TAMPERE UNIVERSITY OF TECHNOLOGY

PRABHAT MAN SAINJU

LTE PERFORMANCE ANALYSIS ON 800 AND 1800 MHz BANDS

Master of Science Thesis

ABSTRACT

Long Term Evolution (LTE) is a high speed wireless technology based on OFDM. Unlike its predecessors, its bandwidth can be scaled from 1.6 MHz to 20 MHz. Maximum theoretical throughputs from the LTE network in downlink can be estimated to range over 300 Mbps. The practical values are however limited by the channel overheads, path loss and cell loading. Its ability to deliver high throughput depends upon its radio access technology OFDM and the high bandwidth usage as well.

The other important feature of LTE is its usage in multiple bands of spectrum. The primary focus in this thesis is on 800 MHz band and its comparison with 1800 MHz band and UMTS coverage. Coverage, capacity and throughput scenario are the essential dimensions studied in this thesis. A test network was set up for LTE measurement and the primary measurement parameters such as RSRP, RSRQ, SINR and throughput were observed for different measurement cases. The measurement files were analysed from different perspectives to conclude upon the coverage aspect of the network.

The basic LTE radio parameters RSRP, RSRQ and SINR tend to degrade as the UE moves towards the cell edge in a pattern similar to the nature of free space loss model. In a way, these parameters are interrelated and eventually prove decisive in the downlink throughput. The throughput follows the trend of other radio parameters and decrease as the UE moves towards the cell edge. The measured values have been compared to the theoretical results defined by link budget and Shannon's limit. The comparison shows that measured values are confined within the theoretical constraints. Theoretical constraints along with the minimum requirements set by the operator have been used to measure the performance of the sites. Similar analysis was also performed with the LTE 1800 network and UMTS 900 network and the result was compared to the coverage scenario of LTE 800. Higher slope of attenuation was observed with LTE 1800 compared to LTE 800 and thus limiting the coverage area. Comparison of radio parameters RSRP, RSRQ and SINR confirm the coverage difference and its consequence on downlink throughput. Performance of UMTS 900 however was not much different to LTE 800 coverage wise.

The measurements have been carried out on LTE test network at Kuusamo, Finland and the commercial UMTS network set up by TeliaSonera for the comparison of LTE 800 with LTE 1800 and UMTS 900.

PREFACE

This Master of Science Thesis has been carried out for TeliaSonera Finland Oyj. from November 2011 - June 2012. The research project was conducted as an attempt by TeliaSonera to obtain a detailed picture on the coverage aspects of LTE 800 MHz band which is due for auction in the 3rd and 4th quarters of 2012.

I am grateful to my instructors Timo Kumpumäki and Kari Ahtola at TeliaSonera and my supervisors Mikko Valkama and Jarno Niemelä at TUT. Their constant guidance and support made it possible for the thesis to churn out into the present state. I also thank Esa-Pekka Heimo and Anssi Vestereinen for providing knowledgebase on the measurement devices and applications. Thank you Teemu Lampila for being with me during the measurements in bone-chilling weather. I also appreciate support team at Anite Helpdesk for their tireless response to my queries.

I finally thank to my family and friends for encouraging and supporting me patiently; you did not lose faith, I did not give up.

Tampere, 5th September, 2012
Prabhat Man Sainju
prabhat.sainju@gmail.com

CONTENTS

LIST OF ABBREVIATIONS

3GPP	3rd Generation Partnership Project
AF	Application Function
AMPS	Advanced Mobile Phone System
ANR	Automatic Neighbour Relation
AuC	Authentication Centre
AWGN	Additive White Gaussian Noise
BLER	Block Error Rate
CDF	Cumulative Distribution Function
CP	Control Plane
CP	Cyclic Prefix
CPICH	Common Pilot Channel
CQI	Channel Quality Indicator
DFT	Discrete Fourier Transform
DHCP	Dynamic Host Control Protocol
DL	Downlink
DSP	Digital Signal Processing
EDGE	Enhanced Data rates for GSM Evolution
EIRP	Effective Isotropic Radiated Power
EMM	EPS Mobility Management
eNodeB	Evolved NodeB
EPC	Evolved Packet Core
EPS	Evolved Packet System
EUTRAN	Evolved-UTRAN
FDM	Frequency Division Multiplexing
FTP	File Transfer Protocol
GI	Guard Interval
GPRS	General Packet Radio Service
GSM	Global System for Mobile Communications
GTP-U	GPRS Tunneling Protocol-User Plane
HO	Handover
HSDPA	High Speed Downlink Packet Access
HSPA	High Speed Packet Access
HSS	Home Subscription Server
HSUPA	High Speed Uplink Packet Access

IFFT	Inverse Fast Fourier Transform
IP	Internet Protocol
IP-CAN	IP-Connectivity Access Network
ISDN	Integrated Services Digital Network
ISI	Inter Symbol Interference
KPI	Key Performance Indicator
LTE	Long Term Evolution
LTE-A	LTE Advanced
MAC	Medium Access Control
MCS	Modulation Coding Scheme
MIMO	Multiple Input Multiple Output
MME	Mobility Management Entity
MMS	Multimedia Message Service
NAS	Non-Access-Stratum
NMT	Nordic Mobile Telephone
O&M	Operation & Maintenance
ODBC	Oracle Database Control
OFDMA	Orthogonal Frequency Division Multiple Access
OLPC	Open Loop Power Control
PAPR	Peak to Average Power Ratio
PBCH	Physical Broadcast Channel
PCC	Policy and Charging Control
PCI	Physical Cell Identity
PCRF	Policy and Charging Resource Function
PDC	Personal Digital Cellular
PDCCH	Physical Downlink Control Channel
PDCP	Packet Data Convergence Protocol
PDSCH	Physical Downlink Shared Channel
PG	Processing Gain
P-GW	Packet Data Network Gateway
PHY	Physical Layer
PLMN	Public Land Mobile Network
PMI	Precoding Matrix Indicator
PRB	Physical Resource Block
PSTN	Public Switched Telephone Network
QAM	Quadrature Amplitude Modulation
QoS	Quality of Service
QPSK	Quadrature Phase Shift Keying
RAT	Radio Access Technology
RI	Rank Indicator
RLC	Radio Link Control
RNC	Radio Network Controller

RRC	Radio Resource Connection
RRM	Radio Resource Management
RSCP	Received Signal Code Power
RSRP	Reference Signal Received Power
RSRQ	Reference Signal Received Quality
RSSI	Received Signal Strength Indicator
SC-FDMA	Single Carrier Frequency Division Multiple Access
SGSN	Serving GPRS Support Node
S-GW	Serving Gateway
SINR	Signal to Interference-Noise Ratio
SISO	Single Input Single Output
SMS	Short Message Service
SNR	Signal to Noise Ratio
SQL	Structured Query Language
TA	Tracking Area
TAI	Tracking Area Identity
TAL	Tracking Area List
TAU	Tracking Area Update
TDMA	Time Division Multiple Access
TTI	Transmission Time Interval
UE	User Equipment
UMTS	Universal Mobile Telecommunication System
UP	User Plane
USIM	Universal Subscriber Identity Module
UTRAN	Universal Terrestrial Radio Access Network
WCDMA	Wideband Code Division Multiple Access
VAS	Value Added Service
VMS	Voice Message Service
X2AP	X2 Application Protocol

LIST OF SYMBOLS

S_{rxlev}	Cell selection Rx level value
$Q_{rxlevmeas}$	Measured Rx level value (RSRP)
$Q_{rxlevmin}$	Required minimum Rx level value (RSRP)
$Q_{rxlevminoffset}$	Offset to signalled $Q_{rxlevmin}$ (dB)
$P_{compensation}$	Power compensation (dB)
$S_{servingcell}$	Serving cell measured value (dB)
$S_{intra-search}$	Intra-frequency cell selection search threshold (dB)
$S_{non-intrasearch}$	Inter-frequency cell selection search threshold (dB)
R_S	Serving cell rank
R_N	Neighbouring cell rank
$Q_{meas,s}$	Serving cell measured value
$Q_{meas,n}$	Neighbouring cell measured value
Q_{hys}	Hysteresis value
Q_{offset}	Offset value
$T_{reselection}$	Time to trigger
I_{own}	Own cell interference
I_{other}	Other cell interference
L	Path loss
I_oT	Interference over thermal
N	Thermal noise
P_{max}	Maximum transmit power
α	Cell-specific path correction factor
P_0	Transmit power
d_{km}	Distance from cell centre (in kilometres)
f_{MHz}	Frequency in Megahertz
h_B	Transmitter antenna height
h_M	Receiver antenna height
P_t	Transmitted power
G_t	Transmitter antenna gain
G_r	Receiver antenna gain
λ	Wavelength of the transmitted signal

LIST OF FIGURES

LIST OF TABLES

1.   INTRODUCTION

From the smoke signals and semaphores to the modern day high speed wireless technology, the world has ever been evolving in the communication timeline. The communication world has taken some giant leaps in past few decades by virtue of wireless communication. The development of cellular technology proved to be the foundation upon which present wireless technology would be laid upon.

Along with the voice, data communication has now also become an integral part of the consumer need. People on the move with smart phones, wireless applications, internet etc. demand high speed data service. Apart from these, consumer satisfaction with greater quality of service also needs to be maintained. All these have brought focus upon the scarce natural resource on which the technology depends upon – Frequency Spectrum.

The evolution of the technology from the 1st to the 4th generation networks have all been based upon more and more efficient use of the frequency spectrum over the capacity and throughput offered.

After the launch of Universal Terrestrial Radio Access Network (UTRAN), the 3rd Generation Partnership Project (3GPP) initiated the research and building specification on Long Term Evolution (LTE) of UTRAN. The first and foremost important change was the switching of radio access technology from Wideband Code Division Multiple Access (WCDMA) to Orthogonal Frequency Division Multiple Access (OFDMA) as the multiple access scheme. LTE with its distinct access technology has proved to be the answer to the bandwidth hungry wireless applications. The first Universal Mobile Telecommunication System (UMTS) standard published in 1999 emphasized more on wireless channels and circuit switched technology. Evolution path from UMTS and then High Speed Packet Access (HSPA) and now to LTE clearly indicates where the technology is heading – a fully Internet Protocol (IP) Switched Network.

1.1.   Evolution of wireless technology

The first of the wireless technologies to emerge were analog radios practically. These 1st generation networks developed in 1980s had two main wireless technologies; Advanced Mobile Phone System (AMPS) in United States and Nordic Mobile Telephone (NMT) in Europe. Global System for Mobile Communications (GSM) evolved of these 1st generation technologies with a major step ahead towards the digital radio. The features such as Short Message Service (SMS), Multimedia Message Service (MMS), Voice Message Service (VMS) and Value Added Services (VAS) made it one of the most used technologies in the world. This firmly established it as a leader in the 2nd generation network.

Other competing technologies were IS-95 CDMA, Time Division Multiple Access (TDMA) and Personal Digital Cellular (PDC).

The network was expanded to include the data service with the addition of General Packet Radio Service (GPRS). Based on Release 97 specifications, GPRS delivered 20 kbps in downlink and 14 kbps in uplink. Enhancements made on Releases R'98 and R'99 increased the theoretical downlink speed to 171 kbps. Addition of GPRS to GSM places it in between the 2nd generation and the 3rd generation. It is often referred to as 2.5 G. Enhanced Data rates for GSM Evolution (EDGE) extended the data services of GSM further up to 384 kbps at max terming the network to 2.75 G. [1]

UMTS can be presented as the 3rd generation network evolved of the 2nd generation GSM networks. Its specification was developed by 3GPP and commercially launched for the first time in Japan in 2001. UMTS is based on WCDMA technology where the user data is multiplied by a high speed chip of 3.84 Mcps to obtain a code division multiplexed output. The radio interface of UMTS is architecturally similar to GSM network although there are distinct differences that make UMTS radio interface unique.

UMTS was succeeded by HSPA which introduced a higher downlink throughput with High Speed Downlink Packet Access (HSDPA) providing theoretical peak downlink data rate of 14.4 Mbps compared to theoretical limit of 2 Mbps for UMTS. High Speed Uplink Packet Access (HSUPA) in the uplink path provides the theoretical peak uplink data rate of 5.7 Mbps. HSPA+ was also introduced with enhanced data rates over preceding HSPA with theoretical data rate extending up to 84 Mbps in downlink and 22 Mbps in uplink. [2]

While the implementation of UMTS was on-going, 3GPP also initiated research on the Long Term Evolution of UMTS Network predicting the increase in the bandwidth demands from the consumer as well as high-end web applications on wireless devices. The motive was mainly to shift current networking trend to an IP switched network. First workshop for LTE was conducted by 3GPP on November 2004 in Canada. Study and research was made on LTE to make it a part of the 3GPP Release 8 Specification. By March 2009, the Protocol freezing was made and the specifications were baselined by 3GPP.

1.2.   Objectives and scope of the research

Coverage estimation is one of the fundamental factors of network planning for all modern wireless technologies. All of the wireless technologies target the users on the move aiming to provide their high Quality of Service (QoS) and customer satisfaction. Theoretical limits set the targets that are hard to achieve in real scenario as there are multiple factors to consider in the practical case; environment, fading, reflections, noise etc. Especially for the users whose position is mobile, situation becomes different. Regardless of this, a provider needs to make sure that sufficient QoS is maintained.

Of many frequency bands in LTE, this research focuses mainly on the 800 MHz band test network installed by TeliaSonera. LTE 800 band in Finland will be made available

for auction in future. Hence, motive behind this thesis and project is to study the coverage performance and limitation of LTE network on this particular band with respect to other bands. Following problem statements have been outlined as the scope of the thesis:

- LTE 1800 MHz band coverage
- Coverage comparison of LTE 800 band with LTE 1800 band
- Coverage comparison of LTE 800 band with UMTS 900 band

Primary radio parameters Reference Signal Received Power (RSRP), Reference Signal Received Quality (RSRQ), Signal to Interference-Noise Ratio (SINR), link adaptation and throughput will be used as tools to provide different dimensions to the coverage perspective of the test network of LTE 800 band and 1800 band. Parameters are also compared to one another to give a comparative analysis. A comparison of LTE 800 band with UMTS 900 band is to be done based on parameters feasible for comparison as not all parameters can be compared to one another between LTE and UMTS. The comparison should give the performance of various network parameters within the coverage area of the both networks.

Interworking between LTE 800 and LTE 1800 bands has been defined as out of scope of this thesis.

1.3.   Research methodology

With the above mentioned objectives for the research, the thesis will primarily include the theoretical background of LTE. With the objectives and the theoretical knowledge in the subject matter clear, measurements will be carried out in a live test network in the Kuusamo area. The network has been installed by TeliaSonera and necessary information, control and access on network have been provided to perform different measurement cases.

The test network has been setup such that the operating band is interference free and isolated. The measurement cases and routes have been defined so as to get the best possible measurement dataset. Suggestions from the Mobility team and Network Planning team at TeliaSonera have been taken while deciding on such matters.

Measurement data is taken along the measurement routes as per the measurement cases. This measurement data will be analysed and reported based on different performance parameters. The analysis will give a measure of coherence of the measured data with different bands (LTE 1800 band) and Radio Access Technology (RAT) (UMTS specifically).

2. LONG TERM EVOLUTION

The need for an evolved technology was felt during the implementation phase of UMTS; a technology that would surpass the other wireless technologies by miles and support the user needs for many more years to come. The rise in the bandwidth demand and the user traffic predicted for the years to come meant that a shift in the mainstream was needed to make that giant leap. Apart from that, it was also felt that the succeeding technology would be compatible with legacy technologies as well for the smoother transition.

The evolution path from the 1st generation to the 3rd generation brought light upon the limitations of different radio access technologies, their pros and cons and most importantly their performance level in terms of throughput, coverage and capacity. With the lessons learned from the previous generation technologies and questions arising on abilities of future wireless technology, the answer that appeared to 3GPP was in the form of LTE.

2.1. LTE requirements

Before the standardization for the LTE in 2004, 3GPP highlighted the most basic requirements for the long term evolution of UTRAN. They are:

- LTE system should be packet switched domain optimized
- A true global roaming technology with the inter-system mobility with GSM, WCDMA and cdma2000.
- Enhanced consumer experience with high data rates exceeding 100 Mbps in DL / 50 Mbps in UL
- Reduced latency with radio round trip time below 10 ms and access time below 300 ms
- Scalable bandwidth from 1.4 MHz to 20 MHz
- Increased spectral efficiency
- Reduced network complexity
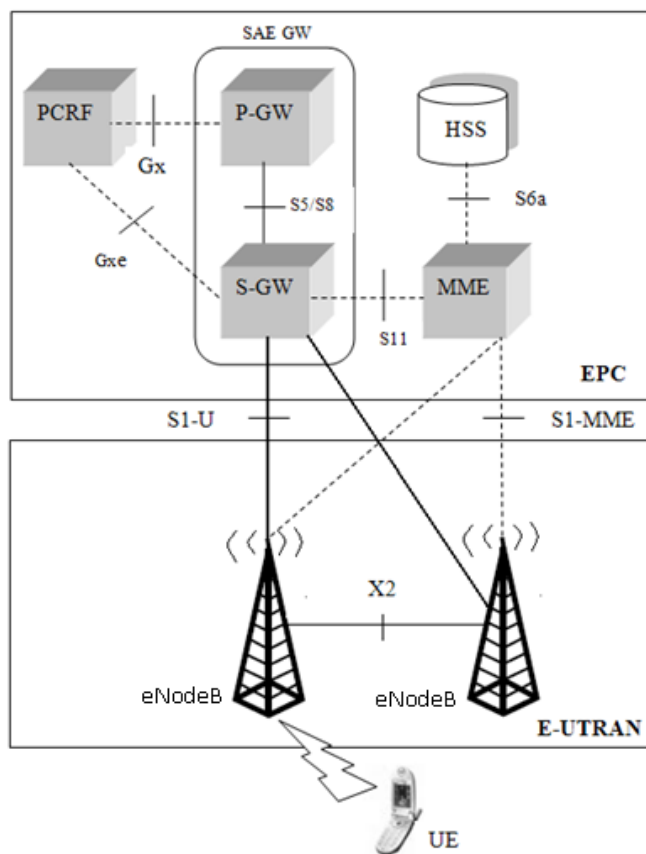
These specifics are based on the visions of 3GPP that concluded in the need of such technology to cope up with the growth predictions of the wireless market. [3]

High data rates and reduced latency are both associated with the better user experience. With the development of high end web applications that demand more bandwidth, these features become a necessity. Apart from these, the system should also be flexible regarding the frequency bands on which the network is deployed with the ability to utilize frequency refarming at different frequency bands. Refarming is the change in the condi-

tions of frequency usage in a given part of radio spectrum. Refarming 900 MHz GSM band together with 800 MHz band is potentially best option as it would provide better link budget and greater coverage at comparatively low cost compared to other higher frequency bands. LTE would be deployed in spectrum bands as small as 1.25MHz and it provides good initial deployment scalability as it can be literally "squeezed" in as the GSM spectrum is freed-up, and grow as more spectrum becomes available. These factors reduce the time advantage of deploying UMTS (HSPA/HSPA+) in the 900 MHz band. [4] Further ahead, the elements of the LTE network and its basic functionalities are explained. The radio interface technology and LTE radio protocols are also explained in brief.

2.2.   Evolved Packet System (EPS)

Evolved Packet System (EPS) is the generalised system architecture which is basically evolved system architecture from that of UMTS Network. In general, the architecture looks similar to the UMTS but holds distinct unique features that ensure the highest level performance and that the requirements set by 3GPP are met.

Figure 2.1: System architecture of EPS

Figure 2.1 shows the system architecture for EPS. The architecture comprises of the Evolved Packet Core (EPC) and Evolved-UTRAN (EUTRAN) as the major building blocks. Appropriate interfaces that connect the modules are indicated with the lines; the

interface names have been included accordingly. The primary functionality of EPS is to provide all IP based connectivity.

The major change in the EPC compared to 3G core is that it does not contain circuit switched domain. Even other circuit switched entities such as Public Switched Telephone Network (PSTN), Integrated Services Digital Network (ISDN) etc. are not directly connected to the EPC but rather connected to the IP cloud. The other major feature change is regarding to the Evolved NodeB (eNodeB). It is the termination point for the radio related functionalities and protocols and these radio functionalities do not exist beyond the eNodeB level in the EPS. One eNodeB is connected with its neighboring eNodeB with X2 interface. The Serving Gateway (S-GW) and the Packet Data Network Gateway (P-GW) together form SAE-GW.

2.2.1.   Logical elements of EPS

2.2.1.1   User Equipment

User Equipment (UE) is the device that a consumer uses for communication. The purpose of communication could be voice oriented or data oriented. The device could be a handheld device or a wireless data card or a modem. Each user is provided with Universal Subscriber Identity Module (USIM). USIM identifies the UE from other UEs and holds the authentication and security keys related operations. Apart from holding these functionalities, UE also forms an important element for mobility management in EPS as it holds key role to operate radio functionalities of EPS.

Table 2.1: Categories of UE in LTE [5]

Category	Maximum Downlink Throughput (Mbits/sec)	Maximum Uplink Throughput (Mbits/sec)	MIMO streams
1	10	5	1
2	50	25	2
3	100	50	2
4	150	50	2
5	300	75	4

Table 2.1 shows the different categories of UEs that are commercially available. As the table indicates, the category is based upon throughput in uplink and downlink for the UE and the number of spatial Multiple Input Multiple Output (MIMO) streams. Currently, only category 3 devices are available commercially and used in the measurements for this thesis.

2.2.1.2   E-UTRAN NodeB (eNodeB)

eNodeB can be considered as a base station that controls all radio related functionalities of the EPS. It is the connecting layer between UE and EPC. All of the radio protocols from UE terminate at eNodeB. eNodeB is the essential part of mobility management in EPS. It also performs encryption/decryption of User Plane/Control Plane data and IP

header compression/decompression as well to decrease the sending of redundant data in IP header.

Beside these basic functionalities, there are other Radio Resource Management (RRM) functionalities conducted by the eNodeB. As a terminating node for the radio protocols, it sets Radio Resource Connection (RRC) and performs radio resource allocations to the users with QoS based prioritization.

Comparing it with UTRAN, it can be seen that the eNodeB performs the functionalities of both NodeB and the Radio Network Controller (RNC). This simplifies the network structure and also in a way reduces the latency in the network as well. As mentioned earlier, the eNodeBs are connected to their neighbouring eNodeBs with the X2 interface. This connection becomes useful during the handover scenarios which will be discussed later.

2.2.1.3   Mobility Management Entity (MME)

MME is an important element of EPC. It is a control plane element and is connected to eNodeBs with S1 interface. Figure 2.1 shows that the MME is connected to Home Subscription Server (HSS) via S6a interface. MME serves for user authentication and security related functionalities in the network via this interface with the help of HSS. MME also takes part in the intra-system handover, a special case which will be discussed in Section 4.3.

The Non-Access-Stratum (NAS) forms the highest stratum of control plane between UE and MME at the radio interface. The major functions of the NAS protocols are:

- Mobility support of the UE
- Session management procedures to establish and maintain IP connectivity between the UE and P-GW
- Tracking area management

More of the NAS is explained in Section 2.2.2. Mobility management in EPS uses the NAS signalling and it is responsible for maintaining functionalities such as cell attach/detach and tracking area management. [6]

2.2.1.4   Serving Gateway (S-GW)

It is a user plane element and forms an important role in inter-frequency handover. During the handover process, the MME commands the S-GW to switch data tunnel from current eNodeB to the target eNodeB. It also relays the data transmission between the serving eNodeB and P-GW. When the UE goes to IDLE mode from the CONNECTED mode while receiving the data packets from the P-GW for a data path, S-GW holds the data packet in buffer. In the meantime, it also requests MME to page the particular IDLE UE. Once the UE resumes to the CONNECTED mode, the buffered packets are delivered and S-GW starts to relay the data from P-GW. Other functionalities of S-GW include entertaining the resource allocation requests from P-GW and PCRF as well. When direct inter-eNodeB connection is not available for the handover, it performs the indirect forwarding of the downlink data. It also acts as a tapping point for monitoring

and security related issues. Apart from these, the packet flow via S-GW can also be used for charging purposes.

2.2.1.5   Packet Data Network Gateway (P-GW)

P-GW is the element of EPS that connects the EPS to the external data network. It can be compared to a router that connects EPS to external network. Just like a router, it allocates the IP addresses to the UE attached to the EPS using the Dynamic Host Control Protocol (DHCP). It could also provide the requested IP via externally connected dedicated DHCP server.

The user plane data is communicated between UE and external data networks in the form of IP packets. P-GW interacts with the PCRF for appropriate policy control information. When the UE switches from one S-GW to another, the bearers need to be switched in the P-GW. Alike S-GW, the P-GW can also be used for monitoring and charging purposes.

2.2.1.6   Policy and Charging Resource Function (PCRF)

PCRF maintains Policy and Charging Control (PCC) rules in the EPS. It handles the PCC requests from the other elements in the network such as P-GW and S-GW. Apart from these, it also acknowledges the PCC requests from the external networks and provides decisions for the EPS bearer setup procedure. A bearer is a transmission path of defined capacity, delay and bit error rate etc. [7].

A simple example would be an attach request case. The UE initially attaches to the network with the default bearer and will eventually acquire the dedicated bearers. The primary functions of PCRF are:

- Charging control
  - PCC rule identifies the service data flow and specifies the parameters for charging control. The charging models available are volume based / time based / event based / no charging.
- Policy control
  - There are two main aspects of policy control; gating control and QoS control
    - In the gating control, PCRF controls the packet flow based on the Application Function (AF) reports of session events.
    - QoS control includes the authorisation and enforcement of the maximum QoS that is authorised for a service data flow or an IP-CAN bearer. [8]
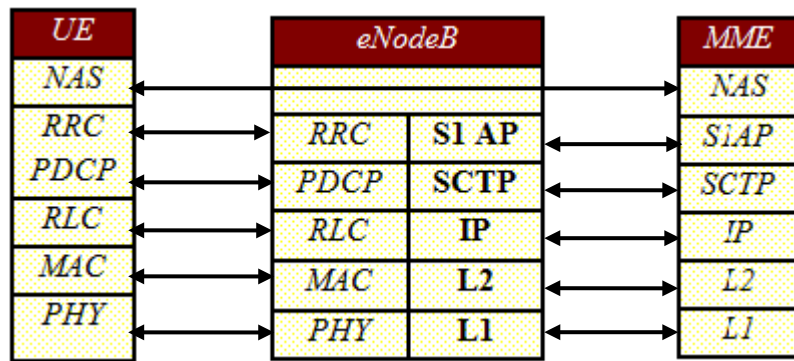
      IP-Connectivity Access Network (IP-CAN) is the collection of network entities and interfaces that provides the underlying IP transport connectivity between the UE and the IMS entities. [7]

2.2.1.7   Home Subscription Server (HSS)

HSS is a server that holds the users data. It contains the master copy of user profile, available services to the user, roaming information etc. Authentication Centre (AuC) is integrated with HSS, which holds the master key for all of the subscribers for security and encryption reasons. HSS also keeps track of the location information of UE with the assistance of MME.

2.2.2.   Interfaces and Protocols

Similar to S1-MME interface, X2 interface needs to be setup for the inter-cellular mobility. Initially the eNodeB will set X2 connection between the eNodeBs suggested by O & M. Later the connection might vary as the eNodeB chooses better neighbour based on Automatic Neighbour Relation (ANR) functionality.
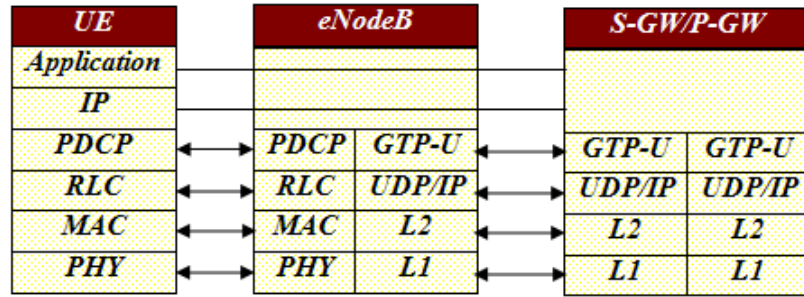
Figure 2.2: Control Plane (CP) protocol stack from UE to MME

Figure 2.2 shows the hierarchical layers of CP protocols with the inter-connections from UE to MME. NAS as explained earlier is a control plane protocol. It connects UE to MME directly. NAS has EPS mobility and session management protocols.

EPS Mobility Management (EMM) is responsible for UE attach/detach process that occurs in the IDLE mode and Tracking Area Updates (TAU). Apart from these, there are security and authentication related features handled by EMM. Other protocols are:

- RRC: Manages the radio resource usage between the UE and the eNodeB. Functionalities include signaling, handover control and cell selection / re-selection.
- Packet Data Convergence Protocol (PDCP): IP header compression and security related functionalities.
- Radio Link Control (RLC): Performs the segmentation and concatenation of the data sent by PDCP and error correction as well.
- Medium Access Control (MAC): scheduling and prioritizing of the usage of physical layer.
- Physical Layer (PHY): Refers to the transmission medium. It involves the usage of code division multiplexing functionalities.
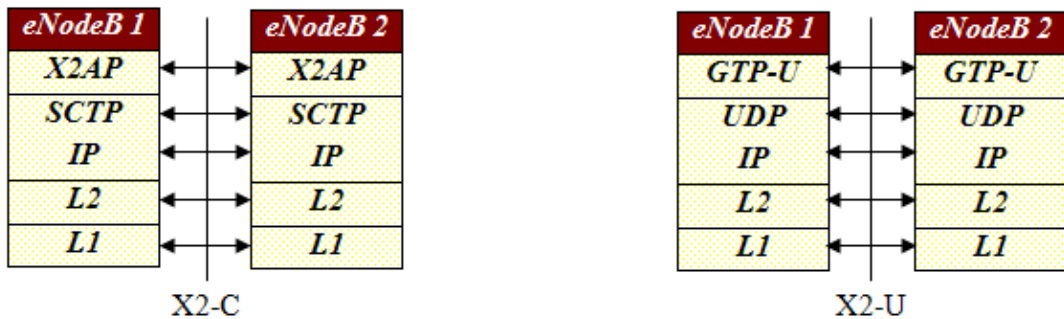
The interface between the UE and eNodeB is referred as LTE-Uu interface and the interface between the eNodeB and MME is referred as S1 interface.

Figure 2.3*: User Plane (UP) protocol from UE to S-GW/P-GW*

Figure 2.3 shows the UP protocol that exists between UE and S-GW/P-GW. Again the UE-eNodeB interface is governed by LTE-Uu interface and eNodeB-S-GW interface is governed by S1 interface. S-GW and P-GW are connected by S5/S8 interface. UP protocol is similar to the CP protocol with the basic difference that the CP carries signaling data packets while UP carries user data packets.

GPRS Tunneling Protocol-User Plane (GTP-U) is used to communicate the end user IP packets belonging to single EPS bearer between the EUTRAN and the EPC. X2 interface is the interface of eNodeB with its neighboring eNodeBs. It becomes an important element in the mobility. X2 protocol addresses both UP and CP connection.

Figure 2.4: *X2 interface in Control and User Plane*

Figure 2.4 shows the X2 protocol architecture. X2 Application Protocol (X2AP) layer manages the handover function between the eNodeBs. Other protocols have already been discussed earlier. The role of X2 interface based handover will be discussed in Section 4.3.1.1.
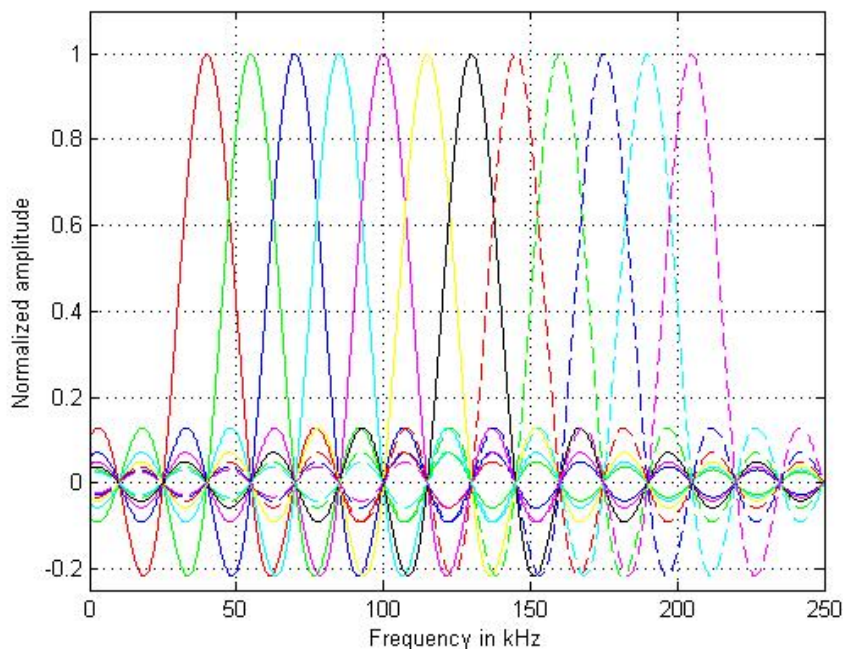
3.   LTE RADIO ACCESS TECHNOLOGY

The legacy technologies like UMTS uses WCDMA as the multiple access technique while GSM used the TDMA approach of multiple access with the frequency division multiplexing. All of these technologies had their set of pros and cons. Most of access methods in the legacy technologies imposed the limitation on capacity / coverage / throughput of the system. With the requirements of 3GPP specified for LTE, the change in the access technology was felt and thus the technology directed towards OFDMA.

3.1.   Introduction to OFDM

Before entering into OFDM, the need of OFDM should be understood; the reason why orthogonality is preferred in the signals. In frequency division multiplexing, users are separated from one another spectrally with multiple users using separate frequency channels and channel bandwidth being equal to the transmission bandwidth.
A simple Frequency Division Multiple Access (FDMA) arrangement would be that multiple frequency channels are arranged serially. For lower adjacent channel interference, guard band is necessary which eventually increases the bandwidth of the system and lowers the spectral efficiency.

Figure 3.1: *12 OFDM sub-carriers in a single resource block*

Basic idea is to use a large number of narrow-banded orthogonal sub-carriers simultaneously. Figure 3.1 shows the orthogonal sub-carriers placed together overlapping each other in such way that the interference experienced in each sub-carrier due to the neighbouring sub-carriers during the sampling is minimum. The sub-carrier spacing in the above figure is 15 kHz i.e. the spacing between the peaks of each sub-carrier is 15 kHz. The phenomenon that haunts most of the radio access technologies is the Inter Symbol Interference (ISI). ISI is caused by multipath propagations which causes the elongation of the received signals in the time domain. This causes the bits to interfere each other and degrade the received signal. To prevent this, a Cyclic Prefix (CP) is added to the symbol which is simply a copy of the tail of the same symbol added at the start of the symbol. CP is preferred to Guard Interval (GI) which is the separation of the symbols in time domain by a time interval to neutralize the delay spread caused by the multipath. This is because with the use of GI, the receiver filter has to consider the delay added to the delay spread. With the use of CP, the data stream becomes continuous and this shortens the receiver filter delay.

There are effectively two sets of CP used based on their duration; Long CP with a duration of 16.67 µs and short CP with a duration of 4.67 µs. Long CP is used in the challenging multipath environments where the delay spread of the received signal is much longer. The inherent properties that make OFDM a better choice for radio access are:

- Better tolerance against frequency selective fading due to the use of multiple sub-carriers
- Link adaptation and frequency domain scheduling
- Simpler receiver architecture based on Digital Signal Processing (DSP)
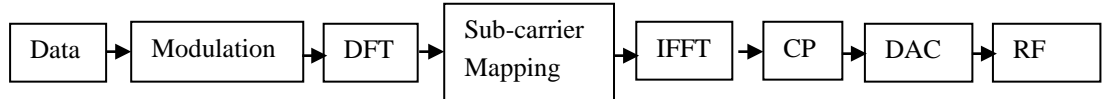
Figure 3.1 shows the bunch of 12 sub-carriers that are placed orthogonally to each other. These blocks of 12 sub-carriers form a Physical Resource Block (PRB) with a bandwidth of 180 kHz. In time domain, these sub-carriers are allocated for duration of 0.5 ms.

3.2.   Single Carrier FDMA

Single Carrier Frequency Division Multiple Access (SC-FDMA) is the preferred uplink multiple access technology over OFDMA in LTE. The problem associated with the OFDMA in the uplink direction is its high Peak to Average Power Ratio (PAPR). This means that the operating point of the power amplifiers in the transmitter needs to be lowered off which in turn lowers the amplifier efficiency. This is not much of an issue in the downlink as the power is much more abundant at the eNodeB side compared to the battery operated UEs. Hence for a longer battery life at the UE end, SC-FDMA is used.
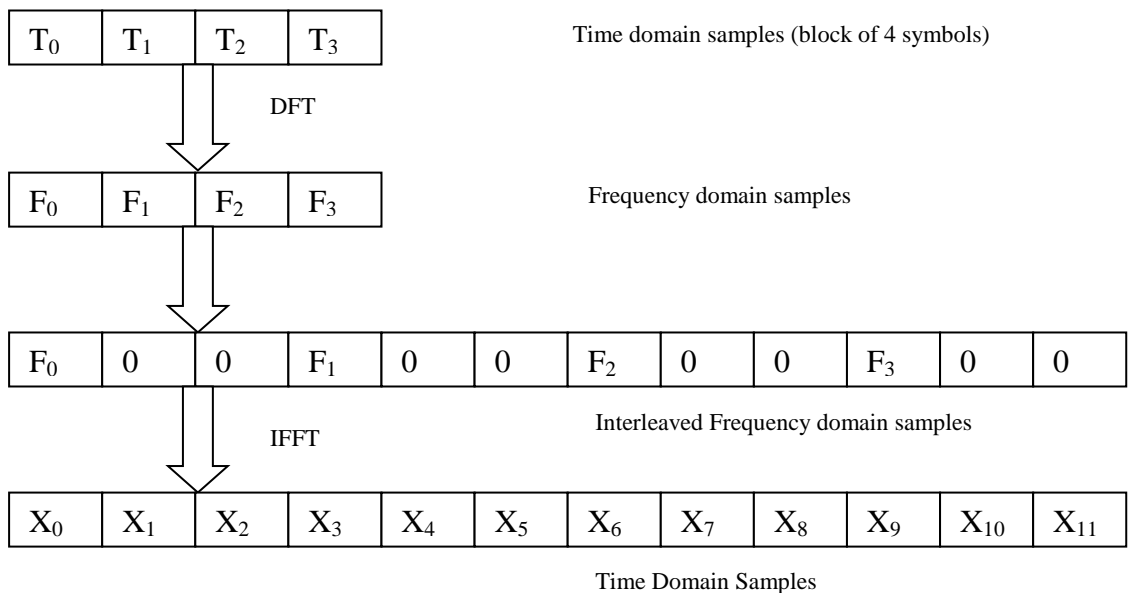
SC-FDMA is also referred as Discrete Fourier Transform (DFT) based OFDMA as it uses DFT mapper to generate frequency domain symbols which would be mapped throughout the different sub-carriers with the subcarrier mapping techniques such as localized mapping or interleaved mapping. Thus the main difference between OFDMA

and SC-FDMA in data wise perspective is that in the OFDMA, the symbols are carried by individual sub-carriers while in the SC-FDMA, the symbols are carried by a group of sub-carriers simultaneously.

| Data | Modulation | DFT | Sub-carrier Mapping | IFFT | CP | DAC | RF |

Figure 3.2: SC-FDMA modulation scheme

Figure 3.2 shows the flow of data for SC-FDMA. 64-Quadrature Amplitude Modulation (64-QAM) is performed to the data chain. DFT is then performed to obtain the data in frequency domain. Sub-carrier mapping is the process to spread the frequency domain samples of the modulated data.

| T_0 | T_1 | T_2 | T_3 |

Time domain samples (block of 4 symbols)

DFT

| F_0 | F_1 | F_2 | F_3 |

Frequency domain samples

| F_0 | 0 | 0 | F_1 | 0 | 0 | F_2 | 0 | 0 | F_3 | 0 | 0 |

Interleaved Frequency domain samples

IFFT

| X_0 | X_1 | X_2 | X_3 | X_4 | X_5 | X_6 | X_7 | X_8 | X_9 | X_{10} | X_{11} |

Time Domain Samples
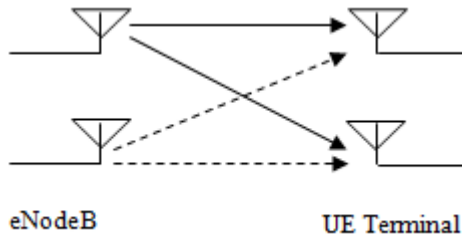
Figure 3.3: Time domain representation of interleaved SC-FDMA

Figure 3.3 shows the sub-carrier mapping process performed above with simple interleaving technique. The frequency domain samples obtained after DFT are interleaved and placed in the block of 12 subcarriers. The remaining vacant sub-carriers are filled with zero. Inverse Fast Fourier Transform (IFFT) is performed to the frequency domain samples to obtain the time domain samples that are evenly spread throughout the sub-carriers. [9]

3.3.   Multiple Input Multiple Output (MIMO)

The major shift in the technology in the LTE suggested by 3GPP in its Release 8 was the implementation of MIMO in the radio environment. The use of MIMO has been made mandatory as per Release 8 to all the devices except for the category 1 device.

Figure 3.4: *A 2x2 MIMO configuration*

Figure 3.4 shows a 2x2 MIMO configuration with two transmitting antennas at the eNodeB side and two antennas at the UE end. Two simultaneous streams of different set of data are transmitted from each transmitting end and both are received simultaneously. Basic idea to separate data streams from one transmitting antenna to another at the receiving end is to use the precoding technique and the reference symbols.

Unlike WCDMA where the pilot channels are used to estimate the channel quality, reference symbols are used in the LTE for the channel estimation. Different set of reference symbols are used for different transmitting antennas so that the receiving antenna can differentiate signals coming from different antennas. Also since the data stream is now divided, better Signal to Noise Ratio (SNR) for each channel needs to be ensured. The UE makes the channel estimation based on the reference symbol measurements, calculates the coefficient of the weight matrix and reports back to the serving eNodeB. eNodeB then adjusts the power level for different channels according to the weight matrix to maximize the capacity. The process is called closed loop spatial multiplexing and the weight matrix is called Precoding Matrix Indicator (PMI).
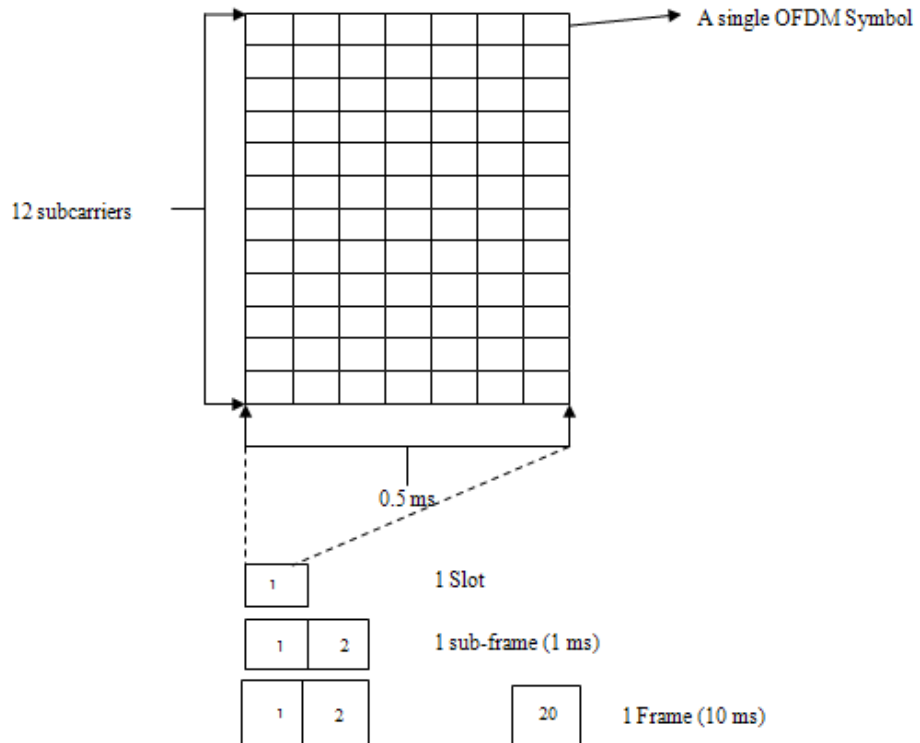
3.4. Modulation techniques

There are three different modulation techniques used in the LTE downlink. They are Quadrature Phase Shift Keying (QPSK), 16-QAM and finally 64-QAM. These different modulation schemes are applicable only in the downlink. The use of the modulation schemes depend upon the channel quality estimation. If the channel is better, higher order modulation like 16-QAM or 64-QAM is used. Higher order means that the alphabet size is high but the alphabet spacing is lesser. This works out well when the channel quality is good and the noise and interference to the received signal is less. But if the channel quality is bad, interference and noise overcome the actual signal and decoding the bits from the received signal becomes impossible. With the signal power remaining constant, the separation between the alphabets needs to be increased to maintain the readability of the signal. This means the modulation has to be lowered to QPSK.

3.5. LTE frame structure

A single PRB is considered the smallest unit in a LTE frame. A single PRB is allocated for time duration of 0.5 ms. A single PRB can be considered of a two dimensional grid

of sub-carriers and symbols. A single PRB consists of 12 sub-carriers grouped together. A single PRB has 6 or 7 symbols depending upon the CP length.

Figure 3.5: *LTE frame structure*

Table 3.1: *Resource block configuration in EUTRAN channel bandwidths*

Channel bandwidth (MHz)	1.4	3	5	10	15	20
Number of resource blocks	6	15	25	50	75	100

Figure 3.5 shows the LTE frame structure. A single PRB is referred as a slot in the LTE frame. Two slots make a sub-frame with duration of 1 ms. 20 PRBs form a single frame and is 10 ms long. The frame structure is same for the downlink (OFDMA) and the up-link (SC-FDMA). Reference symbols are used for the channel estimation. The reference symbols are placed with specific pattern in the PRBs for the efficient channel estimation. Table 3.1 shows the standard list of resource block configuration for different allowable bandwidths in LTE. [10]

4.   EPS MOBILITY MANAGEMENT (EMM)
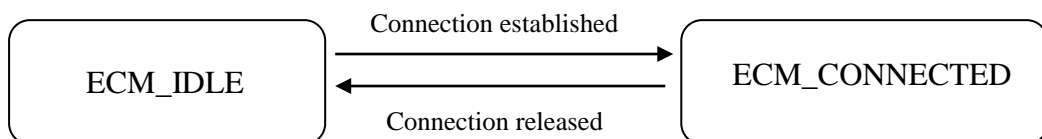
Mobility is an important issue in cellular networks. End users demand flawless network access for both voice service as well as data service. As the users move from one cell to other, the performance of the network has to be high enough to ensure that users do not experience any breakage in the service. Mobility also needs to be ensured in the vehicular environment throughout the coverage area.

4.1.   EPS connection procedure

EPS connection procedure is necessary for UE to establish connection to EPC. The procedure is carried out by the specific EMM message ATTACH REQUEST that operates in NAS signalling layer. The UE-MME connection resides in two main states; EMM-DEREGISTERED and EMM-REGISTERED. Two more intermediate states exist between these two states during the transition.

- EMM-DEREGISTERED: In this state, EMM context is marked as detached. However, MME is able to answer the attach procedure or TAU procedure initiated by UE.
- EMM-COMMON-PROCEDURE-INITIATED: EMM enters this state once it initiates the EMM common procedure and is waiting for the UE response.
- EMM-REGISTERED: In this state, the EMM has successfully established context and a default EPS bearer has been activated in the MME.
- EMM-DEREGISTERED-INITIATED: It enters this state after MME has initiated the DETACH procedure and is waiting for UE response.

Transition from EMM-DERIGISTERED to EMM-REGISTERED occurs when the ATTACH procedure from EMM-DERIGISTERED state or the COMMON procedure from EMM-COMMON-PROCEDURE-INITIATED state is successful.

Figure 4.1: EPS connection management states

Transition from EMM-REGISTERED to EMM-DEREGISTERED state happens when the DETACH procedure from EMM-REGISTERED state is accepted or the TAU request is rejected by MME. Other conditions that lead to DERIGISTERED state when the service request procedure is rejected or when the UE deactivates all EPS bearers. UE is also in the same state when it is just switched ON. [11]

The other two major and familiar states that exist in the EPS connection management are: ECM_IDLE and ECM_CONNECTED modes. Figure 4.1 shows the transition between the IDLE mode and CONNECTED mode in ECM. The mode transition is basically ruled by the Radio Resource Control (RRC) state. The UE could be in DEREGISTERED state or REGISTERED state during the ECM_IDLE mode. The features of IDLE mode are:

- No RRC connection exists.
- UE monitors the paging channel to detect incoming calls
- UE acquires system information from the paging channel
- IDLE mode mobility through cell selection / re-selection

The features of CONNECTED mode are:

- RRC Connection between EUTRAN and UE
- Transfer of unicast and broadcast data to and from the UE
- UE monitors the control channels
- UE provides channel quality feedback

4.2. IDLE state mobility management

Idle state mobility is similar to that of UMTS. The UEs in the mobile environment that are in IDLE state or DEREGISTERED state exhibit the IDLE state mobility. The process is listed below that begins from the switching ON of UE:

4.2.1. Public Land Mobile Network (PLMN) selection

UE scans for all RF channels in E-UTRA bands to find available PLMNs. On each carrier, the UE shall search for the strongest cell and read its system information. It then reports the strong cells to the NAS as the list of high quality available PLMNs. The quality scale for a high quality PLMN is that the measured Reference Signal Received Power (RSRP) value is greater than or equal to -110 dBm. PLMN search can be optimised by utilizing stored information from previous measurements such as carrier frequencies, cell parameters etc. Once the PLMN selection is performed by UE, cell selection procedure is initiated. [12]

4.2.2. Cell selection

- Initial cell selection: In this procedure, UE scans the frequency bands without the use of prior stored data. Once the suitable cell is found, the UE camps on the selected cell.
- Stored information cell selection: In this procedure, the UE utilizes the carrier frequency information, cell parameters etc. of the previous measurements. Once the suitable cell is selected, UE camps on it.

Cell selection criteria S has to be met to select the suitable cell which states that:

$$S_{rxlev} > 0 \tag{4.1}$$

While,

$$S_{rxlev} = Q_{rxlevmeas} - (Q_{rxlevmin} + Q_{rxlevminoffset}) - P_{compensation} \tag{4.2}$$

Where,

$Q_{rxlevmeas} = Measured\ Rx\ level\ value\ (RSRP)$

$S_{rxlev} = Cell\ Selection\ Rx\ level\ value\ (dB)$

$Q_{rxlevmin} = Required\ minimum\ Rx\ level\ value\ (RSRP)$

$Q_{rxlevminoffset} = Offset\ to\ signalled\ Q_{rxlevmin}(dB)$

$P_{compensation} = Power\ Compensation\ (dB)$

Once the suitable cell has been selected and the camped upon, the UE starts to measure neighbouring cells for the reselection process. UE measures the neighbouring cells in the neighbour cell list of the serving cell. To decrease the frequency of neighbouring cell measurements, a threshold signal level is defined for the serving cell so that UE does not need to perform the measurement if the serving cell measured value exceeds the threshold. The threshold has been defined for both inter-frequency and intra-frequency cell selections.

Intra-frequency measurement criteria is that if $S_{servingcell} \leq S_{intrasearch}$, intra-frequency neighbour search should be initiated and inter-frequency measurement criteria is that if $S_{servingcell} \leq S_{non\text{-}intrasearch}$, inter-frequencies or inter-RAT frequency neighbour search should be initiated. $S_{servingcell}$ is the S_{rxlev} value of the serving cell.

4.2.3. Cell re-selection

Cell re-selection is performed when the above mentioned measurement criteria is fulfilled. In the case of intra-frequency cell re-selection, ranking criteria is used. The serving cell and the neighbouring cells are ranked based on measured data. The best ranked cell is re-selected.
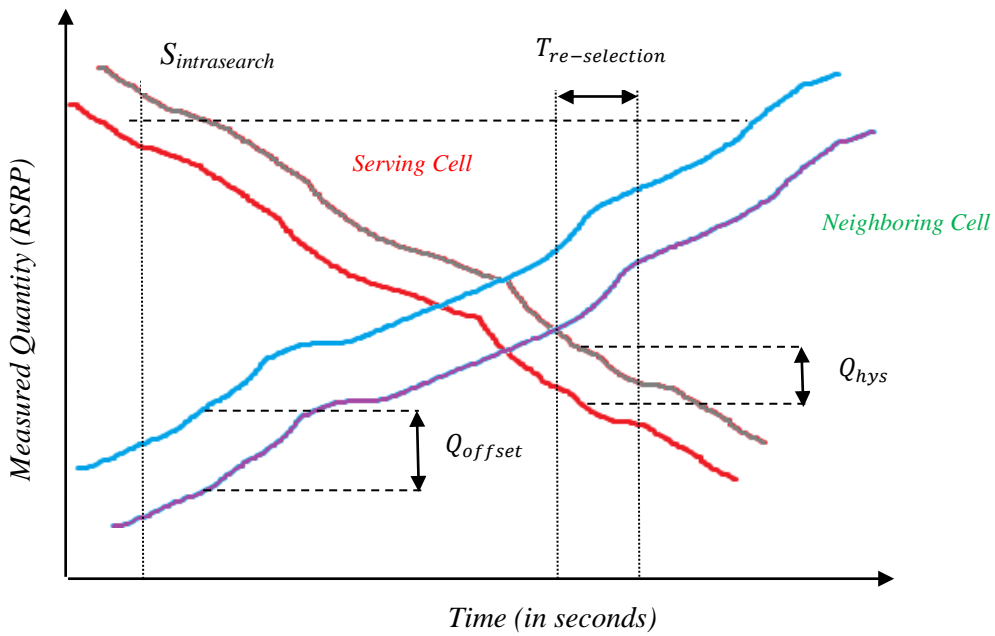
The serving cell is ranked as

$$R_S = Q_{meas,s} + Q_{hys} \tag{4.3}$$

While the neighbouring cell is ranked as

$$R_N = Q_{meas,n} - Q_{offset} \tag{4.4}$$

$Q_{meas,s}$ is the measured RSRP value of the serving cell while $Q_{meas,n}$ is the measured RSRP value of the neighbouring cell. The hysteresis value Q_{hys} is added so that the frequent cell-reselection is prevented. Once the neighbouring cell is better ranked, the cell transition occurs after $T_{re-selection}$ time. This also helps to reduce the frequency of cell re-selection.

Figure 4.2: Cell re-selection during the IDLE mode

Figure 4.2 shows the cell reselection process in the cellular environment. The process begins with the intra frequency measured value of the serving cell getting below the threshold value $S_{intrasearch}$. Without the Q_{hys} and $T_{re-selection}$, the cell re-selection would have begun at the intersection. This would result in the frequent cell re-selection as the UE moves through the serving cell edges or when the link is subject to short term fading. After the serving cell measured value goes below the neighboring cell's measured value, the hysteresis value comes to play. The hysteresis value has to be exceeded for a time of $T_{re-selection}$. After this time interval, the new cell is reselected.

4.2.4. Location Management

The cells in EPS are grouped together based on their physical location. Co-located cells are grouped together to form Tracking Area (TA). A group of cells are provided same Tracking Area Identity (TAI). As the UE moves through different cells, it reports MME to any change in the TAI via TAU message. There are some limitations with the TA. UEs are paged into entire tracking area. A large TA with greater number of cells could cause the paging to UEs fail during the busy hours. This suggests that TA size should be smaller in order to have successful paging. However, smaller TA would mean frequent TAU as the UE moves through the TAs. This creates signaling overhead. To overcome this, 3GPP has suggested for the use of Tracking Area List (TAL). UE maintains the valid list of TAs. Update to the list is made when UE detects it has entered a new TA that is not in the list of TAIs that the UE registered with the network. A TAU is also made when the TA update timer has expired. [13]

4.3.   Handover

Handover (HO) relates to the mobility in the connected mode. Just as explained in the earlier section regarding the cell re-selection that takes place in the IDLE mode, handover operates in the RRC_CONNECTED mode. It is one of the most important features of any of the cellular radio access technologies. As the UE moves throughout the cells in the radio environment, the serving cell might become weak or the neighboring cell might be stronger. This gives option for the UE to switch cell to stronger one. The process is known as handover.

Largely speaking, there are three basic types of handovers in the cellular radio; hard, soft and softer handover. During the hard handover, the connection between the UE and serving cell is temporarily interrupted and the connection is reinstated with the new cell. In the soft handover, the UE is connected with multiple cells at a time. As the UE moves through the cells, weaker connections are released and stronger connections are established. In soft handover, a new connection is first made before breaking previous connection. It is also termed make-before-break connection. Softer handover occurs when the UE switches to the different cells of the same site.

Intra-frequency handovers in LTE are done based on RSRP measurements which should ensure that the users are always connected to the cell with the highest received power. However, in certain environments where interference causes service quality degradation for the user (which RSRP measurement is not able to detect) there might be a situation where a quality based measurement would enable better performance. [14]

Handovers in LTE are different from other access technologies by virtue of its simplified architecture. Unlike UMTS where RNC makes the handover decisions, eNodeB makes the handover decisions in the EPS. UE performs all the handover related measurements and reports them to the associated eNodeB. There are multiple handover schemes available in LTE.

4.3.1.   Intra-LTE handover

4.3.1.1   X2 based handover

Intra-LTE handover involves only E-UTRAN for the handover process. UP is switched from the MME - S-GW source eNodeB to MME - S-GW - Target eNodeB. The handover is referred as UE assisted network controlled handover. The handover process initiates as explained in Figure 4.3:
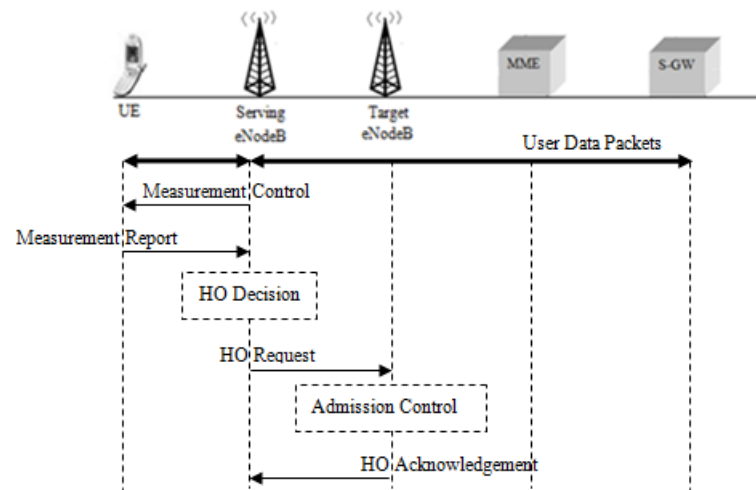
- UE performs the measurements and reports it to the serving eNodeB.
- The serving eNodeB judges the necessity for handover and identifies appropriate target eNodeB.
- The target eNodeB is requested by the serving eNodeB and it then performs Admission Control for the resource allocation to the new client.
- After the resource is allocated, the request from the serving eNodeB is acknowledged.

The handover is executed as explained in Figure 4.4:
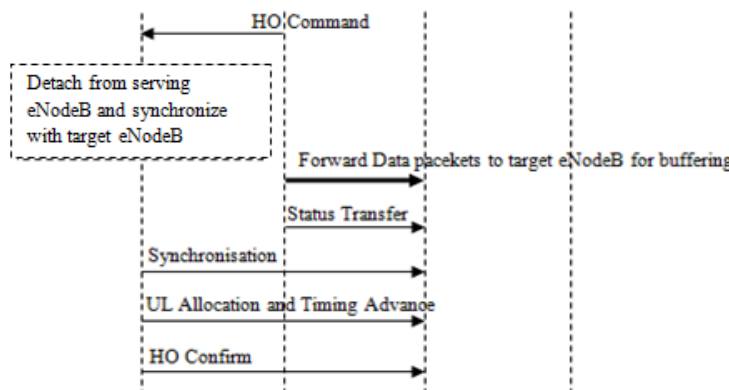
- The serving eNodeB sends the Handover command to UE.
- Serving eNodeB forwards the incoming packets from S-GW - MME to the target eNodeB via the X2 interface while the connection between the UE and E-UTRAN is off.
- The target eNodeB receives the data packets and buffers it till the connection resumes from the target eNodeB.
- The target eNodeB is synchronized with reference to the serving eNodeB.

The handover process is finally completed as explained in Figure 4.5:
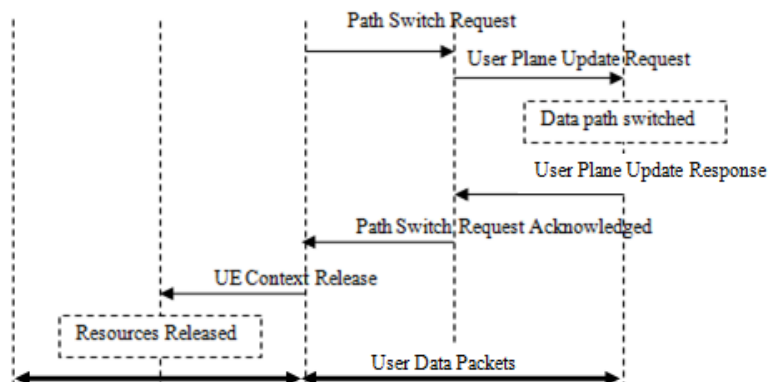
- User plane update request is made to the S-GW.
- S-GW acknowledges the request by changing the data path which would now use the target eNodeB.
- S-GW sends the gives the response back to MME as the data path has been switched.
- MME sends the acknowledgement to the target eNodeB indicating that the user plane has been switched.
- Target eNodeB or the new serving eNodeB now requests the previous serving eNodeB to release the radio resources.
- The resources are released and the data packets are now communicated by UE with the new eNodeB.

Figure 4.3: *Handover preparation over X2 interface [22]*

Figure 4.4: *Handover execution over X2 Interface [22]*

Figure 4.5: *Handover completion over X2 Interface [22]*

4.3.1.2   S1 based handover

S1 based handover is preferred when the X2 based handover cannot be performed. The possible reasons for this could be:

- MME and/or S-GW needs to be relocated.
- X2 interface becomes unavailable during the handover for some reason.
- Error indication from target eNodeB after an unsuccessful X2 based handover.

To show the complete scenario, it is assumed that the serving and target eNodeBs belong to separate MME and S-GW. eNodeB communicates with the MME via S1 interface and MME connects with S-GW via S10 interface.
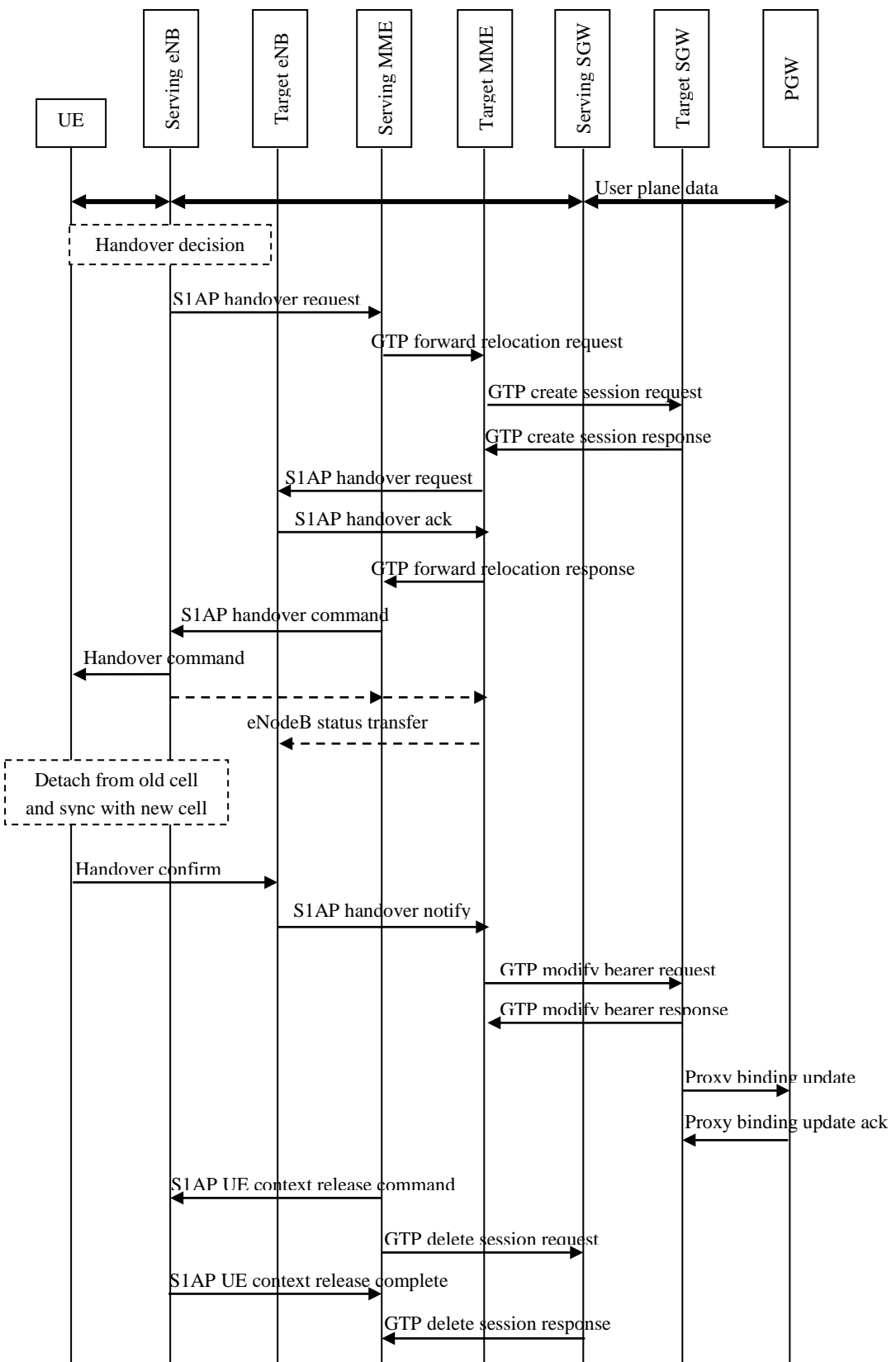
If either of above mentioned conditions is fulfilled, the serving eNodeB opts for the S1 based handover. Figure 4.6 shows the procedure following the S1 based handover. Serving eNodeB sends the S1AP handover request message to the source MME upon the handover decision made at the serving eNodeB and the indication that the direct forwarding is not possible. The message also uniquely identifies the UE to be processed for handover. Serving MME sends the GPRS Tunneling Protocol (GTP) forward relocation request message to the target MME over the S10 interface.

Since the S-GW for serving and target MME is different, the target MME sends the GTP create session request message to the target S-GW. The target S-GW responds by replying with GTP create session response message. Target MME initiates the Handover process at the E-UTRAN by sending the handover request in S1AP interface. Target MME now sends the handover request to the target eNodeB. Target eNodeB replies with handover request acknowledgement in confirmation.

After the handover process set with the target MME and eNodeB, the target MME responds to relocation request of serving MME by sending the S1AP Handover Response Message. Serving MME now sends the handover command to the serving eNodeB. Serving eNodeB now prepares to handover the UE to the target MME by performing the status transfer. The serving eNodeB now detaches from the UE and the UE now starts to synchronize with the new target eNodeB.

UE confirms the attach process with new eNodeB by sending the handover confirm message. Target eNodeB sends the S1AP Handover Notify to the target MME to inform that the UE has attached to it. Target MME sends the GTP modify bearer request message to the target S-GW and it replies with the GTP modify bearer response message.

Serving MME requests serving eNodeB to release the radio resources and delete all the UE Contexts. It also requests the serving S-GW to delete all the EPS bearers associated with that UE. [15]

Figure 4.6: *S1 based handover [15]*

4.3.2.   Inter RAT handover

Just as in the case of S1 based handover, the inter RAT handover is also based on availability of direct forwarding path. A direct forwarding path exists if the X2 connection is available between the source eNodeB and target eNodeB. If the connection is not available, the source eNodeB indicates the indirect forwarding path to source MME. In the case of Inter RAT handover involving the UMTS as the target network, RNC is the target element of the UTRAN. It also involves the Serving GPRS Support Node (SGSN) of the target network analogous to the target MME. The procedure is divided into Preparation and Execution phases.

In the preparation phase, the handover request from the serving eNodeB is forwarded to the source MME. It then sends the Forward Relocation Request to the target SGSN unlike target MME in the S1 based handover. Target SGSN creates session with the target S-GW. Now the target SGSN after creating the session with target S-GW, requests for relocation to target RNC of the UTRAN. After confirmation, the target RNC sends the relocation acknowledge back to the target SGSN.

4.4.   Measurement events and triggers

For a handover decision to be made at the serving eNodeB, a set of measurements need to be carried out and reported to the eNodeB by the UE. The parameters to be measured are configured via the RRC connection reconfigure message. A set of events and triggers have been defined to provide the real time information but with the signaling overhead reduced. An event is a typical condition that occurs in the UE end for the measurement parameters e.g. RSRP value decreasing below a certain threshold. These events are strategically defined such that they are enough for the serving eNodeB to know about the radio environment at the UE. These events trigger UE to send measurement reports to the eNodeB. The report itself has to be concise enough but delivering all the necessary information required for the handover. In addition to event triggered reports, there are also the periodic reports sent by UE.
The measurement configuration parameters are:

- Measurement objects: The network parameter to be measured for
- Reporting criteria: The events for which UE is triggered for the measurement report. A1, A2, A3, A4 and A5 events are used in the intra-LTE measurements while B1 and B2 events are used for Inter RAT measurements.
  - Event A1 : serving becomes better than absolute threshold
  - Event A2 : serving becomes worse than absolute threshold
  - Event A3 : neighbor becomes amount of offset better than serving
  - Event A4 : neighbor becomes better than absolute threshold
  - Event A5 : Serving becomes worse than absolute threshold 1 and neighbor becomes better than another absolute threshold 2
  - Event B1 : neighbor becomes better than absolute threshold

- o Event B2 : Serving becomes worse than absolute threshold 1 and neighbor becomes better than another absolute threshold 2
- Measurement identity: The identifier that relates the measurement object with the reporting configuration.
- Quantity configurations: defines the appropriate filter coefficients for different measurements.
- Measurement gaps: defines the periodic interval upon which the measurement should be carried out.

The measurements in RRC_IDLE state, UE utilizes the measurement configuration defined for cell re-selection. During the RRC_CONNECTED state, UE uses the measurement configuration as per the indication from the serving eNodeB. At least two measurement quantities RSRP and Received Signal Strength Indicator (RSSI) measurement should be supported. [16]

5.   PERFORMANCE INDICATORS

There are various aspects for the assessment of the coverage of LTE Network denoted here as the performance indicators. These various factors are studied and measured to verify the coverage scenario in the radio environment for the LTE test network.

5.1.   Link adaptation

Adaptive link modulation is employed to better utilize the current channel quality. This feature depends upon the Channel Quality Indicator (CQI). UE performs the channel estimate and reports the eNodeB. UE normally reports back the highest CQI index associated with the Modulation Coding Scheme (MCS) for which the DL transport layer Block Error Rate (BLER) does not exceed 10%. The CQI index is reported between 1 and 15 or a CQI index of 0 if the transport BLER exceeds 10%. [17] The modulation schemes available are 64-QAM, 16-QAM and QPSK respectively on the decreasing order of channel quality.

Table 5.1: CQI values and their modulation range

CQI index	Modulation
0	'Out of Range'
1	QPSK
2	QPSK
3	QPSK
4	QPSK
5	QPSK
6	QPSK
7	16 QAM
8	16 QAM
9	16 QAM
10	64 QAM
11	64 QAM
12	64 QAM
13	64 QAM
14	64 QAM
15	64 QAM

Table 5.1 shows the range of the modulation schemes and the CQI levels associated with it. CQI values are reported from 0-15. The highest CQI 15 denotes the best channel quality and thus is supported by highest modulation scheme available i.e. 64-QAM. Apart from CQI, there are other channel estimation reports – Rank Indicator (RI) and PMI that are associated with the MIMO. CQI measurements are reported at an interval of one Transmission Time Interval TTI (1 ms). This causes measurement data to appear redundant i.e. having multiple instances of link adaptations at the same time. [18]

5.2.   Physical Cell Identity (PCI)

PCI is normally used to identify a cell for radio purposes, e.g. camping and handover procedures are simplified by explicitly providing a list of PCIs that UEs must monitor. PCI is part of an initial configuration of the cell, and it is set up by the network designers using network planning tools. In LTE network, a set of 504 unique PCIs are reserved to address a cell. [19]

In LTE radio environment, a UE is served by an active set while the neighbouring cells that are within the threshold limits specified by the Operation & Maintenance (O & M) team after planning and optimization fall under detected set. A measurement tool would identify the active set and detected set cells as the PCIs. Hence, the coverage of a particular cell as the active set can be identified from the set of measurements by filtering out the selected PCIs and making sure that the filtered PCIs are active. PCIs are reused throughput the network. Hence, the PCI distribution needs to be planned such that two cells with same PCIs are separated by considerable radio distance to prevent the cells from interfering each other.

5.3.   Reference Signal Received Power (RSRP)

RSRP is defined as the linear average over the power contributions (in watts) of the resource elements that carry cell-specific reference signals within the considered measurement frequency bandwidth. As the name suggests, reference signal exists as a single symbol at a time, the measurement is made only on the resource elements that contain the cell specific reference signals. RSRP is an important LTE physical layer measurement performed by UE and is mostly utilized during the decision making in the intra-frequency and inter-frequency handovers. [20]

5.4.   Reference Signal Received Quality (RSRQ)

RSRP is an important measure in LTE; however it does not give the measure of quality of the signal. RSRQ parameter gives the measure of the quality of the signal for which the RSRP is measured. Reference Signal Received Quality (RSRQ) is defined as the ratio $N\times$RSRP/(E-UTRA carrier RSSI), where N is the number of resource blocks of the E-UTRA carrier RSSI measurement bandwidth. The measurements in the numerator and denominator shall be made over the same set of resource blocks.

$$RSRQ = N\frac{RSRP}{RSSI} \ in \ dB \tag{5.1}$$

E-UTRA carrier Received Signal Strength Indicator (RSSI), comprises the linear average of the total received power (in watts) observed only in OFDM symbols containing reference symbols, in the measurement bandwidth, over N number of resource blocks by the UE from all sources, including co-channel serving and non-serving cells, adjacent channel interference, thermal noise etc. [20]

5.5.   Signal to Interference-Noise Ratio (SINR)
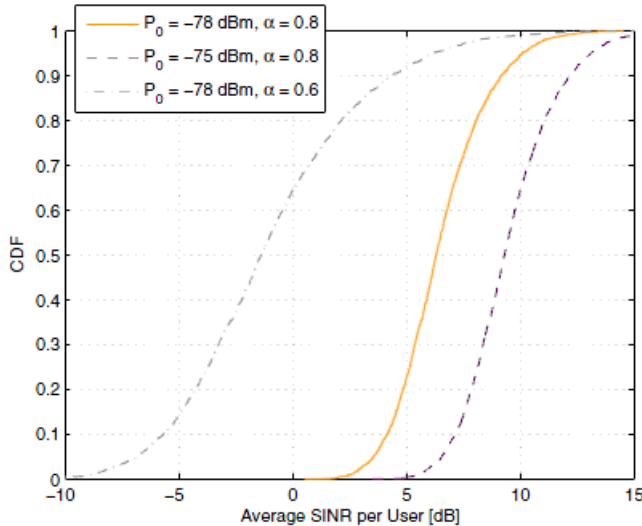
SINR can be defined as,

$$SINR = \frac{S}{I + N} \ in \ dB \tag{5.2}$$

Where S is the average received signal power, I is the interference and N is the noise. I can further be broken down into

$$I = I_{own} + I_{other} \tag{5.3}$$

where I_{own} is the own cell interference while I_{other} is the other cell interference. [21]

Figure 5.1*: Ideal impact on the experienced SINR per user when varying the OLPC parameters, i.e. P_0 and α, assuming a constant I_oT level. This example is shown for Macro 1 [24]*

SINR is one of the most important factors that determine the downlink throughput for the UE. Per UE SINR is highly impacted by power control mechanism. Figure 5.1 shows the CDF plot of average SINR per user. With the Open Loop Power Control (OLPC) implemented, the transmit power is varied by the path loss and the PRB usage. A macro 1 is propagation model simulation scenario with assumption that frequency is 2 GHz, inter-site distance 500 m, bandwidth 10 MHz, UE speed at 3 km/hr and penetration loss at 20 dB. [22] The SINR per user S is given as:

$$S = P - L - I_oT - N \ \ [dB] \tag{5.4}$$

and the transmit power P can be written as,

$$P = min\{P_{max}, P_o + 10.\log_{10}M + \alpha.L\} \quad [dBm] \tag{5.5}$$

Where,

L = Path loss in *dB*,

P_0 = UE specific (optionally cell specific) parameter

I_oT = Interference over Thermal

N = Thermal noise

P_{max} = Maximum transmit power

M = Assigned PRBs

α = Cell-specific path correction factor

With the assumption of P_0 = -78 dBm and α = 0.8 (as mentioned in Figure 5.1), M as 50 (assuming full PRB usage for 10 MHz bandwidth) and L as 130 dB, the transmit power can be calculated from Equation 5.5 as 42.9 dBm. Now utilising this value in Equation 5.4 and assuming *IoT* to be 5 dB (3 to 10 dB for commercial networks [23]) and N to be -104.4 dBm (from the link budget mentioned in Appendix A), S is calculated to be 12.4 dB. Similar collection of data with varying path losses L and PRB usage M in the measurement in a radio environment gives the data that has been plotted in the figure.

The figure depicts that higher P_o causes the increase in average SINR per user while a lower P_o decreases the SINR. A lower α not only decreases the SINR, but also spreads the curve which leads to a higher differentiation in terms of experienced SINR between cell-edge and cell-center users. Apart from P_o and α, interference is also an important factor that has an impact on SINR distribution. [24]

5.6. Capacity of memoryless channels

Shannon bound capacity of Additive White Gaussian Noise (AWGN) channel is obtained by the assumption that the modulated signal *x(t)* (with variance of σ^2) is contaminated by AWGN channel noise (with variance $\frac{N_0}{2}$). When calculating the capacity of Discrete Input Continuous Output memoryless channel, input sequence is assumed to be an equi-probable *M-ary* input symbol having $log_2(M)$ *bits/symbol* information.

The probability of symbol occurrence is given by

$$p(x_m) = \frac{1}{m}, \quad m = 1, \dots \dots M \tag{5.6}$$

Conditional probability of receiving *y* while transmitting *x* over the AWGN channel is given as
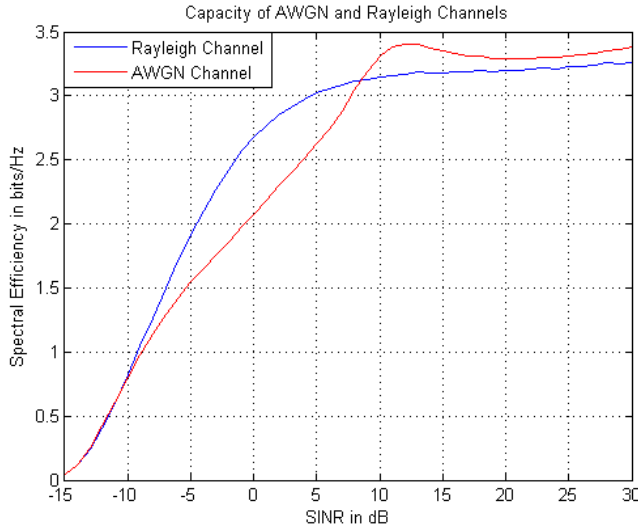
$$p(y|x_m) = \prod_{n=1}^{N} \frac{1}{\sqrt{\pi N_0}} exp\left(\frac{-(y_n - x_{mn})^2}{N_0}\right) \tag{5.7}$$

The simplified channel capacity for *N* = 2 dimensional *M-ary* signal is obtained as

$$C = log_2(M) - \frac{1}{M} \sum_{i=1}^{M} E\left[exp\left(\frac{-|x_m + n - x_i|^2 + n^2}{N_0}\right)\right] \quad bits\ per\ symbol \tag{5.8}$$

Where, *n* is the complex AWGN vector with variance$\frac{N_0}{2}$. [25]

The random characteristics of a radio channel cannot be properly analyzed with the AWGN channel model due to the factors such as reflection, refraction, diffraction, large and small scale fading. Rayleigh fading channel apart from being noise inflicted is also affected by complex channel gain which is a random variable. It is an input-independent time varying channel parameter.

Figure 5.2: Spectral efficiency of AWGN and Rayleigh channel

Capacity of Rayleigh channel is modeled by replacing the effect of AWGN channel model in the Matlab simulation code. The final capacity of both channels is shown in Figure 5.2. [26]

5.7.   Received Signal Code Power (RSCP)

RSCP the received power on one code measured on the primary Common Pilot Channel (CPICH). The reference point for the RSCP shall be the antenna connector of the UE. If Tx diversity is applied on the primary CPICH the received code power from each antenna shall be separately measured and summed together in watts to a total received code power on the primary CPICH. [20]

5.8.   Downlink throughput

The factors governing the application throughput in downlink direction are bandwidth, MIMO usage, modulation and coding. The spectral efficiency offered by different modulation techniques such as QPSK, 16-QAM and 64-QAM for single streamed transmission ranges from 1 bps/Hz to 6 bps/Hz. A 2x2 MIMO usage doubles the bit rate increasing the upper limit to 12 bps/Hz. Number of resource blocks allocated for different bandwidth provide the number of available symbols in a time frame. Various signalling channels consume the allocated resource elements partially. These control channel

overhead bits need to be deducted from the available bit rate to calculate theoretical available bit rate.

Table 5.2: Theoretical downlink bit rates (10 MHz bandwidth)

Modulation Scheme	MIMO Usage	bps/ Hz	Symbols in all PRBs / time slot	PDCCH Overhead Bits / time slot	RS Over- head Bits	Bits /Resource Block	Data Rate (Mbps)
QPSK	SISO	2	4200	1200	400	6800	13.6
16-QAM	SISO	4	4200	2400	800	13600	27.2
64-QAM	SISO	6	4200	3600	1200	20400	40.8
QPSK	2x2 MIMO	4	4200	2400	1600	12800	25.6
16-QAM	2x2 MIMO	8	4200	4800	3200	25600	51.2
64-QAM	2x2 MIMO	12	4200	7200	4800	38400	76.8
QPSK	4x4 MIMO	8	4200	4800	4800	24000	48
16-QAM	4x4 MIMO	16	4200	9600	9600	48000	96
64-QAM	4x4 MIMO	24	4200	14400	14400	72000	144

Table 5.2 shows the theoretical downlink bit rate calculated for different modulation schemes and MIMO usage combinations for 10 MHz bandwidth. Taking an example of 64 QAM Single Input Single Output (SISO), bits per symbol (bps) is 6 and since the MIMO usage is just single stream, bps/Hz is 6x1=6. The rate would have doubled if the stream were 2x2 MIMO or quadrupled if the usage was 4x4 MIMO. Assuming short CP used, number of symbols per sub-carrier is 7 and a single PRB utilises 12 sub-carriers. Total number of symbols in all 50 PRBs allocated for a 10 MHz bandwidth is thus 7x12x50=4200 symbols per time slot. There are 12 Physical Downlink Control Channel (PDCCH) symbols per 0.5 ms time slot. Hence, for 50 PRBs, there are total 6x12x50=3600 bits per 0.5 ms time slot. For Reference Signal (RS) overhead, there are 4 symbols per PRB for single stream, 8 symbols per PRB for 2x2 MIMO and 12 symbols for 4x4 MIMO. Hence, for single stream 64 QAM, total RS bits = 6x4x50=1200 bits. Hence total overhead bits per time slot = 3600 + 1200 = 4800 bits per time slot. Total available bits per time slot in this case is 4200x6=25200. Thus total data bits available = 20400 bits per time slot i.e. 20400 bits per 0.5 ms which results in through-put of 40.6 Mbps. It is to be noted that the above throughput calculation is a near estimate as the other control overheads such as synchronisation signal, Physical Broadcast Channel (PBCH) etc. Result in overhead ranging from 1% at 20 MHz to approximately 9% at 1.4 MHz. [22]

6.   RADIO COVERAGE AND LINK BUDGET

Radio link coverage in the cell site can approximately be modelled by the empirical and deterministic radio propagation models. These models tend to give a clearer picture on the macroscopic radio environment. The propagation models are equipped with the pre-defined set of constants and constraints for different topographies and landscapes. The models also take in to account for the geographical factors such as hills, terrain, lakes, streets, building heights etc. The most important factors that govern the propagation models are:

- Antenna heights (Transmitter and receiver antenna heights)
- Distance between transmitter and receiver
- Frequency of operation
- Transmitted power
- Receiver sensitivity

There are also the radio access technology specific parameters that play important role in coverage calculations. For example, a UMTS or CDMA based radio technology can have its coverage benefitted by the spreading factor. Limitations impeded by the system and the cell loading also affect the coverage.

These factors along with the others can be considered step by step during the path loss calculations to determine the cell coverage. Above all of the propagation models, probably the most famous one and most applicable one in the current measurement case are Free Space model and Okumura-Hata model which is explained below.

6.1.   Free space model

Free space model assumes that there exists a line of sight between the transmitter and receiver and that the radio environment in between is ideal. In such case, the path loss experienced by the radio signal with the distance is given by

$$Path\ Loss\ (dB) = 20log_{10}(d_{km}) + 20log_{10}(f_{MHz}) + 32.46 \qquad (6.1)$$

Where

d_{km} = distance between the transmitter and receiver in kilometres

f_{MHz}= frequency of operation in megahertz

The path loss calculated is in decibel (dB)

However, the free space model does not give the perfect picture of the radio environment. It is highly likely that the line of sight is not always maintained during the communication. There is always possibility of obstacles in the path. Also the multipath ef-

fect is not considered in the free space model. This makes the model practically unusable but provides the theoretical limits of the path loss.

6.2. Okumura-Hata model

It is one of the most popular radio propagation models. It is an empirical model and is based on the measurements carried out by Okumura in the Tokyo area. The measurements made were drafted in graphs and approximations were done by Hata to formulate the path loss expressions which we now refer to as Okumura-Hata model.

The model has validity constraints as below:

- Frequency range f between 150 MHz and 1500 MHz
- Transmitter Antenna Height h_B between 30 and 200 meters
- Receiver Antenna Height h_M between 1 and 10 meters
- Distance d between transmitter and receiver within 20 kilometres
- There are no major obstacles between the transmitter and receiver
- Terrain profiles do not change abruptly

The path loss in dB in this case is generally expressed as

$$PL = A + B log_{10}(d) + C \tag{6.2}$$

Where A and B are,

$$A = 69.55 + 26.16 log_{10}(f) - 13.82 log_{10}(h_B) - a(h_M) \tag{6.3}$$
$$B = 44.9 - 6.55 log_{10}(h_B) \tag{6.4}$$

The factors $a(h_M)$ and C are environment dependent factors.

For rural areas (focusing mainly on the measurement area within the scope of thesis)

$$a(h_M) = (1.1 log_{10}(f) - 0.7)h_M - (1.56 log_{10}(f_C) - 0.8) \tag{6.5}$$
$$C = -4.78[log_{10}(f)]^2 + 18.33 log_{10}(f) - 40.98 \tag{6.6}$$

As stated earlier, the model is valid only for the frequency range of 150-1500 MHz range. Current 2G/3G/4G technologies utilize spectrum in 1800 MHz range as well. The need to model this band has been catered by COST-231 – Hata model. The extension made to the existing model is applicable for 1500-2000 MHz and given as,

$$A = 46.3 + 33.9 log_{10}(f) - 13.82 log_{10}(h_B) - a(h_M) \tag{6.7}$$

The definitions for B, C and $a(h_M)$ are as previously defined. [27]

6.3. Link budget calculations

Link budget is an estimation of the path loss between the transmitter and receiver. In cellular network, link budget is calculated for both uplink and downlink paths. There are several parameters fed to the link budget which in return calculates maximum allowable path loss that exists in the link path. The calculated path loss can be used with the se-

lected propagation model such as Okumura-Hata model to find the cell coverage. It can then be used to compare coverage between different access technologies and frequencies theoretically. The link budgets in Appendix A and Appendix B conclude with the downlink maximum path losses for LTE and UMTS respectively.

6.3.1.   Cell edge SINR calculations

As mentioned earlier, the capacity and SINR are inter-related by the Shannon's formula.

$$C = B \times log_2(1 + SINR) \quad in\ bps \tag{6.8}$$

Where,
C = Capacity of the channel or throughput (bps)
B = Bandwidth of the channel (Hz)
$SINR$ = Signal to Interference-Noise Ratio (in linear scale)
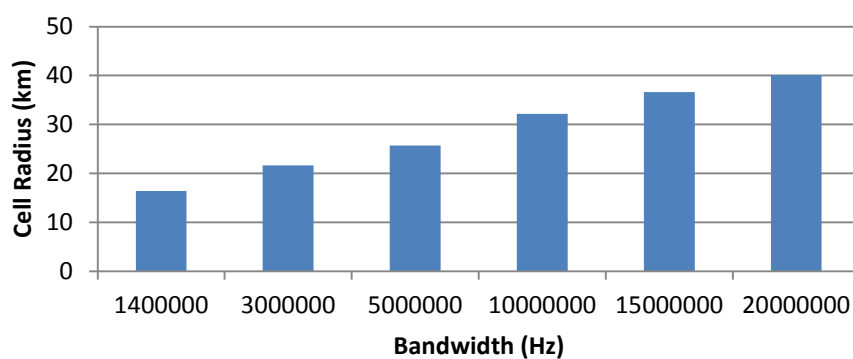
In a region with high $SINR$ which normally occurs near the cell center, the throughput is increased by virtue of MIMO (two fold for 2x2 MIMO and four fold for 4x4 MIMO). But at the cell edge, MIMO becomes ineffective for parallel streaming of data in multiple layers. With the vision of TeliaSonera Mobility and Planning team to provide the cell edge DL throughput of 1 Mbps minimum, required $SINR$ for 10 MHz bandwidth is calculated as,

$$SINR = 10 \times log_{10}\left(2^{\frac{C}{B}} - 1\right)\ in\ dB \tag{6.9}$$

For capacity C = 1 Mbps and bandwidth B= 10 MHz, the cell edge $SINR$ is calculated as -11.4 dB.

**Figure 6.1:** *Cell radii providing 1 Mbps DL throughput under different bandwidths*

Figure 6.1 shows the cell radii for 800 MHz under the assumption of providing throughput of 1 Mbps at the cell edge for different bandwidths. Cell edge SINR for different bandwidths can be calculated using Equation 6.9. The $SINR$ can now be used to calculate the receiver sensitivity where the receiver sensitivity is given as the sum of

Noise Figure (NF), thermal noise power and cell edge SINR. Sensitivity in turn affects path loss and cell radius can eventually be calculated using Okumura-Hata model.

6.4. Theoretical cell coverage calculations

Link budgets give a clear picture of the maximum allowable path losses that occur for the particular radio access technology. Appendix A shows the link budget for the LTE 800/1800. The cell radius for LTE 800 according to the link budget is around 28.9 km while that for LTE 1800 is around 12.3 km. The difference in the coverage radius from the link budget and the result shown in Figure 6.1 for 10 MHz bandwidth operating at 800 MHz band is due to the cell edge SINR calculation assumption. In the figure, the calculation is based on the cell edge throughput limitation while on link budget in Appendix A, the assumption is different. Link modulation of QPSK with coding rate of 0.1 has been taken into account in the link budget. This gives the useful bits per symbol with that particular modulation and coding rate. With this strategy, spectral efficiency for 10 MHz bandwidth is 0.168 bps/Hz and thus the cell edge SINR to be -9 dB using the Shannon's formula stated in Equation 6.9. The difference in SINR with two different assumptions is 2.3 dB and the resulting difference in cell radius calculation is 2.8 km. Similar difference exists in 1800 MHz band as well.

The coverage area for UMTS 900 as calculated from the link budget in Appendix B is 18.9 km. Obvious diminishing factor apart from the network parameters that differentiates two different coverage radiuses is the operating frequency band itself. With rest of the operating parameters maintained equal between the two bands and the allowable path loss in the downlink path is almost equal. A higher frequency signal fades out at much earlier distance from the cell center as the coverage distance of the signal is inversely proportional to the operating frequency.

This fact can also be drawn from free space propagation model which calculates the received signal power as

$$P_r = \frac{P_t G_t G_r \lambda^2}{(4\pi)^2 d^2 L} \tag{6.10}$$

Where P_r = received signal power

P_t = Transmitted power

G_t = Transmitter antenna gain

G_r = Receiver antenna gain

d = distance

L = System loss factor

λ = Wavelength of the transmitted signal

Thus, a signal with higher frequency has a low wavelength and thus gives a low received power P_r at the same distance d compared to lower frequency. A two ray ground reflection model considers both direct path and ground reflected path of the signal to the receiver. However, the ground reflection model does not give a better performance in

short range due to the oscillation caused by constructive and destructive interference of two rays. Before the cross over distance, the received signal power is defined by Equation 6.10. A cross-over distance d_c is given as

$$d_c = \frac{4\pi h_t h_r}{\lambda}$$

(6.11)
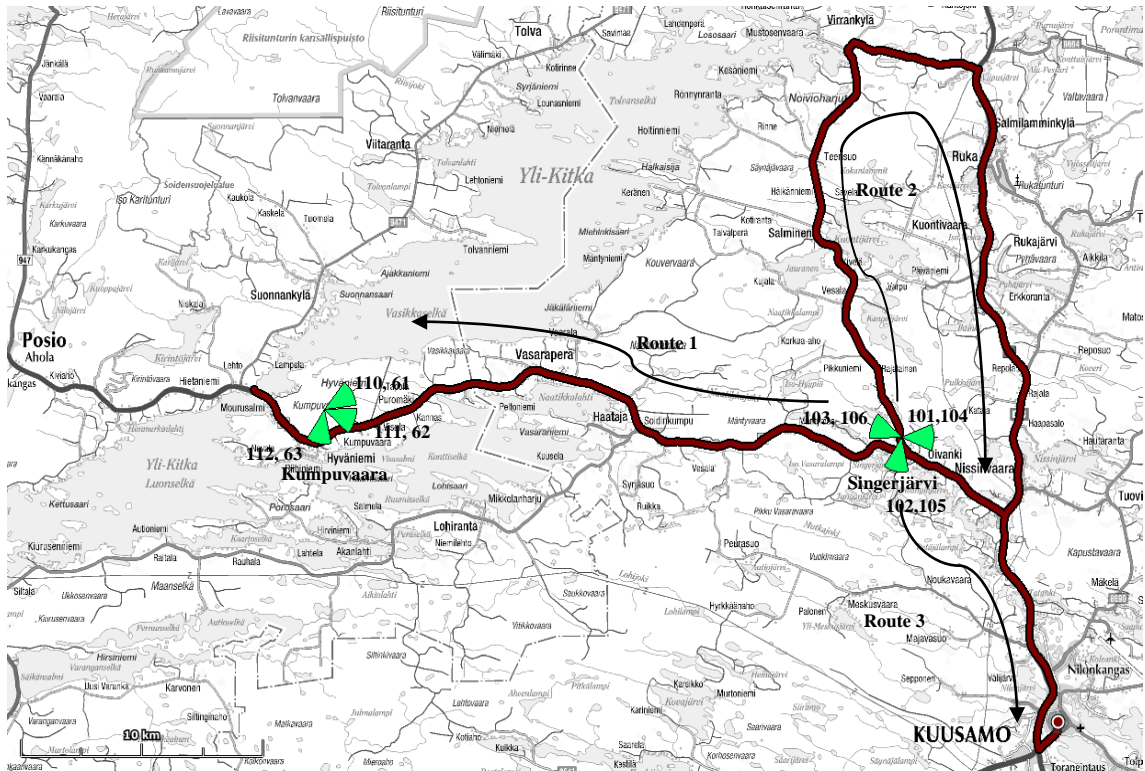
Beyond cross-over distance d_c, two-ray model overtakes and the received signal is given as

$$P_r = \frac{P_t G_t G_r h_t^2 h_r^2}{d^4 L}$$

(6.12)

The combination of free space and two ray ground reflection model provide a better modeling of the radio signal in free space rather than free space model alone. This combination still is not sufficient to describe the radio environment but suffice the fact that coverage radius or distance is inversely proportional to carrier frequency.

7. MEASUREMENTS AND ANALYSIS

The measurement area was near Kuusamo with the test sites located at Singerjärvi (66.069731°, 29.034217°) and Kumpuvaara (66.086234°, 28.481345°).

Figure 7.1: *Measurement route with the eNodeB sites*
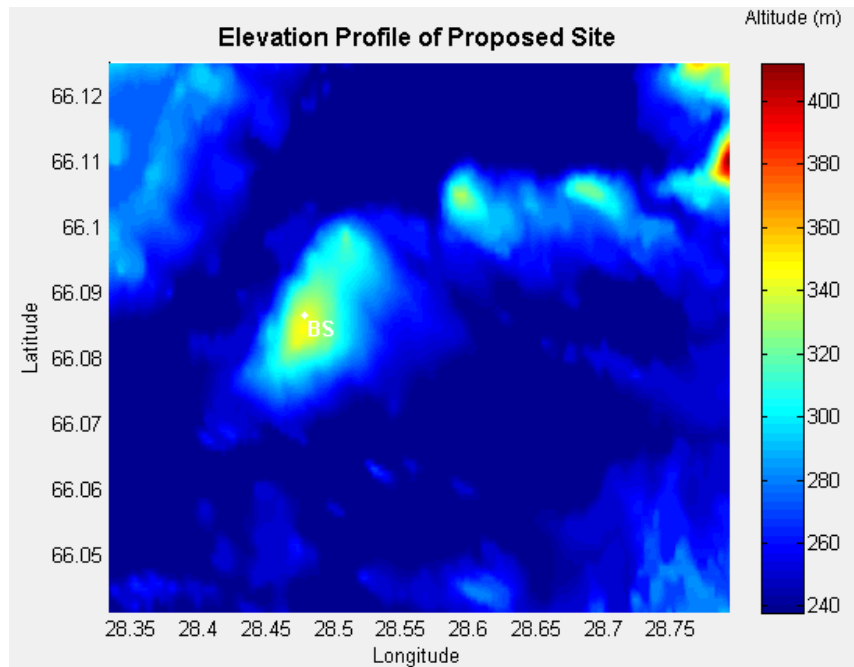
Figure 7.1 shows the measurement routes (marked in red) and the map of the measurement area. Both eNodeBs are marked in green with their cells and corresponding antenna orientations (clear from the antenna beam patterns). The measurements discussed here have been taken with the measurement vehicle at an average speed of 80 km/hr unless specified otherwise. The sites are separated by a distance of 25 km.

Table 7.1: *eNodeB site information*

Site name	RAT	Frequency	Cell ID	DL channel number
Kumpuvaara	LTE	800	110,111,112	6200
	UMTS	900	61,62,63,64	1322
Singerjärvi	LTE	800	101,102,103	6200
		1800	104,105,106	1275
	UMTS	900	11,12,13	1322

The eNodeBs have been chosen so as to provide a no interference scenario as well as to make sure that the cells are unloaded; also that the sites are equipped well to allow all of the features to be tested. $\pm 45^o$ cross polarized antennas have been used in all of the eNodeBs (in LTE) and NodeB (for UMTS). Other necessary parameters have been included in Appendix A and Appendix B. The test was conducted with *ZTE MF820T* USB modem (driver version 14.0.0.162 and *Qualcomm* handler), a category 3 device utilizing 10 MHz bandwidth. A GPS device was also used along with the modem to gather the co-ordinates of the measurement.

A real time outdoor radio environment measurement was carried out with the measurement software *Nemo Outdoor 6.0* from *Anite*. Measured files were imported and analysed with analysis software *Nemo Analyze 6.10.00* from *Anite*. Custom KPIs and user defined SQL queries were constructed in *Nemo Analyze* and third party ODBC SQL query tools. Most of the reports were built within Nemo Analyze; however few have also been analysed by exporting the data to *Matlab, gnuplot* and *MS-Excel*.

Figure 7.2: Elevation profile of the Kumpuvaara site area

Figure 7.2 shows the elevation profile of the measurement area. Elevation data for the area was extracted from NASA's SRTM3 database [28] and expanded in visual form by using Matlab. The resolution of data-grid is approximately 90 m (3 arc seconds). The data set was linearly interpolated to fill in the missing points in the display.

The measurement unit was placed inside a measurement vehicle. A 1 Gigabyte file located in the remote FTP server was to be downloaded using the USB modem while being attached with the test network. Radio parameters during this active connection when the file was being downloaded were measured and recorded by *Nemo Outdoor*. Measurement routes were chosen such that most of the peripheries for both sites were measured. The measurements were however constrained by the roads.
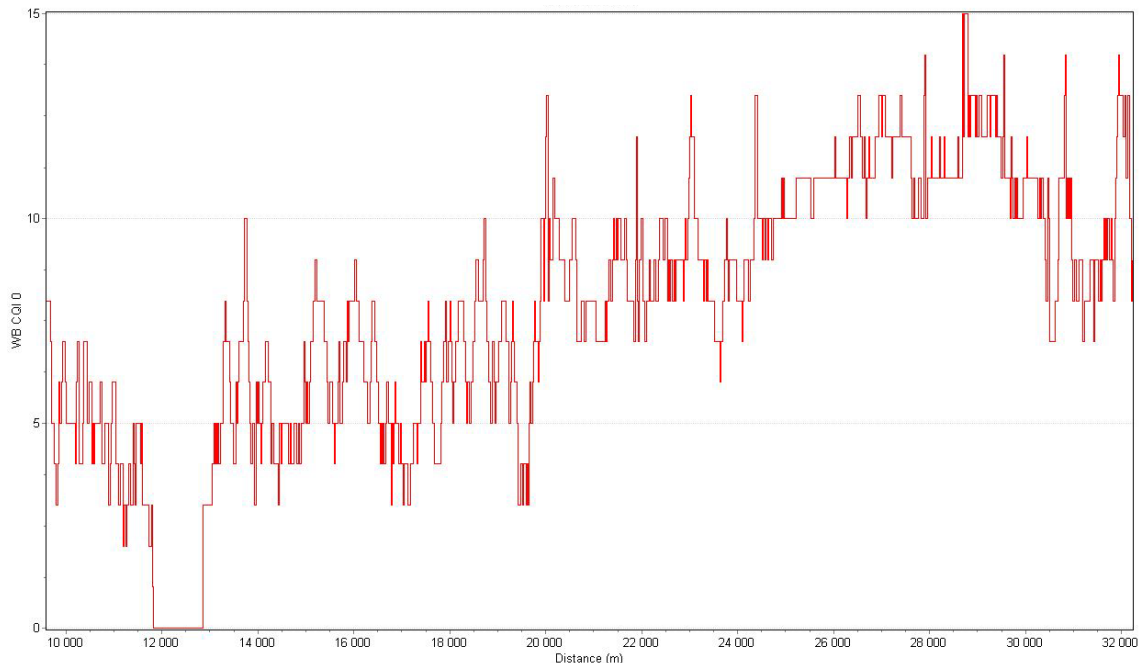
7.1. LTE 800 MHz coverage measurements

7.1.1. Measurement setup

The measurement setup for the LTE 800 coverage was to turn the LTE 1800 in the Singerjärvi site offline. This would mean that only LTE 800 and UMTS 900 would be online. The UE was locked to LTE so that no inter-RAT handovers was possible and the UE was attached to LTE 800 network all the time.

The measurements were taken with both of the sites turned ONLINE. However, when a particular cell or site is being referred in the analysis, the measurement data have been filtered out using custom SQL queries and KPI workbench from Nemo so as to provide only the information regarding particular cell or site.

7.1.2. CQI and link adaptation

Figure 7.3: CQI against Distance for Kumpuvaara site

Figure 7.3 depicts the channel condition along the measurement route. CQI ranges from 0 to 15. The CQI shown above is for codeword 0 i.e. the primary stream of MIMO. The measurement is taken as the UE moves from the cell edge towards the cell center. The trend of CQI can be seen to increase as the UE moves towards the cell center. The mean CQI is 8.23 and median at 8.

CQI can also be taken as a coverage performance indicator as it depicts the coverage condition of the radio environment of the band UE is attached with. CQI is reported as a measure of the channel quality in order to trigger the adaptive modulation. Wideband CQI can be reported for both of the MIMO streams separately.
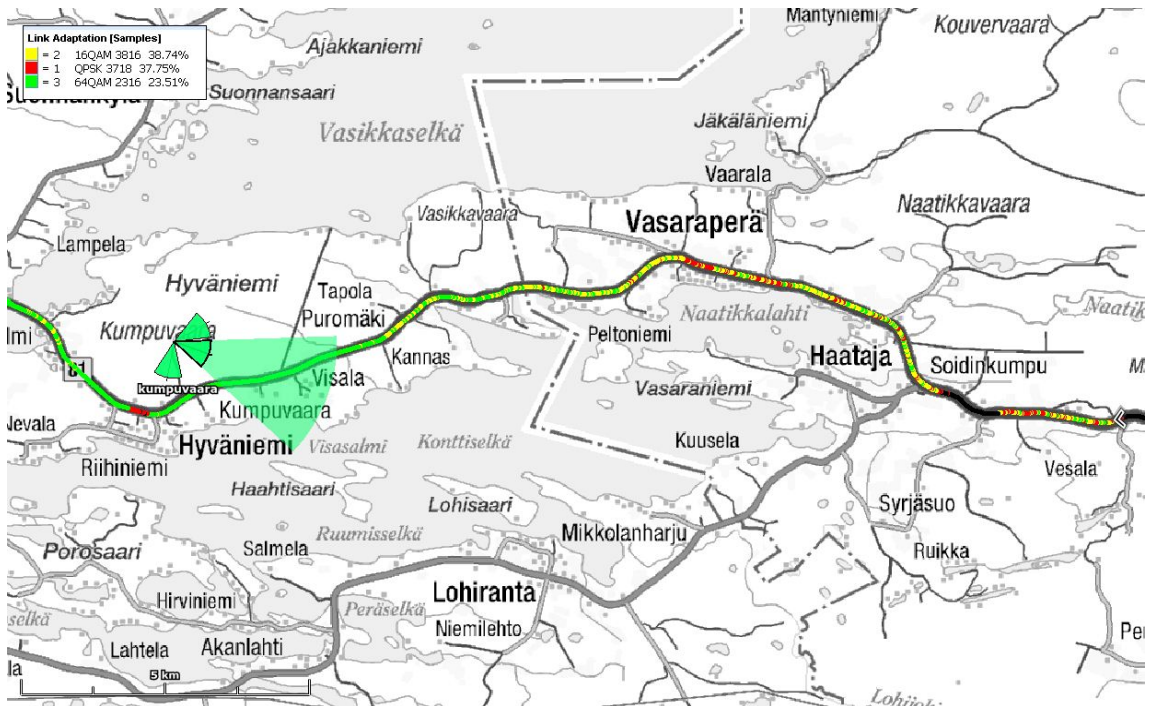
Channel condition of the measurement route made with CQI analysis can now be elaborated with analysis of link adaptation in the coverage area. It is clear with the adaptive

link modulation procedure that the mechanism works in closed loop with the CQI. As long as UE is attached with the serving cell and UE moving to bad radio condition, CQI gets worse. This in turn forces eNodeB to adapt the modulation to lower order.

Table 7.2: Average CQI for different sites at different routes

Site name	Route	Modulation	Average CQI
Singerjärvi LTE 800	Route 2	16 QAM	8
Singerjärvi LTE 800	Route 2	64 QAM	11
Singerjärvi LTE 800	Route 2	QPSK	4
Singerjärvi LTE 800	Route 3	16 QAM	7
Singerjärvi LTE 800	Route 3	64 QAM	11
Singerjärvi LTE 800	Route 3	QPSK	4
Kumpuvaara LTE 800	Route 1	16 QAM	8
Kumpuvaara LTE 800	Route 1	64 QAM	11
Kumpuvaara LTE 800	Route 1	QPSK	4
Singerjärvi LTE 800	Route 1	16 QAM	8
Singerjärvi LTE 800	Route 1	64 QAM	10
Singerjärvi LTE 800	Route 1	QPSK	4

Table 7.2 shows the average CQI experienced with different modulation schemes in different measurement routes and also with different sites. Overall, average CQI with QPSK is 4, with 16 QAM is 8 and with 64 QAM is 11.

Figure 7.4: Link modulation along the measurement route for Kumpuvaara site

Figure 7.4 shows the link adaptation pattern along the measurement route. The serving eNodeB in the above figure is Kumpuvaara. In this case, the UE is moving from the cell edge towards the cell centre. The figure utilises the link adaptation scheme for code-

word 0 in MIMO scenario. Similar analysis can be drawn for codeword 1. Kumpuvaara site has been taken primarily for analyzing purpose because of the reason that the route falls directly under the coverage of cell 111 unlike Singerjärvi site which has cell coverage mostly not falling under the measurement route.
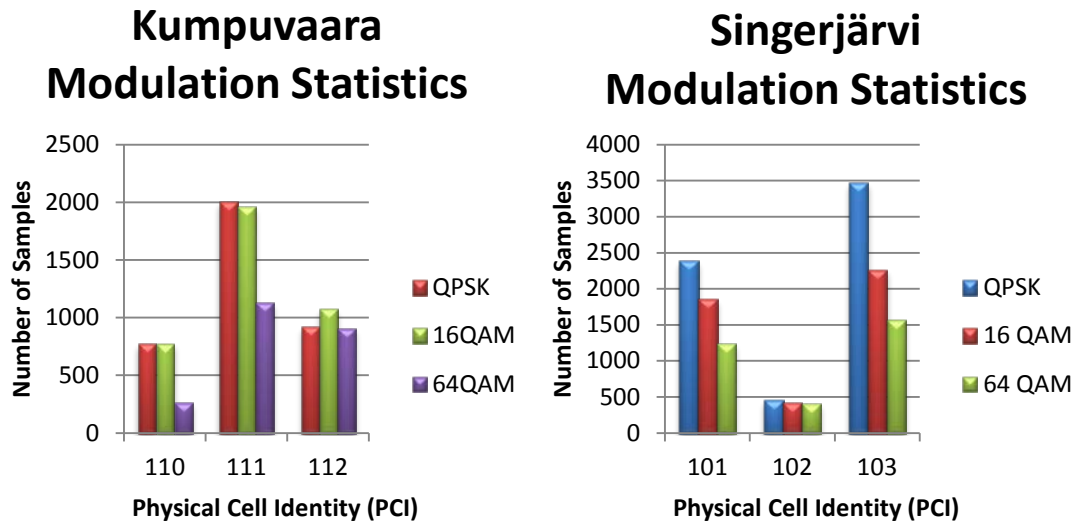
Table 7.3: Link modulation statistics for Kumpuvaara site

PCI	Maximum RSRP	Minimum RSRP	Codeword 0	Codeword 1	Count
110	-82.8	-135	QPSK		323
110	-82.8	-135	QPSK	QPSK	238
110	-82.8	-135	QPSK	16QAM	189
110	-86.1	-101.4	QPSK	64QAM	31
110	-82.8	-135	16QAM		286
110	-82.8	-102.9	16QAM	QPSK	188
110	-82.8	-102.9	16QAM	16QAM	233
110	-83.2	-101.4	16QAM	64QAM	67
110	-82.8	-111.6	64QAM		100
110	-83.7	-102.6	64QAM	QPSK	29
110	-82.8	-102.6	64QAM	16QAM	67
110	-82.8	-101.4	64QAM	64QAM	72
111	-70.1	-117.5	QPSK		1074
111	-68.8	-115.3	QPSK	QPSK	552
111	-70.1	-111.4	QPSK	16QAM	305
111	-71.7	-115.3	QPSK	64QAM	82
111	-70.1	-117.5	16QAM		866
111	-70.1	-112.8	16QAM	QPSK	355
111	-68.8	-111.4	16QAM	16QAM	470
111	-70.1	-112.4	16QAM	64QAM	275
111	-70.1	-114.6	64QAM		359
111	-71.7	-115.3	64QAM	QPSK	112
111	-70.1	-115.3	64QAM	16QAM	321
111	-68.8	-115.3	64QAM	64QAM	344
112	-66.9	-106	QPSK		288
112	-66.9	-106	QPSK	QPSK	374
112	-71.1	-104.1	QPSK	16QAM	194
112	-72.4	-102.8	QPSK	64QAM	68
112	-66.9	-106	16QAM		297
112	-67	-106	16QAM	QPSK	175
112	-66.9	-104.1	16QAM	16QAM	365
112	-66.9	-103.2	16QAM	64QAM	239
112	-66.9	-104.1	64QAM		261
112	-71.6	-104.1	64QAM	QPSK	74
112	-66.9	-103.2	64QAM	16QAM	268
112	-66.9	-103.2	64QAM	64QAM	309

Table 7.3 shows the detailed statistics on the distribution of different modulation schemes partitioned by the serving PCI of the Kumpuvaara site. Maximum and minimum RSRP shows the corresponding floor and ceil of the RSRP distribution for the

particular PCI with the particular combination of modulation in two MIMO layers. The null or blank values in modulation scheme of codeword 1 shows that the Physical Downlink Shared Channel (PDSCH) rank is 1 in that case. Finally the count gives the count of rows for the particular selection combination.

Figure 7.5: Kumpuvaara and Singerjärvi modulation schemes for different PCIs

Figure 7.5 shows distribution of modulation schemes over the coverage of different cells for both sites. In case of Kumpuvaara, the DL path has been associated with QPSK for 37.7% of all time and 38.7% with 16-QAM. For 23.5% of time, the DL modulation was 64-QAM. In case of Singerjärvi, the modulation was QPSK for 47.5% of time, 16-QAM for 30.9% of time and 21.4% for 64-QAM.
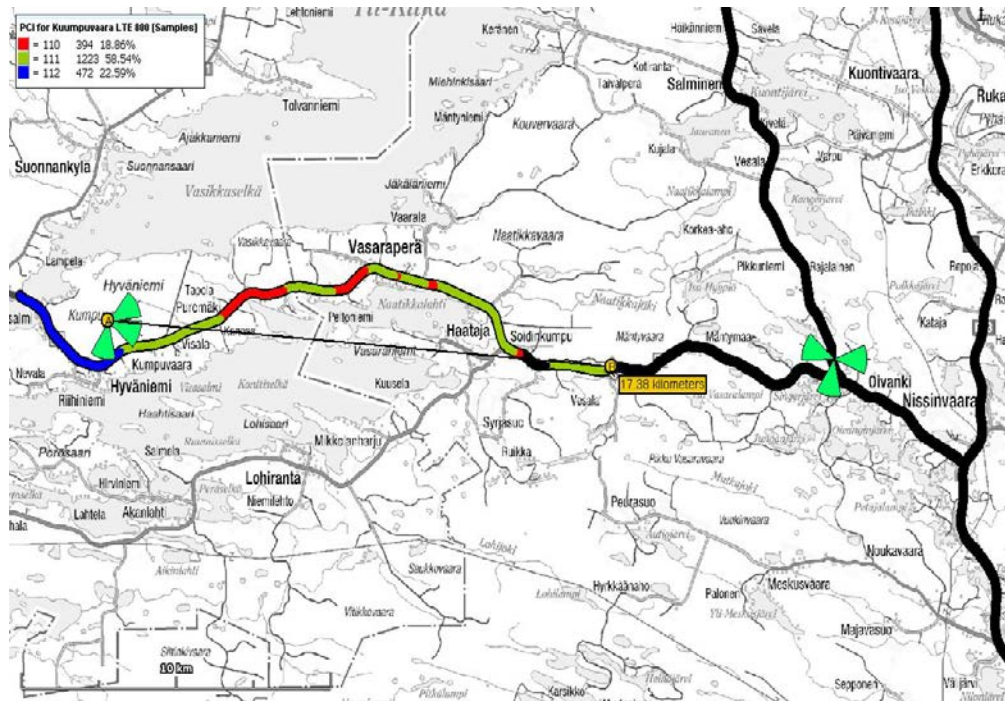
Being associated with QPSK would indicate worse CQI as explained earlier in Section 5.1. For the Kumpuvaara site, it indicates that the site had a poor coverage in terms of link modulation for 37% of time and best coverage for 23.5%. For the Singerjärvi site, the site had poorer coverage for 47.5% of time and best coverage for 21.4% of time.

Recollecting the facts from Figure 7.4, the worst RSRP observed for Kumpuvaara site with QPSK as the DL modulation scheme is -135 dBm and the best RSRP is at -66.9 dBm. Similarly, the worst RSRP observed for Kumpuvaara site with 64-QAM as the DL modulation is -111.6 dBm and the best RSRP being -66.9 dBm.

Link adaptation however may not give a clear picture of coverage area but indicates the channel quality in the coverage area. A point in the measurement route near to the site might have poorer CQI compared to a point farther to the site all depending upon the radio environment.
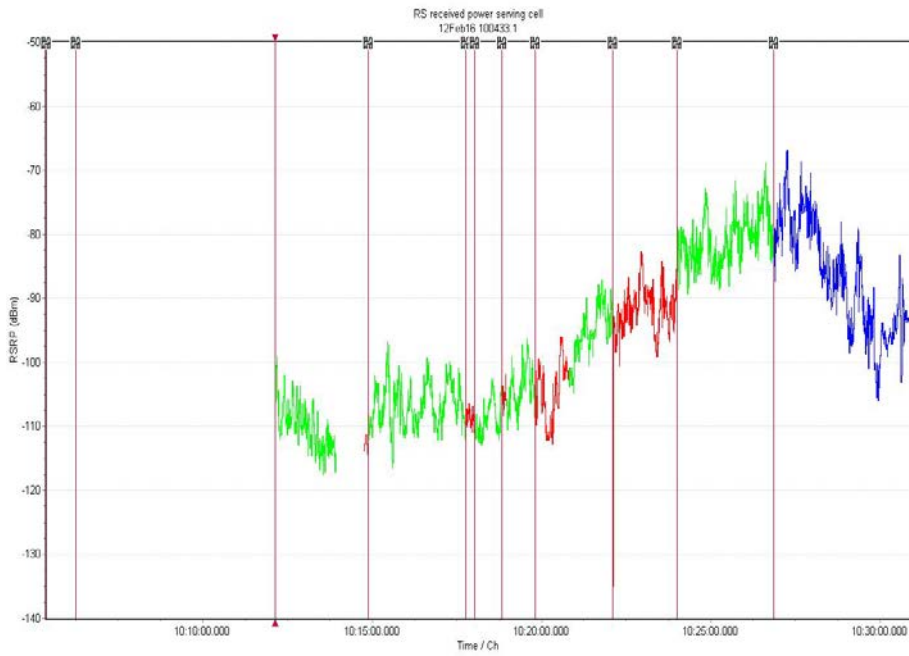
7.1.3. RSRP coverage analysis

7.1.3.1 PCI coverage

Figure 7.6: PCI coverage for Kumpuvaara site

Figure 7.6 shows the distribution of PCIs for the Kumpuvaara site in the measurement route. The measurement points have been filtered to display only the points where the Kumpuvaara site acts as the active/serving cell. PCIs associated with the two test sites are given in Table 7.1.


Figure 7.7: RSRP levels for different PCIs along the measurement route for Kumpuvaara site

Figure 7.7 shows the interpretation of Figure 7.6 on time scale. The eNodeBs have been marked and the PCIs have been color coded. The measurement has been taken from the cell edge towards the cell center (made clear by the rising trend of the serving cell RSRP level). Red, green and blue lines are associated with PCIs 110,111 and 112 respectively. The figure also clearly indicates the handovers between the cells; the transitions made clear by change in PCI as well as with the handover events marked. The blank spots in the timeline are the coverage area of Singerjärvi site. The antenna beam pattern for the site are shown matching to the actual antenna orientation.

Figure 7.6 shows that the measurement points are served mostly by cell 111. The measurement route itself mostly falls under the coverage area of cell 111. The cell edge can be described as the point where the UE last remains attached with the current serving cell. Cell 111 is last traced till the distance of 17.3 km from Kumpuvaara site. The cell edge value for the serving cell 111 is -106.2 dBm. Figure 7.7 shows that the there is a gap in the coverage indicating that Singerjärvi cell is intersecting Kumpuvaara cell.

The coverage of a cell is physically defined by the antenna orientation (the angle at which the cell antenna is fixed on the mast) and the transmit power. Other determining factors are the antenna beamwidth, side lobe levels etc. which are again associated with the transmitting antenna. As seen from Figure 7.6, the measurement route is mostly covered by cell 111. The measurement also verifies that 57% of the measurement events have been associated with cell 111, 20 % with cell 110 and 22% with cell 112.

7.1.3.2   RSRP analysis
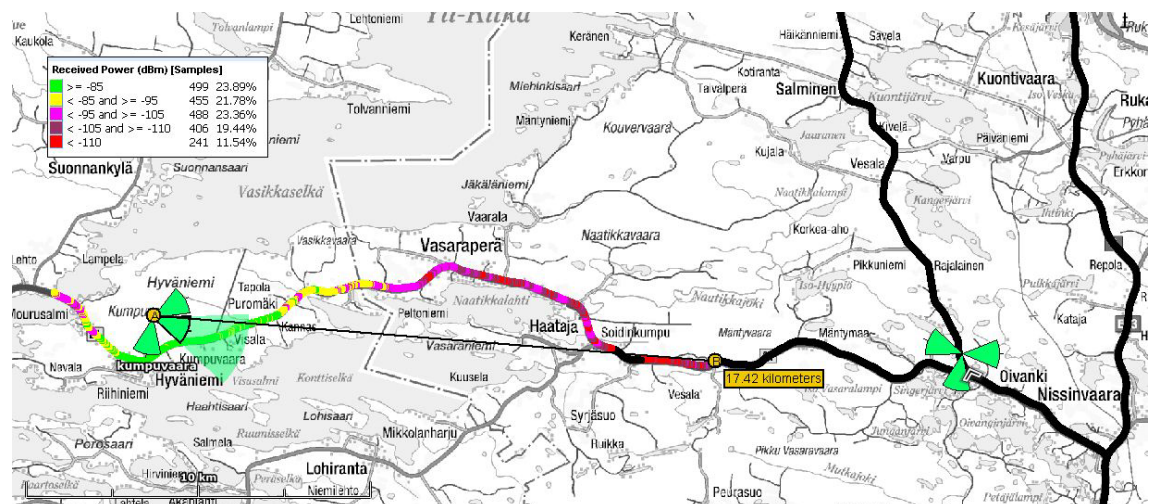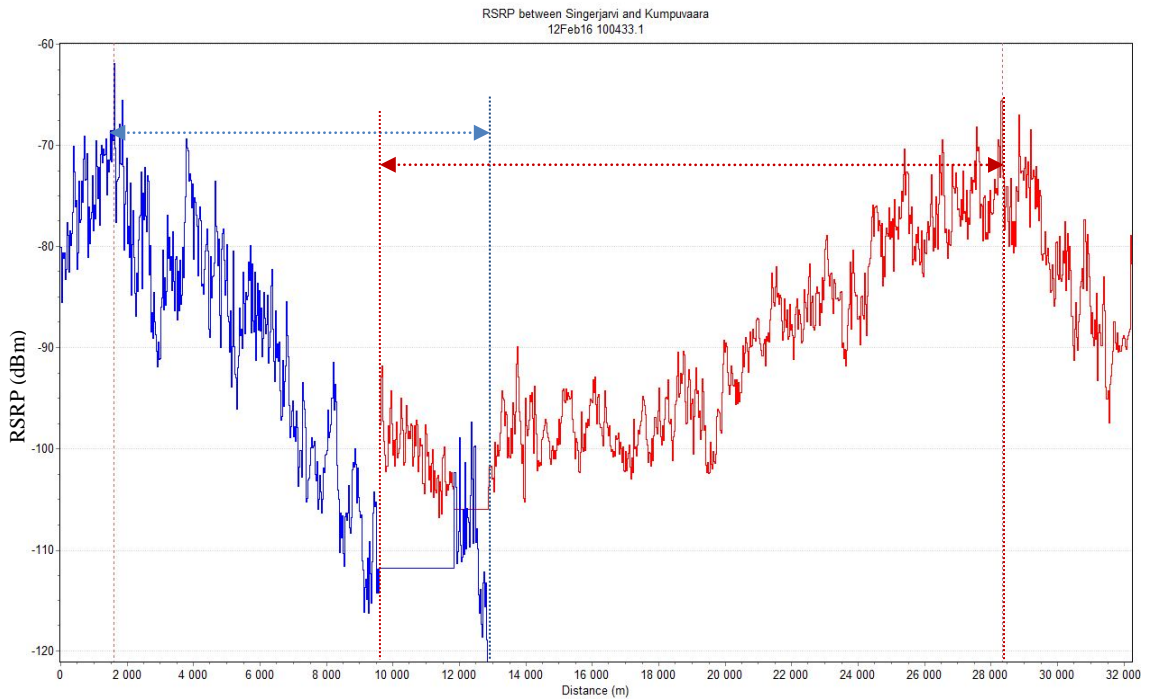
Figure 7.8: *RSRP coverage of Kumpuvaara site*

RSRP is one of the major coverage determination factors in LTE network. Figure 7.8 shows the plot of RSRP with Kumpuvaara site serving as active cell to the UE. The coverage level has been made clear by the color code with green color being the better RF condition (above -85 dBm) and the worst being the red color (below -110 dBm). The farthest point covered by the site towards Singerjärvi was at distance of 17.4 km.

Figure 7.9: RSRP between Singerjärvi and Kumpuvaara against distance
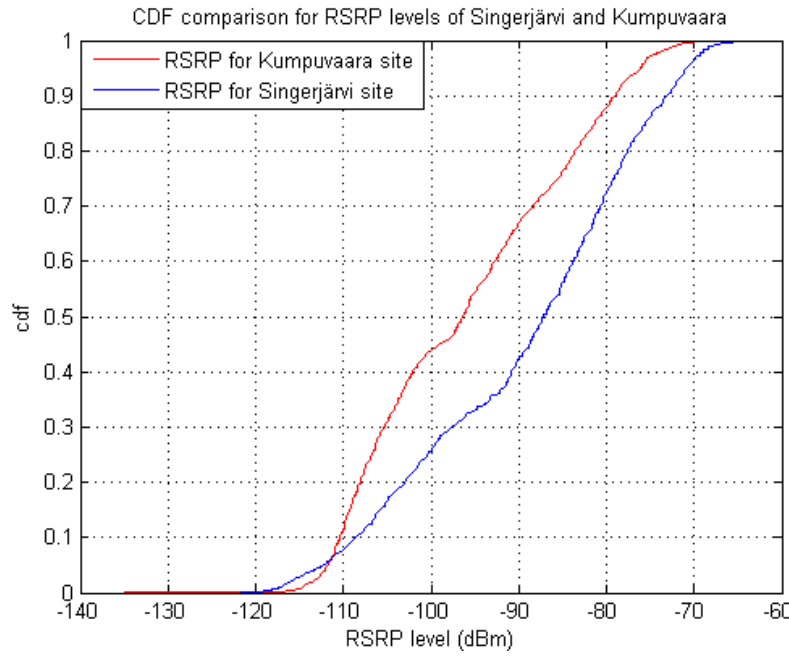
Figure 7.9 shows the RSRP pattern along the measurement route with values of both sites displayed. Blue colored value corresponds to Singerjärvi site and red colored value corresponds to Kumpuvaara site. The RSRP levels are plotted against distance. The obvious trend of received signal level to go down as UE moves towards the cell edge is clear from the figure. Distance is the parameter associated with the GPS data. Distance 0 m is the point where the measurement started for the particular measurement file.

Table 7.4: RSRP statistics between Singerjärvi and Kumpuvaara

Statistics on RSRP	Kumpuvaara Site	Singerjärvi Site
Minimum (dBm)	-135	-121.7
Maximum (dBm)	-66.9	-61.9
Mean (dBm)	-95.9	-89.4
Median (dBm)	-96.3	-87.1
Standard Deviation (dB)	11.8	13.1

Table 7.4 shows the brief statistical values for the RSRP measurements for both sites. Mean RSRP levels for both sites are well within acceptable limits. Peak RSRP is -61.9 dBm for Singerjärvi cell and -66.9 dBm for Kumpuvaara cell. Assuming the peak RSRP point to be the cell center (a near approximation of cell center rather than true cell center) and finding the difference with the distance of last observable value for the particular site gives the cell radius along the particular measurement route.

It is to be noted that cell center here means the point where the eNodeB is located. In this case with Figure 7.9 as reference, the cell radius for Singerjärvi cell along route 1 is approximately 11.3 km. Similar analysis for Kumpuvaara cell gives 18.8 km cell radius from the point of peak RSRP.

Figure 7.10: Comparison of Cumulative Distribution Function of RSRP levels

Figure 7.10 is a comparison of Cumulative Distribution Function (CDF) of RSRP levels of two different sites. It shows that the radio conditions are better for the Singerjärvi site throughout the time the site served the UE compared to that of Kumpuvaara site. Relating Table 7.4 with Figure 7.10, the median value of Kumpuvaara is 9.1 dB below to that of Singerjärvi. This value divides the sample distribution into half. This means half of the data for Kumpuvaara are below -96.3 dBm while only below -87.1 dBm for Singerjärvi site indicating better RF levels at Singerjärvi.

Table 7.5: Active set path loss calculations for LTE 800 cells on different routes

Route	Cells	Minimum RSRP (dBm)	Maximum Path Loss (dB)	Deviation (dB)	Radius (km)	Attenuation (dB/km)
1	110	-135	197.8	31.9	14.1	14
	111	*-117.5*	*180.3*	*14.4*	*17.3*	*10.3*
	112	-106	168.8	2.9	3.1	53
1	101	-85.5	148.3	– 17.5	1.7	85.2
	102	-86.9	149.7	– 16.1	0.8	170.1
	103	*-121.7*	*184.5*	*18.6*	*10.8*	*16.9*
2	101	-116.2	179	13.1	6.0	29.6
	102	-83.6	146.4	– 19.4	0.7	192.6
	103	*-114.9*	*177.7*	*11.8*	*12.0*	*14.7*
3	101	-118.3	181.1	15.2	12.7	14.2
	102	*-123.1*	*185.9*	*20*	*13.7*	*13.5*
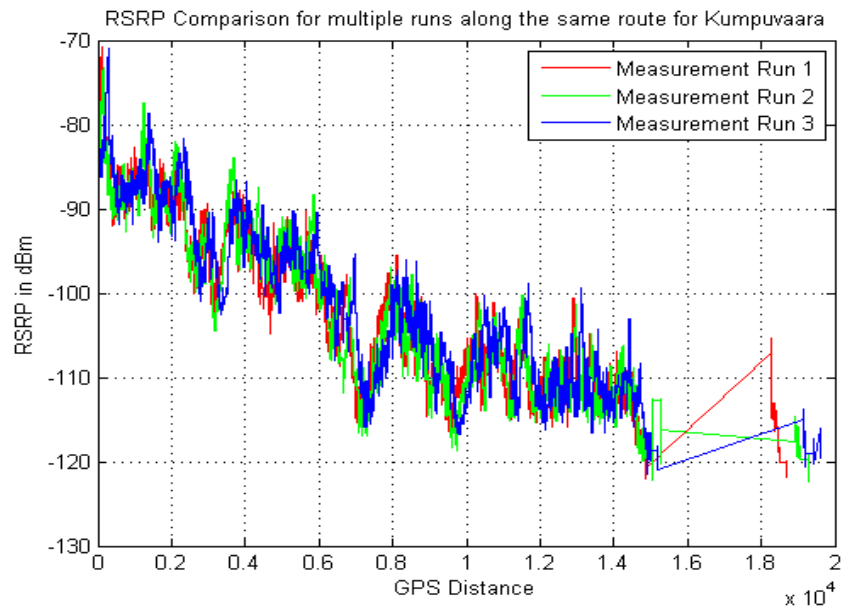
Table 7.5 shows the difference between the measured path loss and theoretical path loss as indicated in the link budget. Considering the EIRP to be 62.8 dBm and maximum

allowable path loss 165.9 dB for LTE 800 taken from Appendix A, the Maximum Path Loss is calculated as the difference of EIRP and Minimum RSRP. The deviation is calculated as the difference of the maximum Path Loss (path loss experienced in the measurement) with the Maximum allowable path loss from link budget. Average maximum path loss observed for all the six cells on different routes is 172.7 dB which is 6.8 dB above the estimated path loss. Radius column is the coverage radius for each routes and cells obtained from *Nemo Analyze*. Attenuation gives the ratio of path loss with respect to cell radius. The dominance area of the cell in a particular route can be decided as the cell with least attenuation slope. The rows of dominant cells in different routes have been italicized in the table for distinction.

One of the reasons for the difference between the calculated and measured path loss could be due to the gains resulted due to the MIMO schemes. Transmit/receive diversity gain in MIMO compared to SISO is about 6-7 dB as the transmit power is doubled by 3 dB due to the use of two Tx paths and the received power is doubled by 3 dB due to the two Rx paths. The diversity gain due to four signal paths adds up additional gain of 0-1 dB or higher depending upon how uncorrelated the signal paths are. [21]

7.1.3.3   RSRP analysis on multiple runs
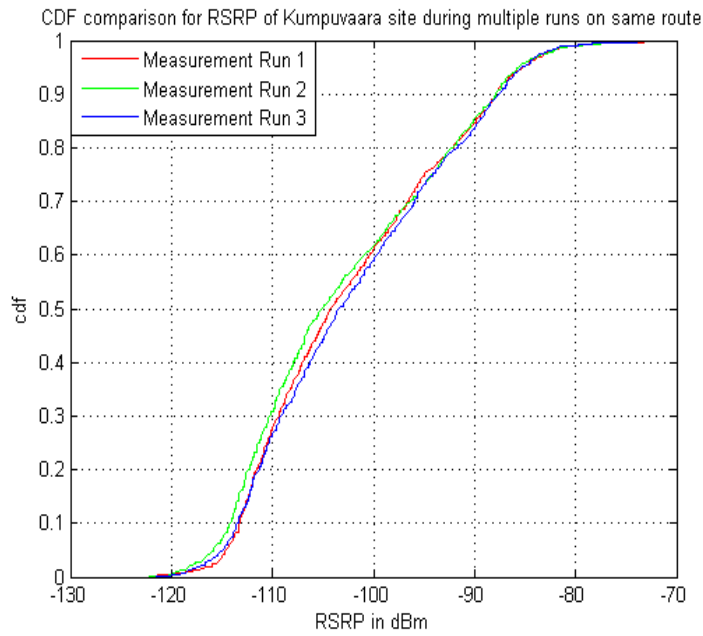
Multiple drive tests were conducted on the same measurement route with the similar measurement scenario. The direction of the measurement was from the cell center of Kumpuvaara site towards the cell edge. Three sets of measurements were taken under the identical measurement setup. LTE network on Singerjärvi site was turned OFFLINE to prevent inter-eNodeB handovers. With a fixed starting point, measurements were taken over and over till the cell edge was reached. The purpose of this measurement is to trace the reliability of the data during multiple tests.

Figure 7.11: Comparison of RSRP distribution for multiple runs of Kumpuvaara site

Three similar measurements were made along the route from Kumpuvaara towards Singerjärvi under the same condition indicated in Figure 7.11 as Measurement Run 1,

Measurement Run 2 and Measurement Run 3 respectively. The variance among the data as seen from the figure is minimal. Statistical differences among the different runs are clarified from the CDF plots. The figure above confirms the RSRP distribution result obtained for the route with the data almost overlapping one another. Mean RSRP (refer to Table 7.6) varies among the measurements by around 1 dB which can be judged nominal given the number of samples the statistics are based on. Cell edges for all three measurements falls at around 19.5 km with a deviation of around 1 km.

Figure 7.12: CDF plots for multiple runs of measurements along Kumpuvaara route

Table 7.6: RSRP statistics for multiple runs along the same route

RSRP statistics	Run 1	Run 2	Run 3
Min (dBm)	-122.1	-122.3	-121.5
Max (dBm)	-70.8	-73.3	-70.9
Mean (dBm)	-102.1	-102.7	-101.7
Median (dBm)	-104.2	-105.1	-103.4
Standard deviation (dB)	9.78	10.1	9.8
Cell edge (km)	18.8	19.8	19.74

Figure 7.12 is the CDF plot of RSRP distribution of all three measurements. The statistics confirm the results explained for Figure 7.11. All of the statistical parameters mentioned in Table 7.6 agree with conclusions drawn earlier. The measurements are statistically aligned indicating very small deviation from each other.
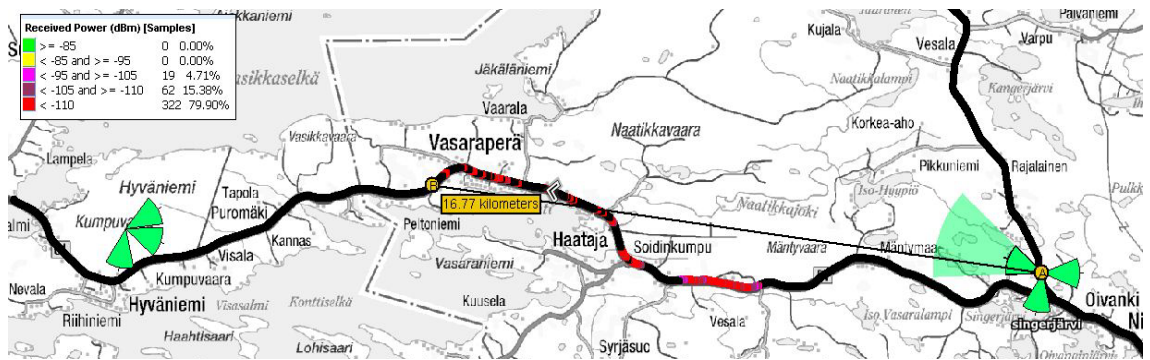
7.1.3.4   Detected set analysis

In this section, the coverage of both of the sites in terms of site's signal appearing in the detected set of UE is analyzed. A site may appear in the detected set range while the other site is serving. UE measures the neighboring cells of the cells have RSRP above a

pre-defined threshold limit during an active connection. This can also be taken as the coverage range of the site as the site can be detected by the UE.

Figure 7.13: Kumpuvaara cells appearing in detected set
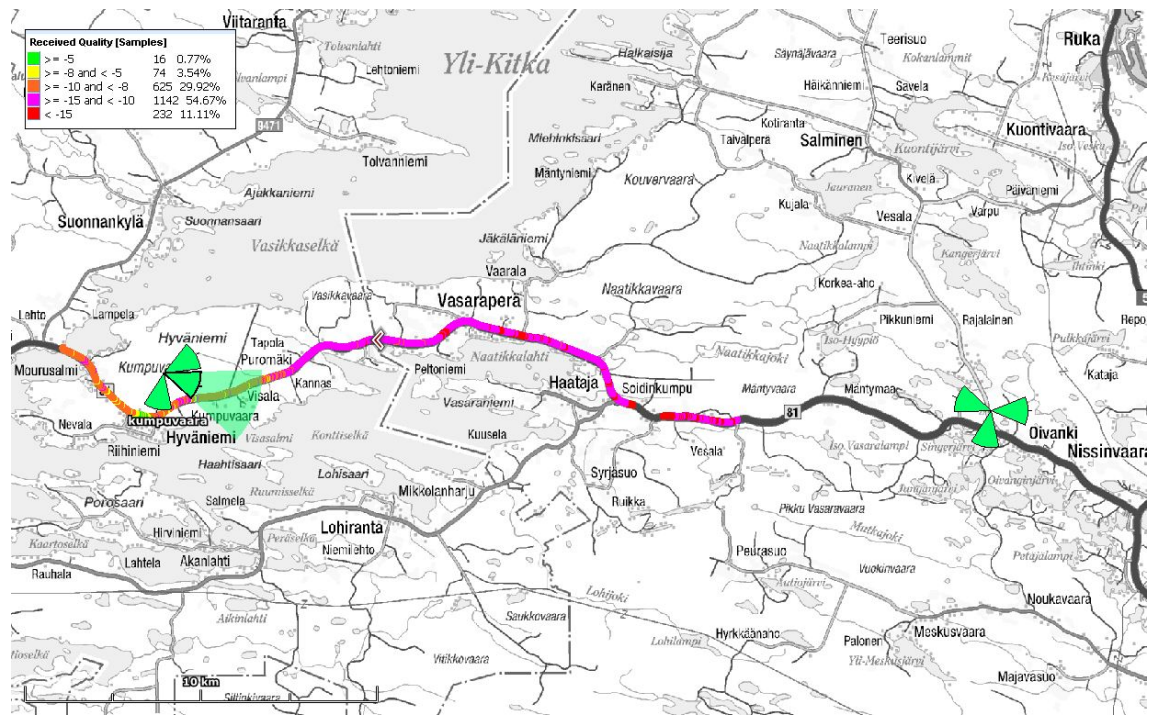
Figure 7.14: Singerjärvi cells appearing in detected set

A cell falling under detected set means that the serving cell is dominating the coverage. The measurement routes are taken such that they cover the vicinity of both of the sites. Figure 7.13 and Figure 7.14 show the appearance of the cells of Kumpuvaara site and Singerjärvi site in the detected cell list. The cell ranges for detected set are 30.2 km and 16.7 km respectively. RSRP in both cases is below -115 dBm.
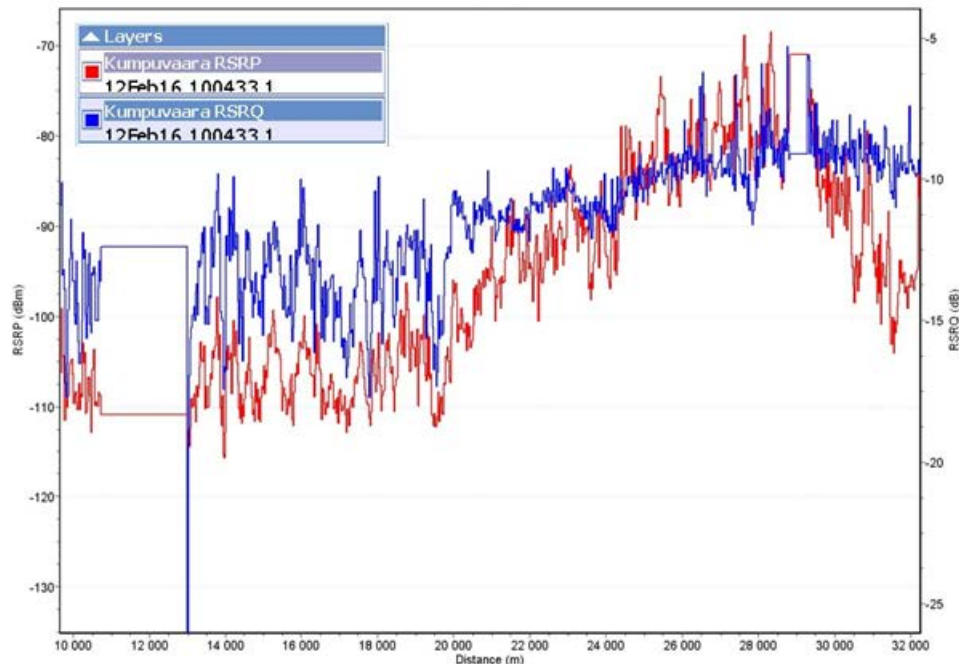
The case of Kumpuvaara cells is taken as suitable candidate to analyze the coverage as the measurement route is better covered by the site antennas. Comparing cell radius measured to the one calculated in the link budget in Appendix A, the cell radius differs approximately by 2 km.

7.1.4. RSRQ coverage analysis
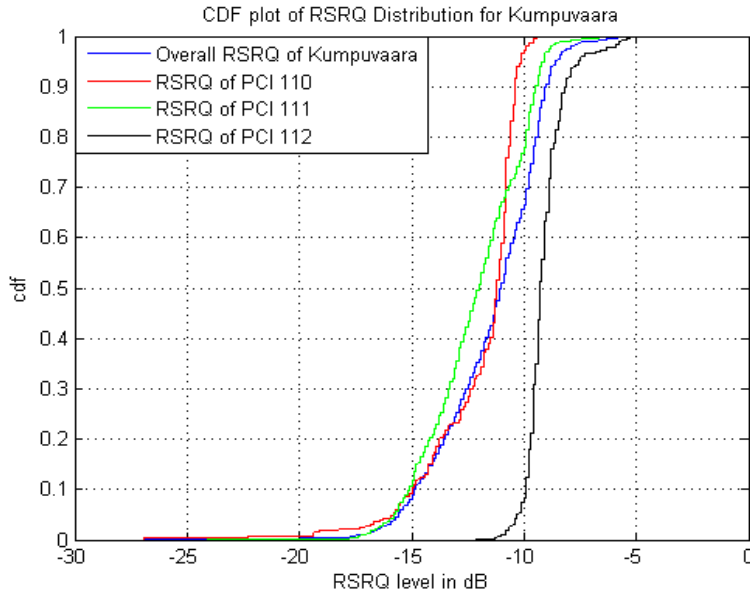
Figure 7.15: RSRQ levels for the Kumpuvaara site

Figure 7.15 shows the plot of RSRQ along the measurement route with Kumpuvaara site as serving cell. At the near proximity of the site, the RSRP is observed to be good. The value deteriorates as the UE is moved away from the center of the cell. For most of the coverage, the RSRQ value is less than -10 dB. RSRQ is mathematically associated with RSRP as seen from Equation 5.1. It follows the RSRP pattern which can be seen in Figure 7.16.

Figure 7.16: RSRP and RSRQ distribution against Distance for Kumpuvaara site

Figure 7.16 is the plot of RSRP and RSRQ levels when the UE was served from Kumpuvaara site, plotted against the distance. The UE moved from cell edge towards the cell center. RSRQ seems to follow the general trend of RSRP i.e. to increase as the UE moves towards the cell center. The gap seen at the beginning is because UE was attached with Singerjärvi site. The RSRQ at the cell edge was around -18 dB. Best RSRQ was observed to be at around -5 dB approx. near the cell center.

Figure 7.17: RSRQ distribution for different PCIs associated with Kumpuvaara site

Figure 7.17 shows the RSRQ distribution along the measurement route of Kumpuvaara site. The overall RSRQ has also been broken down into RSRQ levels of individual PCIs.

Table 7.7: CDF statistics for RSRQ of Kumpuvaara

RSRQ statistics	PCI 110	PCI 111	PCI 112
Minimum (dB)	-26.9	-24.1	-12.1
Maximum (dB)	-9.2	-6.2	-4.9
Mean (dB)	-12	-12.1	-9.1
Median (dB)	-11.2	-12	-9.3
Standard deviation (dB)	2.1	2.2	0.8
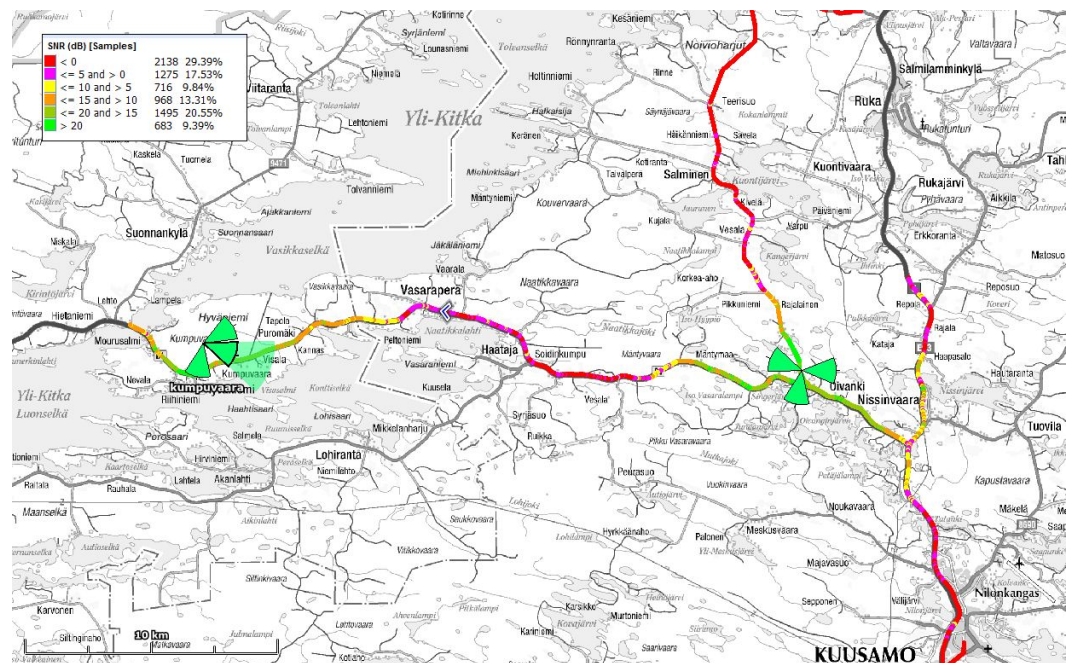
Table 7.7 shows the RSRQ statistics as per the CDF plots made in Figure 7.17. The figure and table collectively show the quality of received signal from the Kumpuvaara site throughout its coverage area. Statistically, PCI 112 is offering a better quality signal in its coverage area with a mean RSRQ of -9.1 dB while the worst has been seen with the PCI 110 with -12 dB mean RSRQ. PCI 111 offers a signal quality that is near to the overall RSRQ distribution observed in the coverage area for the Kumpuvaara site. The median for overall RSRQ distribution for Kumpuvaara is -11 dB.

The measure of RSRP gives the received signal level however the measure of RSRQ also takes into account for the interference in the operating band and noises apart from

the received signal. The RSRQ level indicates that the overall signal level during the coverage of the Kumpuvaara network has been average.
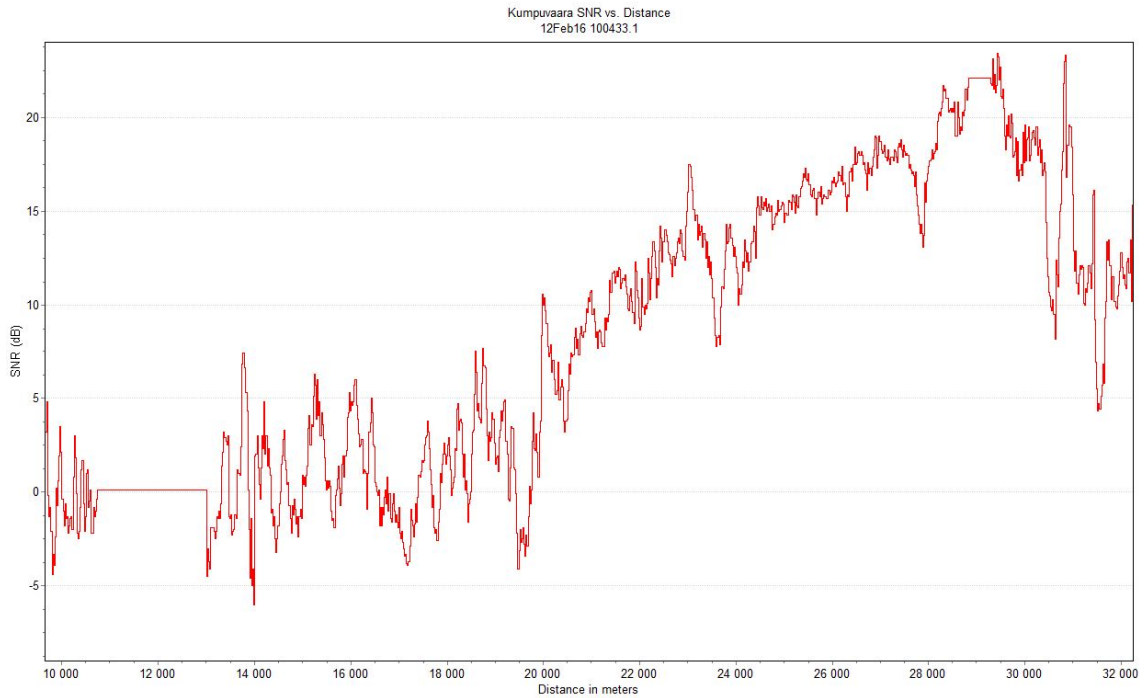
RSRQ is directly proportional to RSRP value but inversely proportional to RSSI level. RSRP is normally always less than RSSI. Hence, lesser the difference between RSRP and RSSI means lesser is the interference and ultimately resulting in better received signal quality. As the UE is farther from the cell center, received signal level goes down and the difference between RSRP and RSSI increases. It can also be considered that interference and noise start to take over to the received signal when the UE is farther from the cell. 50% of the measured data has RSRQ level below -11 dB. The interfering source was the Singerjärvi site in this case. The site antennas are not directed exactly in line with the measurement route as well. This in turn reduces the RSRP level and eventually the quality of the received signal is compromised.

7.1.5. SNR analysis
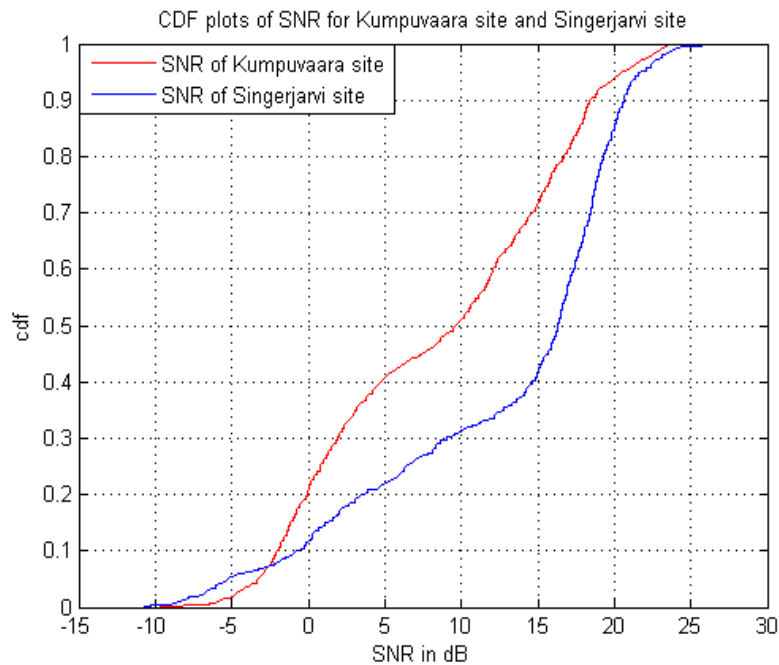
Figure 7.18: SNR plot for Singerjärvi and Kumpuvaara sites

Figure 7.18 depicts the SNR pattern with both of the sites online and measurements made throughout most of the possible coverage routes. The measurements have been done with completely unloaded network i.e. with just a single UE online and both sites considerably far apart. For a coverage limited environment as with the test network, the SINR can be approximated as SNR.

Figure 7.19: SNR vs. Distance for Kumpuvaara site

Figure 7.19 shows SNR distribution along the route of Kumpuvaara site. Please note that distance shown in the figure is the GPS distance as moving away from Singerjärvi towards Kumpuvaara site. SNR ranges from 24 dB to -10 dB approx. SNR follows the trend similar to that of RSRP (refer to Figure 7.9). SNR at the cell edge or the point after which the UE is handed over to Singerjärvi site is 3.2 dB.

Figure 7.20: CDF of SNR measured for Kumpuvaara and Singerjärvi sites

Table 7.8: *SNR statistics of Kumpuvaara and Singerjärvi sites*

SNR Statistics	Kumpuvaara site	Singerjärvi site
Minimum (dB)	-9.7	-10.7
Maximum (dB)	24	26.3
Mean (dB)	8.4	12.6
Median (dB)	9.7	16.3
Standard Deviation (dB)	8.1	8.5

Figure 7.20 and Table 7.8 show the SNR distribution for both of the test sites along the measurement route from Singerjärvi towards Kumpuvaara. The sites are dominant in different measurement routes. Referring to Figure 7.18 it is clear that signal from Kumpuvaara site prevails mostly in the route east from the site while Singerjärvi site is dominant in all three directions except west of the site.
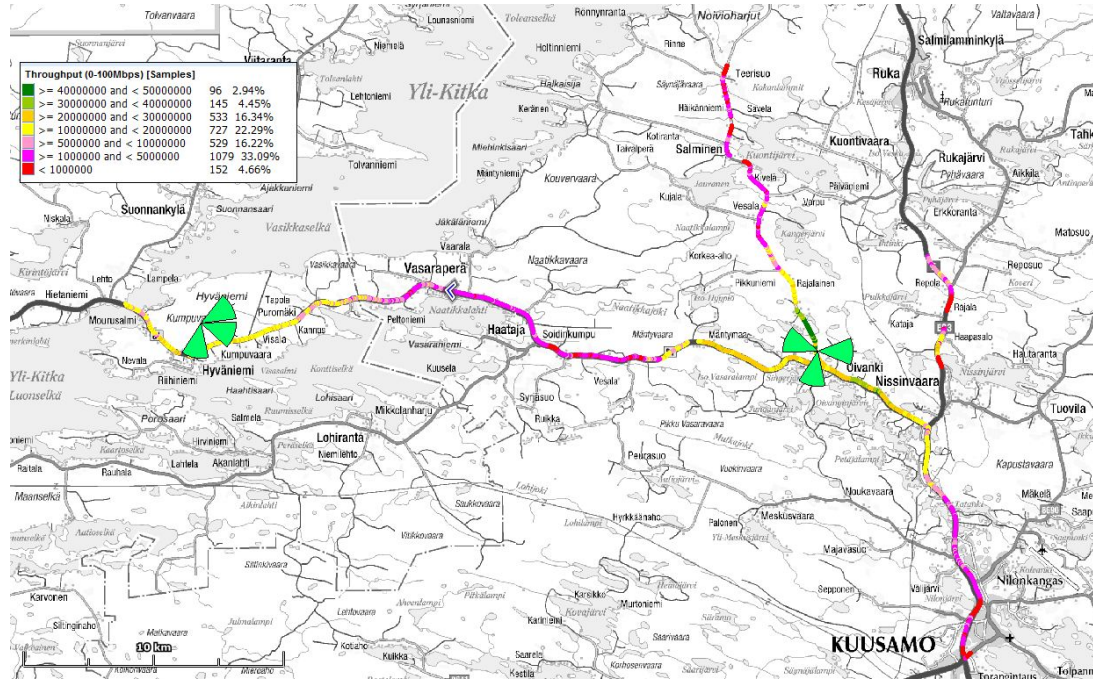
The maximum SNR observed for Kumpuvaara site was 24 dB while for Singerjärvi site was 26.3 dB. The mean SNR for Singerjärvi site is higher than Kumpuvaara site by around 4 dB. Half of measurement data for Singerjärvi has SNR above 16.3 dB while half of measurement data for Kumpuvaara has SNR above 9.7 dB. Standard deviation for both of the measurement cases is higher which indicates a big fluctuation in SNR.

High SNR for both sites was seen at the proximity of the sites which is an obvious case because the signal level near the site is high and dominates the noise and interference. Poor SNR was observed in places where the Line of Sight (LOS) was not possible with the serving site due to hills and forest. Singerjärvi has a mean SNR of 12.6 dB while Kumpuvaara has 8.4 dB which shows that Singerjärvi offers a better radio condition and signal level compared to Kumpuvaara. Interestingly however, the standard deviation for both sites is around 8 dB indicating a huge fluctuation in SNR. Figure 7.18 shows that there are regions of good SNR as well as the regions with poor SNR throughout the measurement route.

SINR or SNR (in present case) at the cell edge for RAT with frequency reuse factor N =1 is worse. Every cell acts as an interferer to the neighboring cells resulting in no dominant server condition mostly at the cell edge where composite signal level is high but SINR from any cell is poor due to the interference. Also in a vehicular environment, cell edge SINR can worsen due to handover dragging effect. When a UE moves across cell edge before handover completion, it is served by the original cell which has become second or third best serving cell. UE will still not be served by the best cell until the handover is successful. Handover trigger condition A3 (refer to Section 4.4) specifies that RSRP of new cell should be better than RSRP of serving cell with a hysteresis margin for a time period defined as time-to-trigger. Hence with the RSRP and time margins beyond the handover point, a UE could be served by a second best cell with poorer SINR. [29]
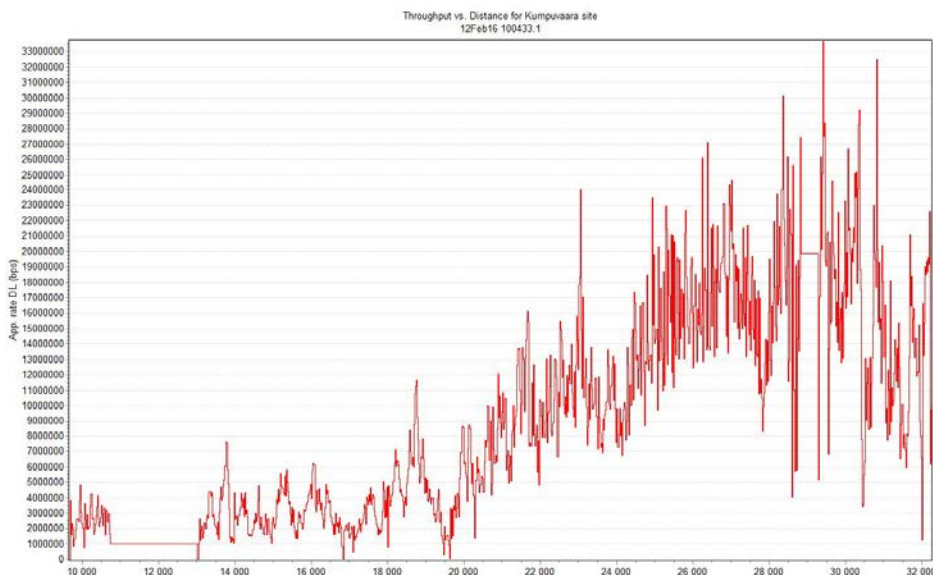
7.1.6. Downlink throughput analysis

Application downlink throughput is one of the most revealing parameters on characterizing the performance of a radio network.
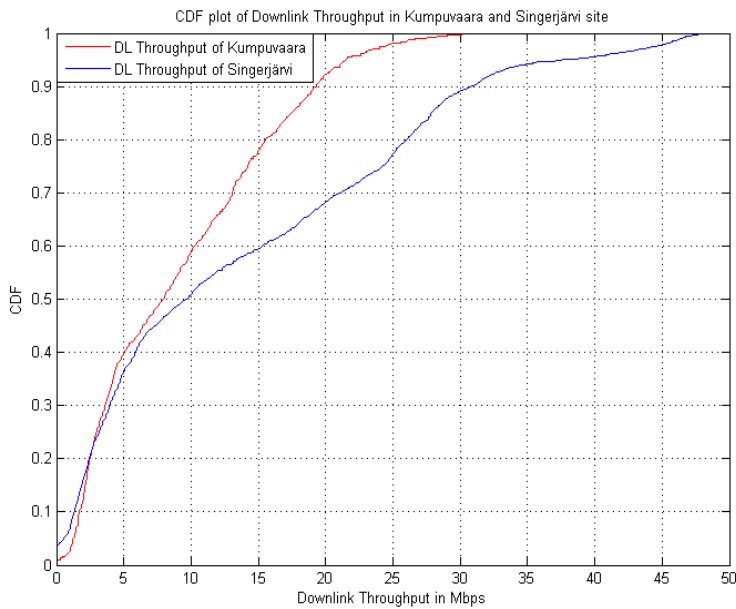
Figure 7.21: *Application downlink throughput for Kumpuvaara and Singerjärvi sites*

Figure 7.21 gives a general picture of application downlink throughput in the entire LTE coverage region. Contribution of both test sites Kumpuvaara and Singerjärvi have been considered above. A throughput of above 10 Mbps have been observed at a distance of 7.1 km for Singerjärvi site while similar range of throughput was observed up to a distance of 9.3 km for Kumpuvaara site. Throughput of 1 Mbps was observed up to a distance of 11.8 km for Singerjärvi site and at a distance of 17.3 km for Kumpuvaara site.

Figure 7.22: *Throughput vs. Distance for Kumpuvaara site*

Figure 7.22 is the measure of downlink throughput taken against the distance. Assuming the cell center to be at the point with the highest throughput, the figure confirms that cell radius is around 18 km. Throughput milestones discussed for Figure 7.21 can be verified in the plot.

***Figure 7.23:*** *CDF of Throughputs for Kumpuvaara and Singerjärvi*

Figure 7.23 shows the CDF plot of downlink application throughput for Kumpuvaara and Singerjärvi sites. It is the statistical measure for the same measurement plotted in Figure 7.22. Data extracted for the throughput measurements are for entire measurement routes. The maximum throughput seen for Kumpuvaara site was at 33.6 Mbps approximately and 48.8 Mbps approx. for Singerjärvi site.

50 % of the measurement data have throughput above 8 Mbps for Kumpuvaara site and above 9.6 Mbps for Singerjärvi site. Mean throughput for Kumpuvaara site was 9.2 Mbps while that for Singerjärvi was 13.8 Mbps. This implies that application level throughputs are in somewhat similar scenario for both sites in terms of median of data but Singerjärvi offers a better throughput on average compared to Kumpuvaara. The standard deviation for Kumpuvaara site was 6.9 Mbps while that for Singerjärvi was 12.3 Mbps. It suggests that the variation in throughput is greater for Singerjärvi and that the radio environment change drastically within the coverage area yielding large throughputs as well as very poor throughputs.

Figure 7.3 shows the CQI variation in measurement route. This CQI result when compared with Table 5.1 gives the corresponding link modulation. As we see the poor CQI at the cell edge, which in turn means a lower order modulation possibly QPSK with lower coding rate as well. Number of bits per symbol with QPSK is lower compared to 16 and 64-QAM. The spectral efficiency goes down and thus the downlink throughput towards the cell edge goes down. Similarly, higher order modulation such as 64-QAM with higher coding rate prevails near cell center and thus spectral efficiency goes higher and so does the downlink application throughput.
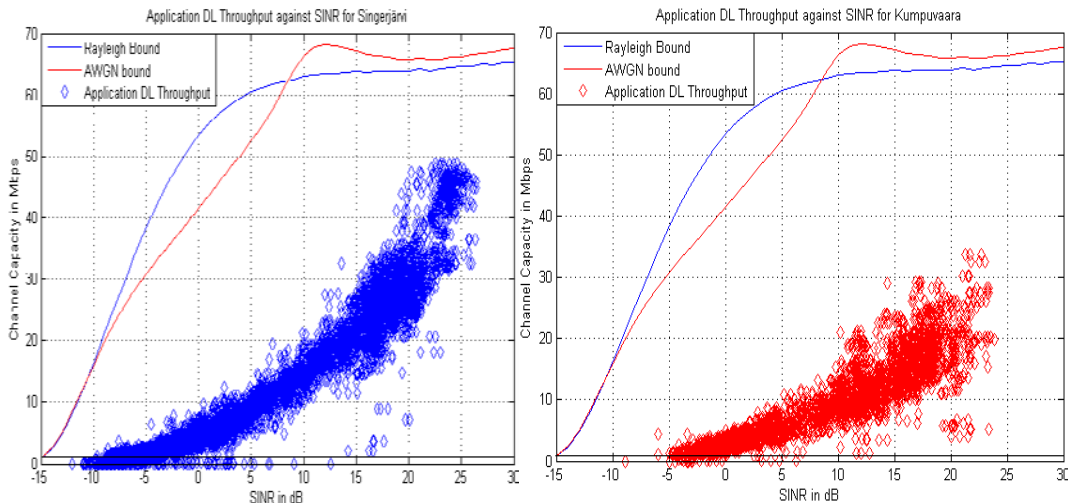
Figure 7.24: Singerjärvi and Kumpuvaara throughputs plotted against SNR

Figure 7.24 shows the smooth trend of throughput against SNR for both sites Singerjärvi and Kumpuvaara respectively for all the measurement routes. Singerjärvi site plot on the left has more data points in the figure as different routes were taken for the measurement. In comparison to it, the plot of Kumpuvaara is much sparse. However, both of the plots suggest that application throughput is directly proportional with SNR. Highest throughput seen for Singerjärvi site is about 48 Mbps at 22 dB SNR. The downlink throughputs obtained can be compared with the theoretical downlink throughputs listed in Table 5.2. The maximum theoretical downlink throughput for a 64-QAM modulation with 1/1 coding rate utilizing 2x2 MIMO stream is about 76 Mbps. It is much higher than the observed maximum downlink throughput of 48 Mbps as the path loss and BERs associated with the noisy channel has not been accounted for in Table 5.2.
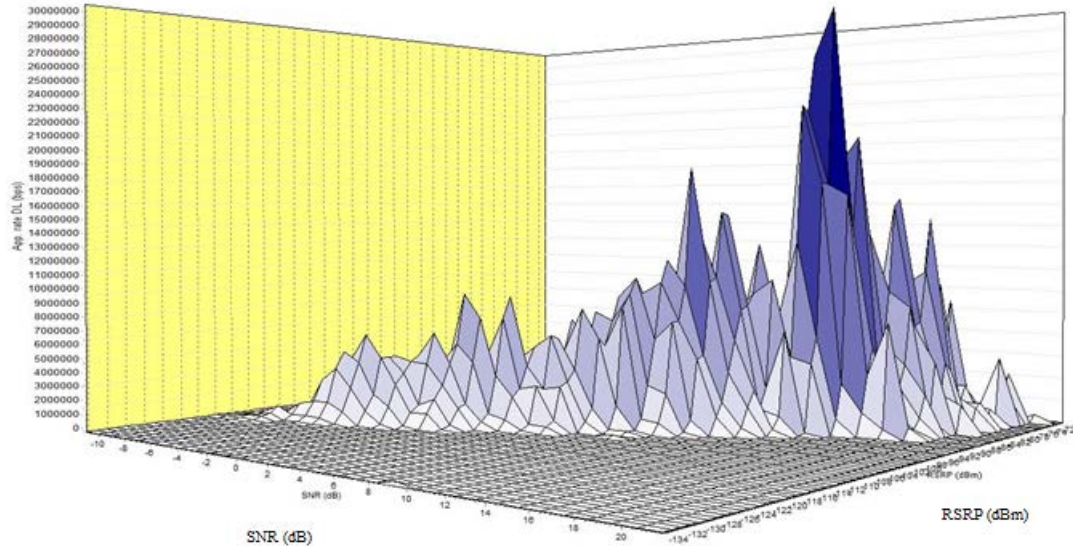
The threshold requirement of 1 Mbps at the cell edge for the operator has been marked in the both plots. 1 Mbps DL throughput requires a cell edge SINR of -11.4 dB marked by the vertical line for the Singerjärvi site while no such marks have been made in Kumpuvaara plot as all the SNR values are well within the cell edge limit.

For Singerjärvi site, 6.9% samples are above the SINR limit of -11.4 dB but throughput below 1 Mbps while similar statistics for Kumpuvaara site is at just 1.5%. This means the UE in the Singerjärvi site is served within the operator's requirement inside the site coverage for approximately 93% while UE in Kumpuvaara site coverage is served within the operator's requirement for approximately 98% of time. With SINR limitation of -11.4 dB at 1 Mbps throughput, the calculated cell radius (refer to Figure 6.1) with 10 MHz bandwidth operating at 800 MHz shows 32 km approx. while the observed cell radius with 1 Mbps limit is 19.8 km. for Kumpuvaara and 11.6 km for Singerjärvi.

The blue and red lines mark Shannon bounds for Rayleigh and AWGN channel models providing the theoretical throughput limit. The lines are based on Equation 5.8 with the multiplicative effect on throughputs due to the spatial multiplexing feature of MIMO. High throughput gain due to MIMO is due to the factors: rich scattering conditions within a cell and UE utilizing the advantage of multipath condition. These scenarios in

radio environment ensure that the each layer of spatial multiplexing under MIMO operation is orthogonal with each other. [30]

7.1.6.1   Throughput analysis on multiple runs

Figure 7.25: SNR, RSRP and downlink application throughput for Kumpuvaara site

Figure 7.25 shows the three dimensional relation between SNR, RSRP and application downlink throughput for the Kumpuvaara site. Multiple runs of data were taken on the Kumpuvaara route for the analysis. A region of low SNR also mostly has low RSRP and a low application throughput. Highest application throughput for the route is observed to be at around 30.4 Mbps with SNR of 18.8 dB approx. and RSRP of -88.9 dBm.

The results support the fact that application throughput in general trend tends to increase with the increment in RSRP and SNR. As the coverage of the radio network goes down due to the distance from the site or due to obstacles in the line of sight, SNR goes down and so does RSRP. These factors ultimately reduce the application throughput. As the UE closes in towards the site, SNR and RSRP go up that can be confirmed from Figure 7.9 and Figure 7.19, and so does the throughput.

7.2. LTE 1800 MHz measurements and comparison

LTE 1800 measurements were done with the Singerjärvi site as the test eNodeB. LTE 800 was shut down for both of the test sites Singerjärvi and Kumpuvaara.

7.2.1. CQI and link adaptation comparison
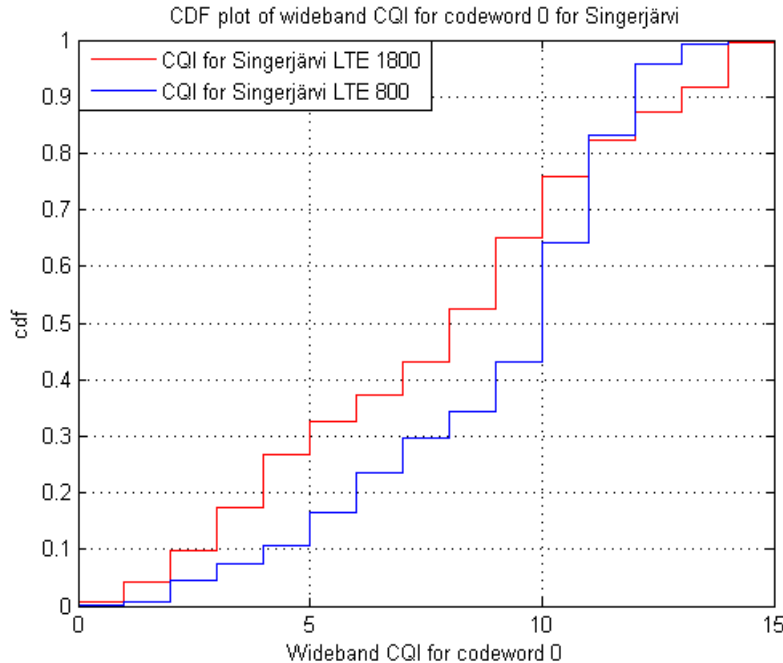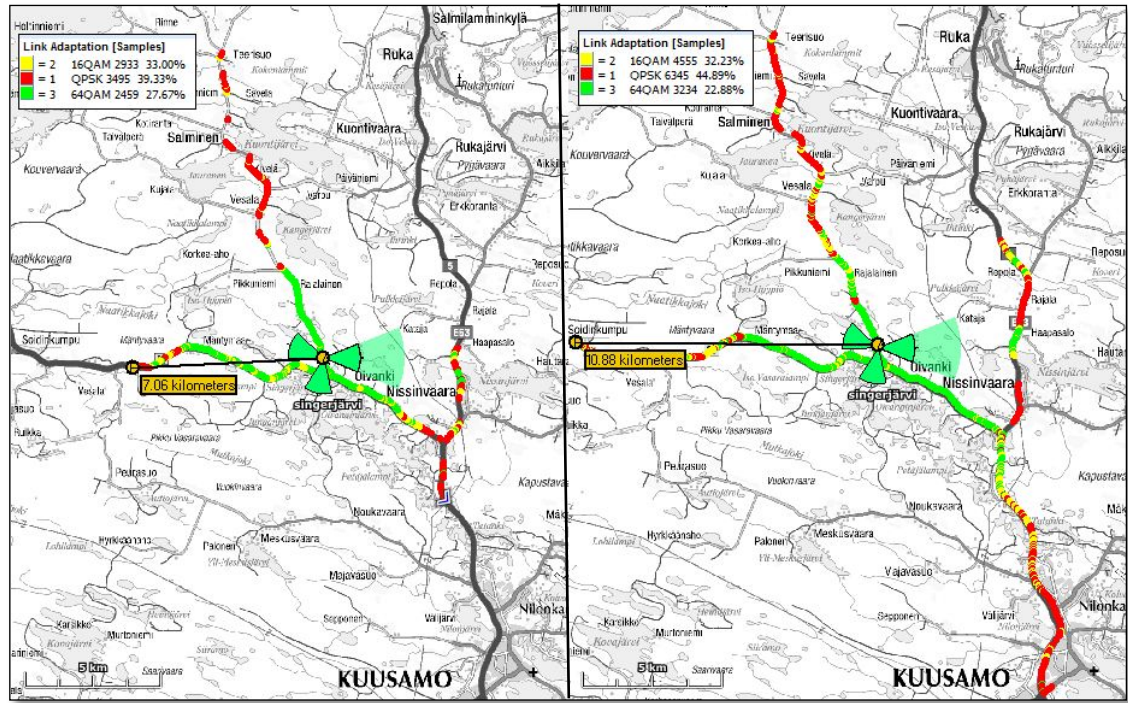
Figure 7.26: CDF plot of CQIs for LTE 1800 and LTE 800 of Singerjärvi

Table 7.9: CQI statistics for LTE 1800 and LTE 800 of Singerjärvi

Statistical Parameters	LTE 1800	LTE 800
Minimum CQI	0	0
Maximum CQI	15	15
Mean	7.7	8.8
Median	8	10
Standard Deviation	3.7	2.9

Figure 7.26 gives the CDF plot of the CQIs compared for the same measurement routes for LTE 1800 and LTE 800. Both CQIs are wideband CQI for codeword 0. The statistical parameters listed in Table 7.9 are the statistical measures drawn from the figure. Minimum CQI is 0 and maximum CQI is 15 for both cases. 50% of CQI samples are below 8 for LTE 1800 and below 10 for LTE 800. The deviation is higher for LTE 1800. CQI index values reported range from 1 to 15. CQI 0 indicates that the transport layer BLER exceeded 10% and the measurement point was out of range. [14]

CQI statistics indicate that LTE 800 has better channel condition than LTE 1800. The link budget in Appendix A shows that the coverage of LTE 1800 is weaker than that of LTE 800. Hence, the coverage of LTE 1800 deteriorates with a greater slope compared to LTE 800. A measurement point which has a better coverage with LTE 800 could be at a poorer coverage with LTE 1800. As UE moves away from the cell center, the difference in the channel condition between two bands becomes larger.

Figure 7.27: *Link adaptation comparison between LTE 1800 and LTE 800 in Singerjärvi*
Left: Link adaptation of LTE 1800 and Right: Link adaptation of LTE 800

The coverage area has been marked with the presence of the modulation schemes in the above figure. The modulation schemes marked in both cases above utilizes PDSCH modulation for codeword 0 as with the similar case analyzed in Section 7.1.2.

Figure 7.27 shows the comparison of link adaptation between LTE 800 and LTE 1800 with the measurements carried out in the same route. The number of samples in the LTE 1800 is lesser than that of LTE 800 as the coverage of LTE 1800 is weaker.

Performance wise, QPSK has highest percentage in both cases with 39.33% availability in LTE 1800 and 44.89% in LTE 800. 64-QAM served the area for 27.6% of samples for LTE 1800 while 22.8% for LTE 800. Distance of cell edge towards Kumpuvaara for LTE 1800 is about 7 km while that for LTE 800 is about 11 km. The route north of Singerjärvi is sparsely served by QPSK modulation of LTE 1800 while the service of LTE 800 is, moreover continuous till the cell edge. Service of the LTE 1800 site towards Kuusamo is also confined to 6.7 km while that for LTE 800 is 13.9 km.

The result indicates that QPSK is the most dominant modulation in the coverage of both bands. It also suggests a poorer radio condition for LTE 800 compared to LTE 1800 but this is due to the fact that coverage of LTE 1800 itself is limited as seen from Figure 7.27. Thus number of samples collected for the downlink link adaptation is 10887 for LTE 1800 while that for LTE 800 is 14134. The measurement routes not covered by LTE 1800 are covered by LTE 800 but with poor radio condition as the cells are not aligned with the measurement routes.

7.2.2. RSRP comparison
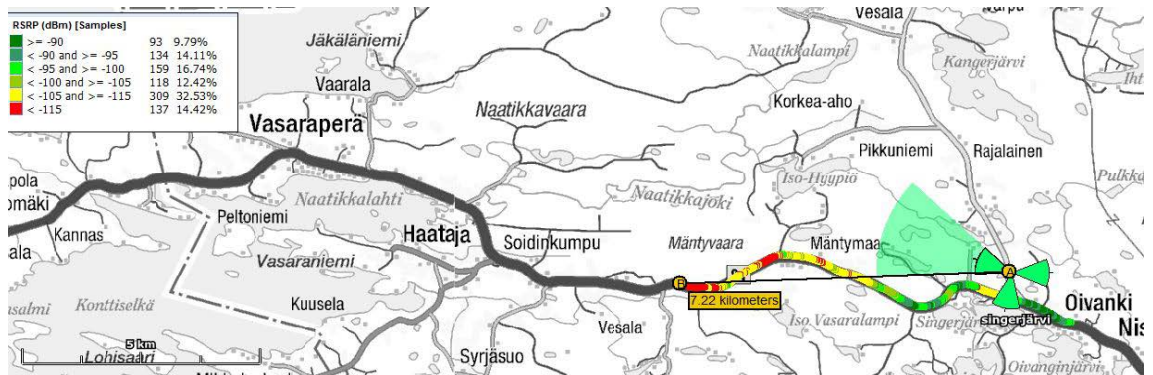
Figure 7.28: *RSRP of Singerjärvi LTE 1800 on the measurement route towards Kumpuvaara*

Figure 7.29: *RSRP of Singerjärvi LTE 800 on the measurement route towards Kumpuvaara*

Figure 7.28 and Figure 7.29 show the RSRP levels in the measurement area. The measurement route is the road between Singerjärvi and Kumpuvaara. The coverage area in the measurement route is 7.2 km for LTE 1800 and 16.7 km for LTE 800. The coverage radius for LTE 800 shown in Figure 7.29 includes both active set and detected set samples (refer to Section 7.1.3.4 for more on detected set). Detected set analysis was not needed in case of LTE 1800 as it was the only site during the measurement.
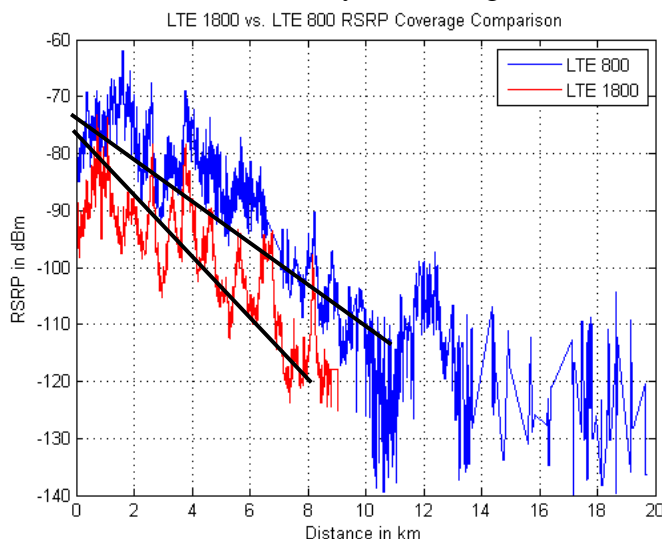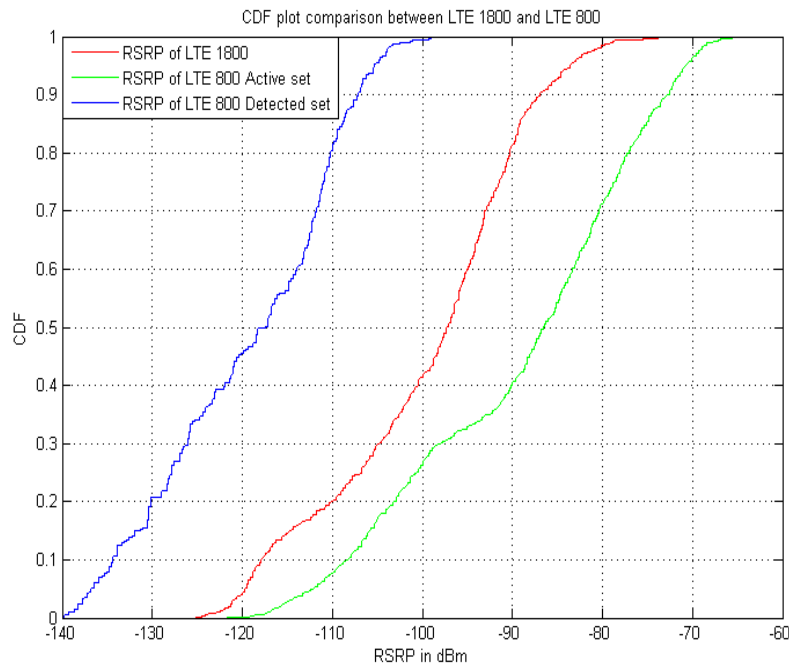
Figure 7.30: *RSRP comparison between LTE 1800 and LTE 800*

Figure 7.30 is the graphical representation of measurement result presented in Figure 7.28 and Figure 7.29. RSRP level plotted against the distance gives a measure of coverage. RSRP measure for LTE 800 includes the active set and detected set measurements combined together. Considering the combination of free-space loss and two-ray model as the basic path loss model, theoretical frequency dependent nature observed of the measured RSRP can be explained as in Section 6.4.

As the combined model depicts, free space loss is frequency dependent till the cross-over point. Using the same principle, the signal theoretically attenuates at 7.8 dB/km for 800 MHz band and approximately 8.5 dB/km for 1800 MHz band. But from the figure, the slope attenuates roughly at 3.7 dB/km for 800 MHz band and 5.3 dB/km for 1800 MHz band. Calculated path loss slopes of the measured data (for individual active sites) have been elaborated in Table 7.5 for 800 MHz band and Table 7.11 for 1800 MHz band. Assuming the peak value of RSRP as the cell center, the cell edge beyond which the coverage does not exist is around 7 km for LTE 1800 while the radius for LTE 800 beyond which the cell does not support either in active set or in detected set is around 17 km.

Figure 7.31: CDF plots of RSRP level of LTE 1800 and LTE 800

Table 7.10: RSRP statistics for LTE 1800 and LTE 800 for Singerjärvi

Statistical Parameters	LTE 1800	LTE 800 (Active set)	LTE 800 (Detected set)
Minimum RSRP (dBm)	-125.2	-121.7	-139.8
Maximum RSRP (dBm)	-73	-61.9	-99
Mean RSRP (dBm)	-99.6	-89.1	-119.4
Median (dBm)	-97.2	-86.5	-117.4
Standard Deviation (dB)	11.1	13.2	10.1

Figure 7.31 is the CDF plot of the measurement results obtained for LTE 1800 and LTE 800 taken along the measurement route specified in Figure 7.28 and Figure 7.29. CDF for active set and detected set have been separately analyzed. Maximum RSRP for LTE 1800 is considerably lower than LTE 800 differing by almost 9 dB. Mean RSRP seen for LTE 1800 is less than that of LTE 800 by around 9 dB. Mean RSRP for LTE 800 under detected set is -119.4 dBm. 50% of the measurement samples for LTE 1800 have RSRP level below -97.2 dBm while the same for LTE 800 is below -86.5 dBm. Similar figure for LTE 800 under detected set is -117.4 dBm. Standard deviation for LTE 800 is highest among the three sets of data while that of LTE 800 under detected set is the lowest.

The minimum RSRP observed for LTE 1800 was at the distance of 7.2 km from the cell center (practically can be referred as cell edge) while the minimum RSRP of -121.7 dBm for the LTE 800 active set was observed at a radius of above 10 km and minimum RSRP of 139.8 dBm for LTE 800 in detected set range was observed at a distance of 17 km approx.. This comparison shows that RSRP levels are better off with LTE 800 compared to LTE 1800. The statement is also confirmed by the mean RSRP and median of the measured data. A median of -86.5 dBm for LTE 800 is an indicator that the radio condition with LTE 800 is lot better as half of the data is above -86.5 dBm which is a good value. Figure 7.29 shows that nearly 41% of data has RSRP level above -90 dBm (marked in green) which shows that the radio condition have in overall been good for LTE 800 in Singerjärvi. It is to be noted that the data shown in Figure 7.29 is for the combined data set (active set and detected data set merged) while the CDF plots have been separately analyzed.

Table 7.11: Path loss statistics of LTE 1800
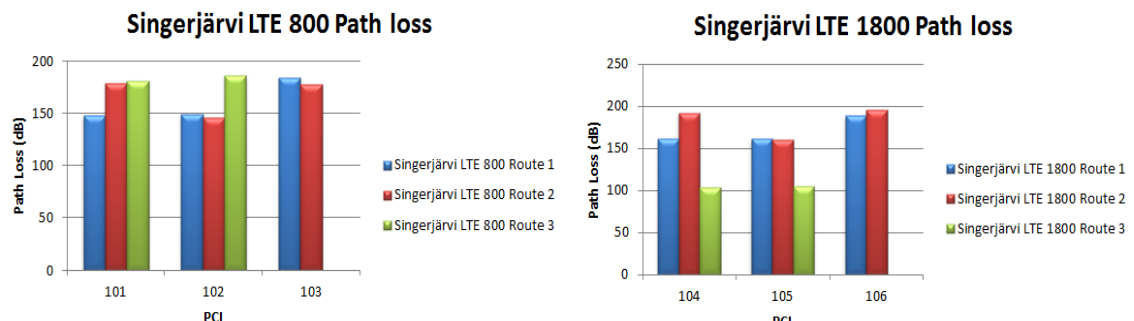
Route	Cells	Minimum RSRP (dBm)	Maximum Path Loss (dB)	Deviation (dB)	Radius (km)	Attenuation (dB/km)
	104	-98.3	161.7	-4.7	1.7	91.9
1	105	-98.4	161.8	-4.6	1	160.2
	106	*-125.2*	*188.6*	*22.1*	*7*	*26.6*
	104	-128.8	192.2	25.7	5.4	35.2
2	105	-97	160.4	-6	0.7	216.8
	106	*-132.4*	*195.8*	*29.3*	*12*	*16.2*
3	*104*	*-131.1*	*194.5*	*28*	*6.9*	*27.8*
	105	-121	184.4	17.9	6.4	28.5

Maximum path loss in Table 7.11 is calculated as a difference of EIRP for LTE 1800 (calculated in Appendix A) i.e. 63.4 dBm and minimum RSRP for the particular LTE 1800 cell. The deviation again is calculated as the difference of observed maximum path loss with maximum allowable path loss (calculated in Appendix A) i.e. 166.5 dB. Average path loss observed for LTE 1800 is 179.9 dB which is 13.4 dB above the maximum allowable path loss calculated in the link budget. When compared to the similar statis-

tics shown in Table 7.5, the observed average maximum path loss for LTE 800 is 172.7 dB which is 7.2 dB below the observed average path loss of LTE 1800 although the maximum allowable path loss for LTE 1800 exceeds to that of LTE 800 by only by 0.6 dB. Radius column is the coverage radius for each routes and cells obtained from *Nemo Analyze*.

Attenuation finally gives the ratio of path loss with respect to cell radius. The dominance area of the cell in a particular route can be decided as the cell with least attenuation
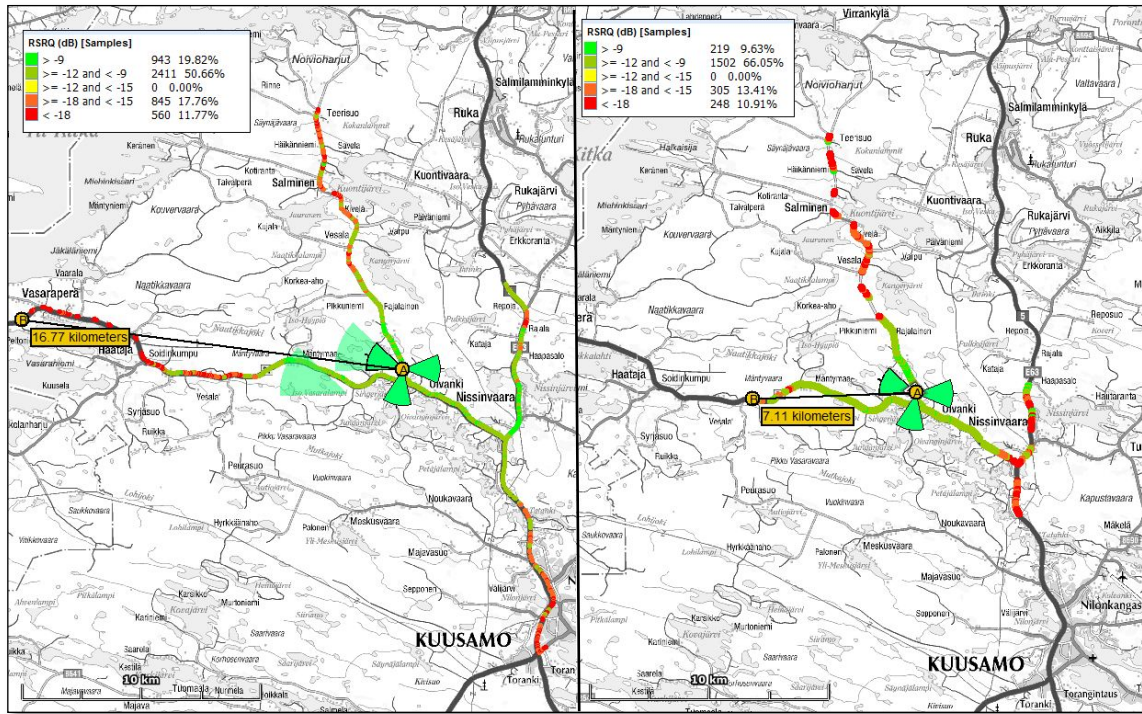
slope. The rows of dominant cells in different routes have been italicized in the table for distinction. Yet again, one of the reasons for higher observed path losses could be the exclusion of MIMO gains from the link budget.

Figure 7.32: Singerjärvi LTE 800 and LTE 1800 path loss in figure
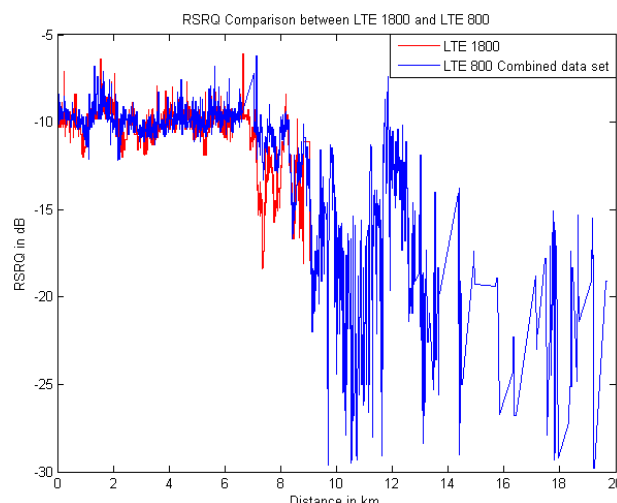
Figure 7.32 shows the path loss statistics of LTE 800 and LTE 1800 RSRP measurements. Basically, the statistics indicated in Table 7.12 have been shown in the figure. Path losses measured on route 3 for LTE 1800 have relatively very low path loss. This is due to the fact that the coverage range of the cells in Route 3 is very low compared to other routes. The above figure and table clearly distinguish the coverage of LTE 1800 with LTE 800. While the path loss suffered for two bands differ by 7.2 dB, the coverage radius differs by 9.5 km.

7.2.3. RSRQ comparison
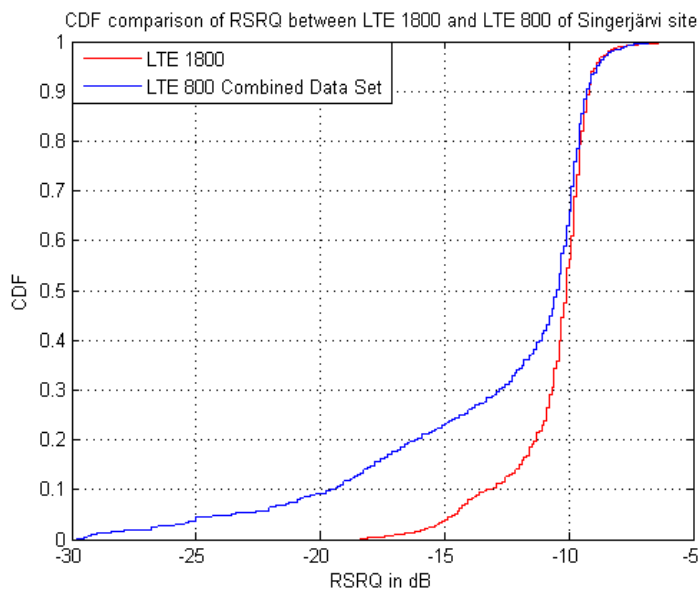
Figure 7.33: RSRQ scenario in Singerjärvi
Left: RSRQ for LTE 1800   Right: RSRQ for LTE 800

Figure 7.33 is the comparison of RSRQ levels around Singerjärvi site for both LTE 800 and LTE 1800. Coverage for LTE 1800 as discussed in earlier sections is smaller than that of LTE 800. RSRQ level of LTE 1800 is above -12 dB for nearly 75% of sample data. Comparing this with LTE 800, nearly 70% of sample data are above -12 dB. The statistics suggest that signal quality in both cases remain much similar. However, LTE 800 served much larger distance. Considering the route marked by blue arrow in the figure, the quality of signal for LTE 1800 is all most coherent with LTE 800 till the distance of 6.3 km from the site. Beyond this, LTE 1800 coverage deteriorates and coverage ends.

Figure 7.34: RSRQ Comparison between LTE 1800 and LTE 800

Figure 7.34 shows the RSRQ pattern compared for LTE 1800 and LTE 800 along the same measurement route. Measurement values for LTE 800 again have been merged to include the active set and detected set data. The pattern almost matches for both LTE 1800 and LTE 800 till the distance of 7 km from the initial point of measurement beyond which LTE 1800 RSRQ starts to deteriorate much worse than LTE 800 and finally the coverage of LTE 1800 ends at around 9 km. The worst RSRQ observed for LTE 1800 is -18.4 dB at a distance of 7.3 km. while that at the cell edge is -17.9 dB. The worst RSRQ level observed for LTE 800 when the site is serving as active set is -22 dB. The point is at a distance of 7.1 km approx. from the cell center. The worst RSRQ with LTE 800 in the detected set is -29.8 dB at a distance of 18 km.
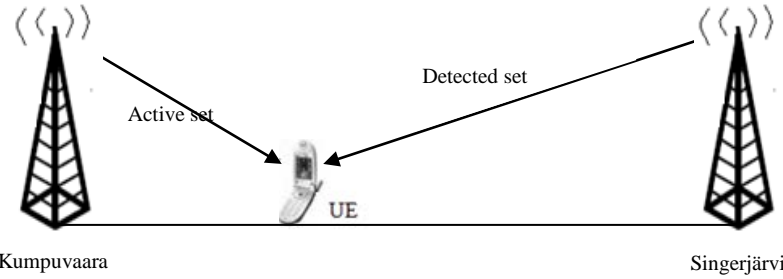

Figure 7.35: CDF comparison of RSRQ between LTE 1800 and LTE 800

Figure 7.35 shows CDF plots of RSRQ levels for LTE 1800 ad LTE 800 measured along the route marked in Figure 7.33. As indicated in the CDF plot, the CDF of LTE 800 includes the RSRQ level for both active set and detected set combined together. The upper and lower extremes for LTE 800 is greater compared to LTE 1800. But the distribution catches up with that of LTE 1800 seen clearly with the 50th percentile which is at -10.1 dB for LTE 1800 and -10.5 dB for LTE 800. But the lower limit is definitely much lower for LTE 800 compared to LTE 1800. This poor RSRQ is observed at the cell edge and is clear from Figure 7.34.

Noise and interference scenario is similar for both of the frequency bands. But as the coverage for the 1800 band closes down, the received signal level goes down as indicated in the RSRP analysis made in Section 7.2.2. With the RSRP level going down, the difference of RSRP with the total received signal RSSI increases and thus the RSRQ level goes down as indicated in Equation 5.1. LTE 800 measurement has been done with both test sites active. Singerjärvi LTE 800 active and detected set data as mentioned previously has been filtered out by removing Kumpuvaara site data from the measurement file. With the signal of Kumpuvaara existing in the measurement of LTE 800 as well, this would mean a considerable rise in RSSI level at the UE but with the

deteriorated RSRP level of Singerjärvi LTE 800 site. This resulted in the poor RSRQ levels at the cell edge for LTE 800.
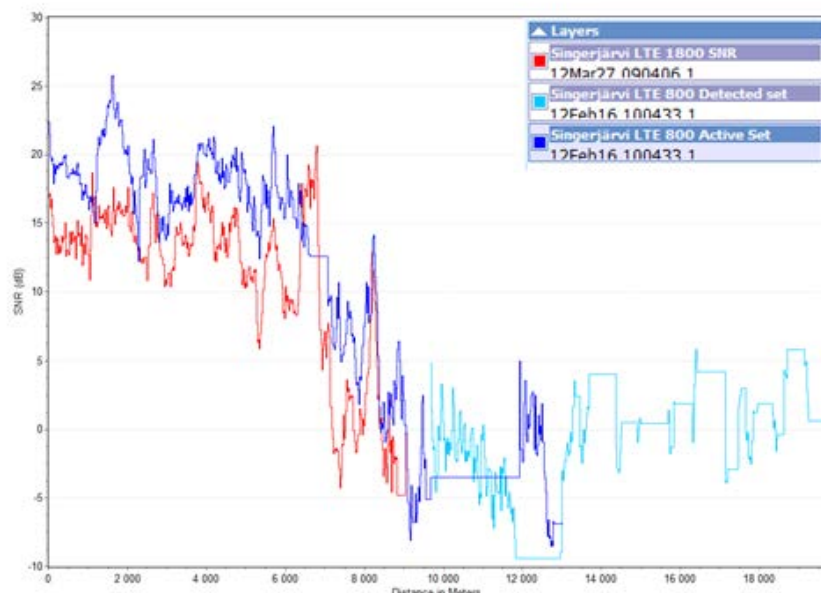
Figure 7.36: Measurement scenario of LTE 800 with both of the test sites

The case explained above can be clarified with Figure 7.36. At a point where the Singerjärvi LTE 800 is observed in the detected set list will obviously be served by Kumpuvaara LTE 800. Hence at that point, the RSSI level of the UE includes received signal or RSRP of both Kumpuvaara and Singerjärvi. For example in above figure, let the measured RSRP for active set (from Kumpuvaara) is -90 dBm, RSRP for detected set (from Singerjärvi) is -105 dBm and RSSI level be approximately -80 dBm.
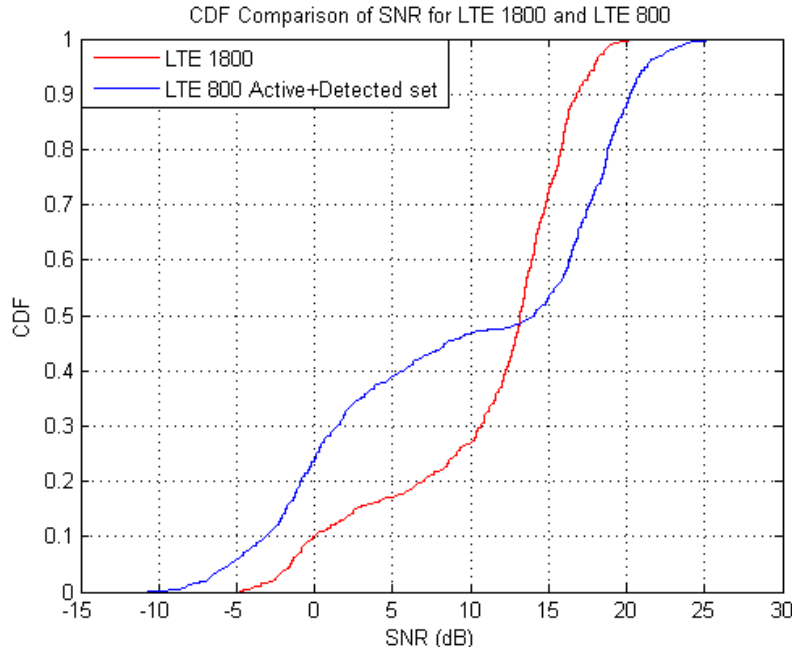
Utilizing Equation 5.1, RSRQ of detected set would be -8 dB approx. But in case of only site available as for LTE 1800, RSSI level at the same point will be lower for example at -85 dBm. In that case, the RSRQ level with the single active set (assuming the RSRP level be same i.e. -105 dBm) would be -3 dB approx. This is the reason why the RSRQ values are poorer at the detected set region of Singerjärvi LTE 800. In the current test network with just two sites, RSRQ might seem irrelevant. But with a loaded multi-site network, triggers based on RSRP do not exactly give the interference scenario. In such cases, adding RSRQ based triggers become handy.

7.2.4.   SNR comparison

Figure 7.37: SNR Comparison between LTE 1800 and LTE 800

Figure 7.37 shows SNR levels along the measurement route indicated in Figure 7.33 for LTE 1800 and LTE 800 (Combined data set of active and detected set). Line in red marks the SNR of LTE 1800 against the distance while line in blue and its shade mark the SNR of LTE 800 active set and detected set respectively. The figure shows that the plot of SNR of LTE 800 almost envelopes SNR of LTE 1800 for most of the active set region. SNR for LTE 1800 starts approximately 5 dB below LTE 800 and remains mostly below LTE 800 throughout the coverage of LTE 1800.
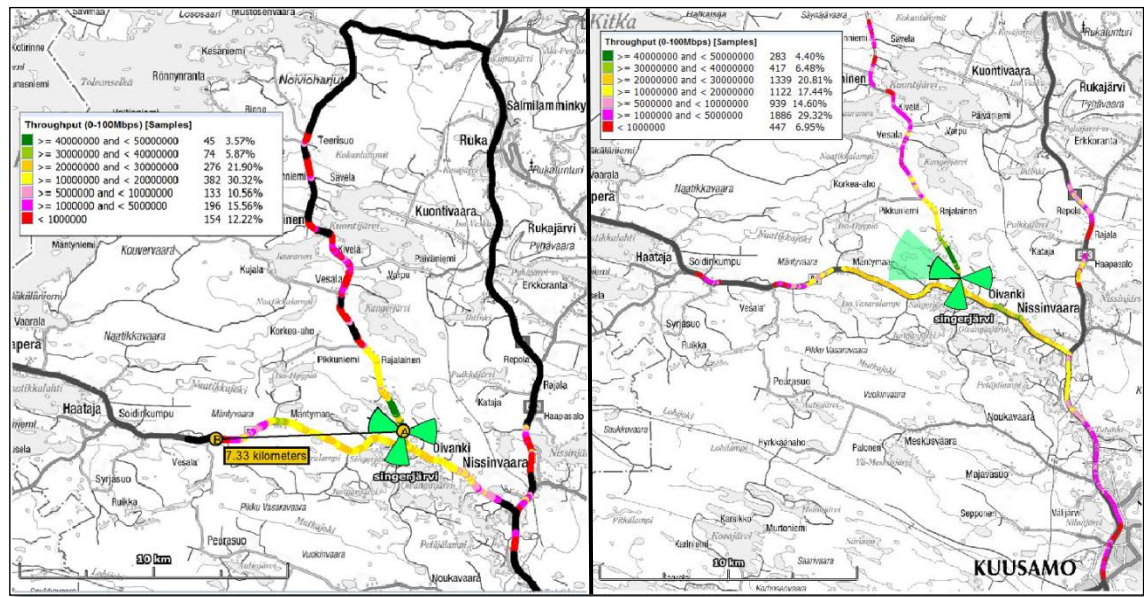
Figure 7.38: Comparison of CDF of SNR between LTE 1800 and LTE

Figure 7.38 shows the statistical comparison between SNR of LTE 1800 and LTE 800. Maximum SNR for LTE 1800 is 20.6 dB and for LTE 800 is 26.3 dB while the worst SNR for LTE 1800 is -4.8 dB and for LTE 800 is 26.3 dB. 50th percentile for LTE 1800 is 13.2 dB while that for LTE 800 is 14.1 dB. These values though seem quite closer but percentiles below 50 indicate that SNR for LTE 800 deteriorates much worse than that of LTE 1800. 90 % of LTE 1800 data is above 0 dB while the same figure is above -3 dB for LTE 800.
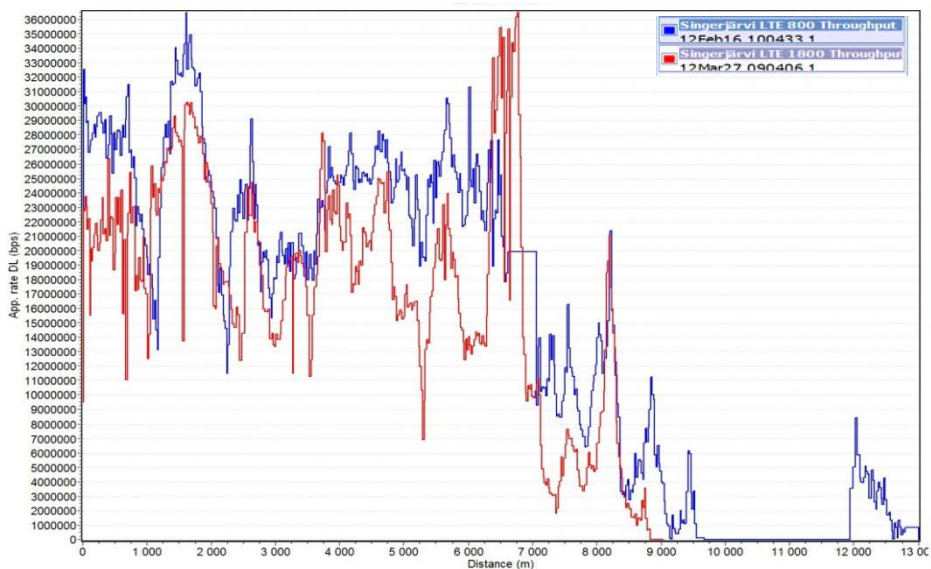
If the SNR of LTE 800 only during the active set has to be considered, Figure 7.20 can be referred. The figure and statistical results listed in Table 7.8 indicate a better SNR performance with LTE 800 compared to Figure 7.38. 50th percentile or the median of the LTE 800 (with active set only) is 2.2 dB higher than the LTE 800 (combined set). The trend of the graph of LTE 1800 is similar to the simulated result explained in Figure 5.1 while the CDF of LTE 800 bulges out on the lower percentiles. The measurement scenario can be considered interference free as the test sites for LTE 800 are considerably far (25 km approx.) while the LTE 1800 site in Singerjärvi is the only LTE site operating in that particular band in the region. The reason for the deterioration of lower percentiles in LTE 800 is mostly due to inclusion of SNR values from detected set.

7.2.5. Throughput comparison
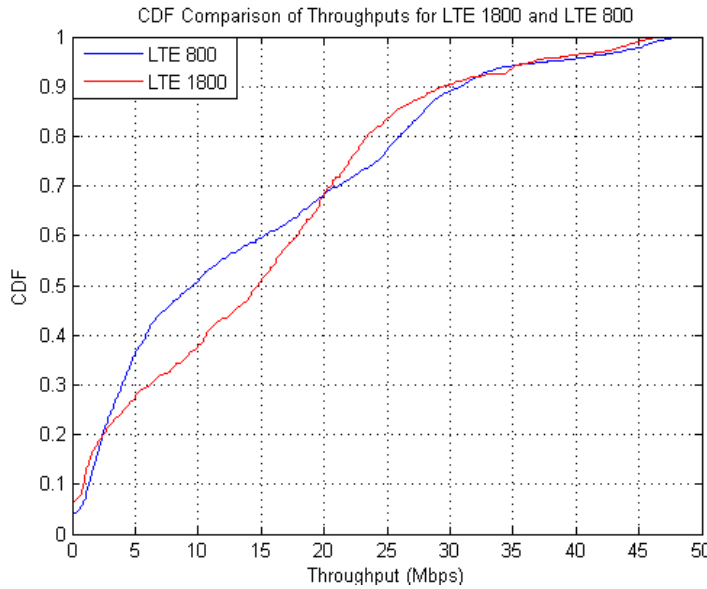
Figure 7.39: *Application downlink throughput coverage*
Left: Singerjärvi LTE 1800 and Right: Singerjärvi LTE 800

Figure 7.39 shows the throughput pattern of LTE 1800 and LTE 800 at Singerjärvi site. The coverage range indicated in the figure left is directed to the route towards Kumpuvaara. For LTE 1800, throughput of above 40 Mbps was observed at a radius of 1.2 km, above 10 Mbps was observed till 5.2 km. The range is 7.3 km approx. towards that particular direction for LTE 1800. Maximum throughput was observed to be 47.4 Mbps. For LTE 800, throughput above 30 Mbps was observed at a radius of 1.8 km, above 10 Mbps at a radius of 6.2 km and cell edge with 1 Mbps throughput at a distance of 10.8 km. Maximum throughput was observed to be 48.8 Mbps.

Figure 7.40: *Application throughput comparison between LTE 1800 and LTE 800*

Figure 7.40 shows the comparison of throughput between LTE 1800 and LTE 800 along the measurement route that heads from Singerjärvi towards Kumpuvaara. LTE 1800 is as seen engulfed by the curve of LTE 800 for most of the coverage area. The figure gives a clear picture of throughput distribution against the distance for both bands. Surprisingly, the peak DL throughput for LTE 1800 was observed at a distance of around 6.5 km.

Figure 7.41: *CDF comparison of throughputs for Singerjärvi LTE 1800 and LTE 800*
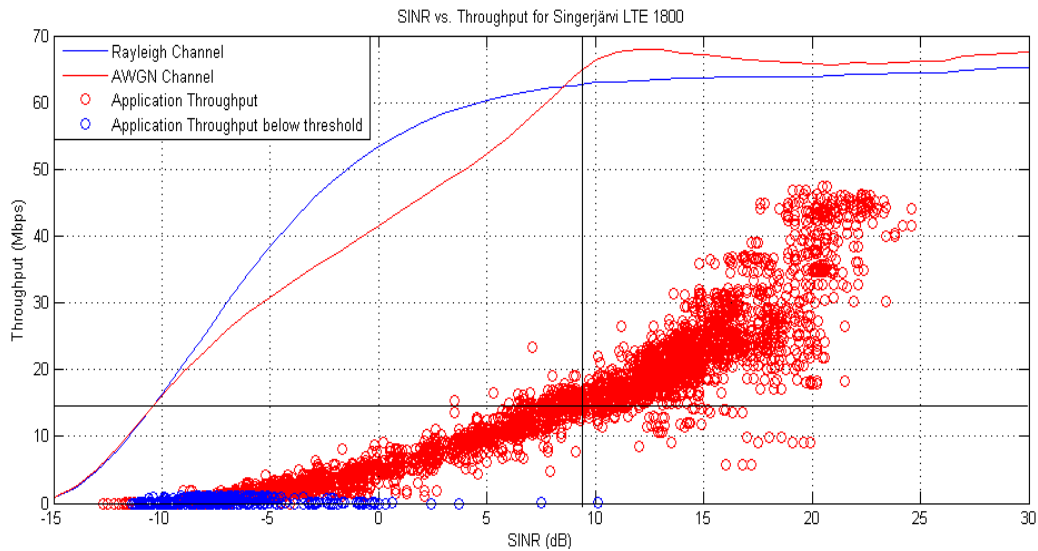
Figure 7.41 shows the statistical comparison of throughputs observed for LTE 1800 and LTE 800. Data from all of the measurement routes (as seen in Figure 7.39) have been taken for the CDF analysis for both LTE 1800 and LTE 800.

Table 7.12: *Statistical parameters of LTE 800 and LTE 1800 throughputs*

Statistical Parameters	LTE 800	LTE 1800
Minimum (Mbps)	0	0
Maximum (Mbps)	48.8	47.4
Mean (Mbps)	13.8	14.8
Median (Mbps)	9.6	14.7
Standard Deviation (Mbps)	12.3	11.4

Table 7.12 draws the summary from the CDF in Figure 7.41 for both bands. The minimum is 0 for both the cases as the measurement route includes values beyond the coverage area as well. The mean throughput for LTE 800 is 13.8 Mbps while that for LTE 1800 is 14.8 Mbps differing by 1 Mbps approx. Median or 50th percentile for LTE 800 is 9.6 Mbps while that for LTE 1800 is 14.7 Mbps differing by 5 Mbps approx. The deviation in throughputs measured in 12.3 Mbps for LTE 800 while that for LTE 1800 is 11.4 Mbps. This huge deviation in both cases is because the test network consists of only one site and as the coverage deteriorates moving towards the cell edge, the throughput degrades. The measurements were taken from the cell center towards the

cell edge in different directions. Thus, the presence of lower throughput in the cell edge region for both of the bands causes the throughput deviate in large proportion.

Figure 7.42: SNR vs. Application Downlink Throughput for LTE 1800

Figure 7.42 shows a scatter plot of application downlink throughput vs. SNR for LTE 1800 band. The Shannon bounds for Rayleigh and AWGN channels are given in Figure 5.2. The measurement points are for all of the measurement routes. SNR in the measurement routes ranges from -12 dB to 24 dB. The throughput reaches to 47 Mbps approx. supported by the peak SNR. The curve swing is similar to the ones in *Figure 7.24* plotted for LTE 800. As the SNR decreases, the downlink throughput decreases and vice versa which is fairly predictive. The median of the data which falls at 14.7 Mbps approx. and 9.4 dB SNR divides the data into 4 quadrants marked by black line. The blue colored line marks the cell edge defined by SNR and throughput thresholds of -11.4 dB and 1 Mbps respectively (as calculated in Equation 6.9).
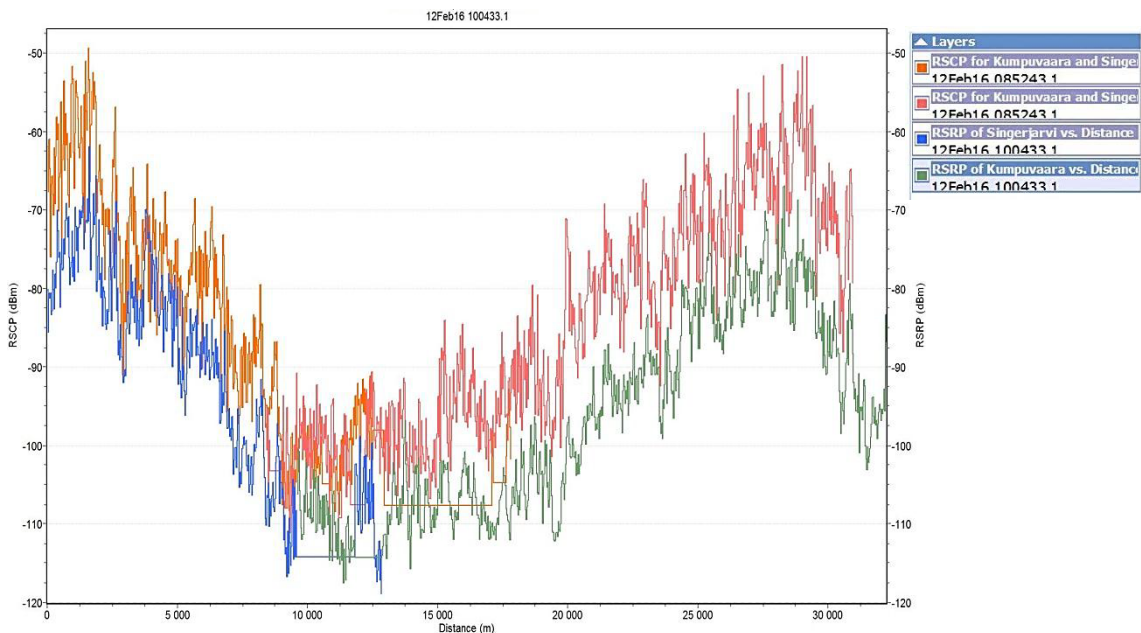
The blue circles in the figure fall in the region where SNR is above -11.4 dB but the throughput is below 1 Mbps. 10.1% samples of LTE 1800 fall under this region. There are no samples that are above 1 Mbps threshold having SNR below -11.4 dB. With the operator's requirement of providing 1 Mbps throughput limit at the cell edge, approximately 90% of samples have met the operator's performance requirement.

The results when compared with that of LTE 800 results for both Singerjärvi and Kumpuvaara sites (refer to Figure 7.24) show that LTE 800 has outperformed LTE 1800 in terms of service quality provided within its coverage limits. Of all, the Kumpuvaara LTE 800 has best performed with site meeting the requirement 98% of sample time.

7.3. UMTS 900 comparison

A detailed one on one comparison of LTE 800 MHz and UMTS 900 MHz cannot be made as in case of LTE 800 and LTE 1800. This is because of underlying differences in access technologies and other issues. One of the major obstacles faced during the comparison is that LTE network set up in the Kuusamo is only a test network consisting of two test sites. However, the UMTS 900 network in the region is commercially on air. It consists of multiple sites and multiple users as well. The test environment for LTE can be termed as coverage limited environment while that of UMTS can be termed as interference limited environment comparatively. However, filtering out the other neighboring sites except Kumpuvaara and Singerjärvi from the measurement files could give some measures of comparison. CQI reporting for link adaptation (QPSK and 16 QAM) range from 0 to 30 (for category 10 HSDPA devices) giving different transport block sizes. RSRQ measurement in LTE can be termed analogous with E_c/N_0 in UMTS but with the difference of PRB usage that contributes to RSRQ.
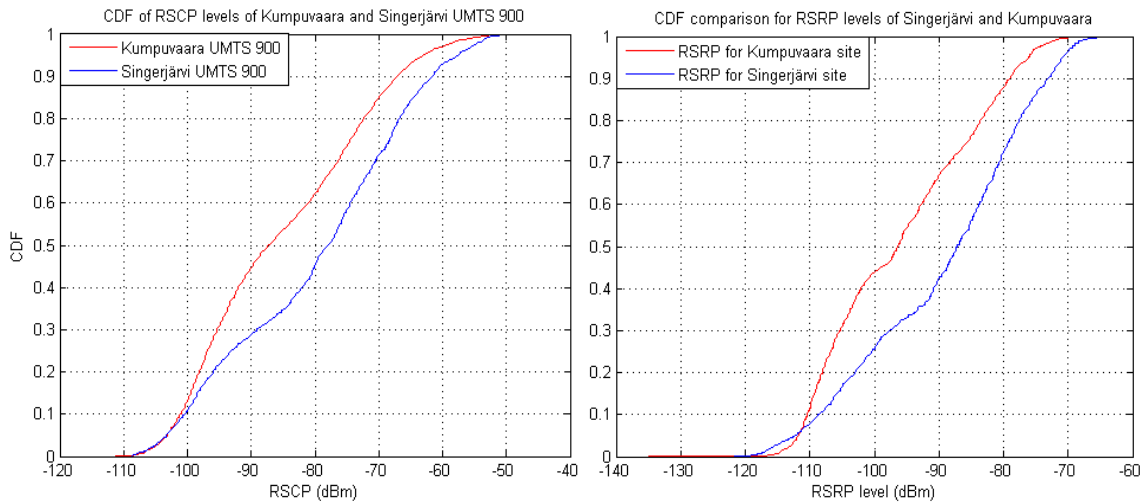
7.3.1. RSRP vs. RSCP

Figure 7.43: RSRP vs. RSCP comparison between Kumpuvaara and Singerjärvi

Figure 7.43 shows the comparison of RSRP of LTE 800 and RSCP of UMTS 900 against distance. The measurement file has been filtered out for both cases to consider only the Kumpuvaara and Singerjärvi sites. Kumpuvaara site for UMTS 900 has one extra cell with scrambling code 64 which is not co-located with the LTE cells. Measurement points with 64 as active scrambling code has been filtered out. Both of the measurements RSCP (orange and red line) and RSRP (blue and green line) have been plotted in same scale. RSRP level throughout the coverage area has been below UMTS's RSCP level. The peaks seen at the beginning and end of the measurement

align indicating the presence of cell center. Cell radius in terms of received signal level for Kumpuvaara UMTS is 18.5 km approximately while that of Singerjärvi UMTS 900 is 10.9 km.
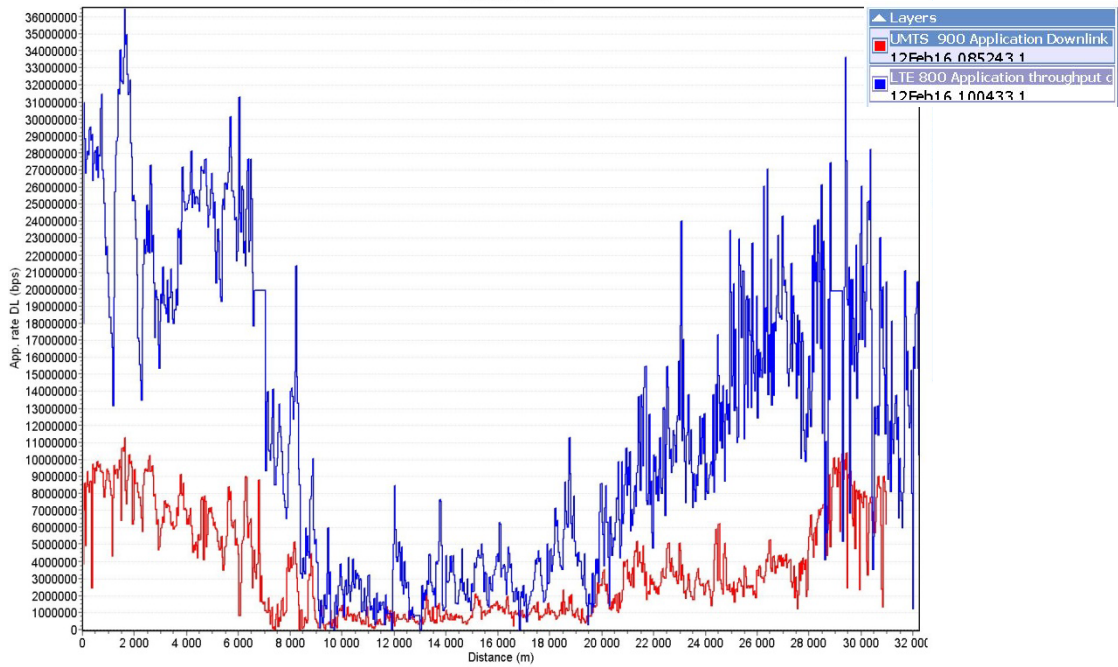
Figure 7.44: CDF comparison between two sites in UMTS 900 and LTE 800

Figure 7.44 shows the CDF for RSCP and RSRP levels of Kumpuvaara and Singerjärvi UMTS 900 and LTE 800 sites. RSCP level of Kumpuvaara ranges from -48 dBm to -111 dBm while RSCP of Singerjärvi ranges from -49 dBm to -109 dBm. Mean RSCP for Kumpuvaara is -85 dBm and that for Singerjärvi is -79 dBm. 50th percentile is -87 dBm for Kumpuvaara while -78 dBm for Singerjärvi. LTE 800 CDF plot is similar to that of UMTS 900 exception being the difference in the lower and upper limits.

The CDF plot and Figure 7.43 indicate that RSRP level has remained almost below the RSCP level. Theoretically the received signal levels should be similar in both cases as the transmit power levels and the RF Noise Figure for the UE and eNodeB are almost same (Appendix B). However, UMTS has the advantage of Processing Gain (PG) which boosts the descrambled signal power level; an advantage to UMTS inherent of its RAT which LTE does not have. This causes descrambled RF levels of UMTS to be higher than reference power level of LTE.
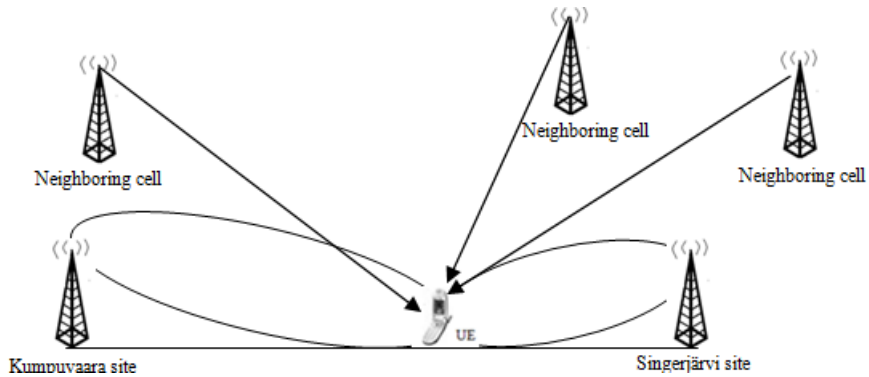
7.3.2. Throughput comparison

Application throughput as always is one of the most important performance indicating parameters in wireless technologies. This section compares the application downlink throughput between LTE 800 and UMTS 900. UMTS 900 is equipped with HSDPA+ technology which supplements its downlink throughput theoretically to 21 Mbps. Again, the lower limit or the cell edge limit requirement of the operator i.e. to provide 1 Mbps downlink throughput minimum at the edge is valid for UMTS as well.

Figure 7.45: Application downlink throughput comparison between UMTS 900 and LTE 800

Figure 7.45 shows the plot of application downlink throughput measurements plotted against the distance for both UMTS 900 and LTE 800 along the same measurement route i.e. from Singerjärvi towards Kumpuvaara. The peak throughput for UMTS 900 at Singerjärvi is 11.2 Mbps while that of Kumpuvaara is 14.2 Mbps. The average down-link throughput in the measurement route with UMTS 900 is 3.8 Mbps. Throughput for LTE 800 is above UMTS 900. But the throughput for LTE 800 has also suffered steep degradation towards the cell edge. The deviation for the LTE is 9 Mbps while that of UMTS is 3.2 Mbps. The peak throughput in case of LTE on the same measurement route is 36.4 Mbps. The minimum throughput for UMTS network is 8.8 Kbps while that of LTE Network is measured to be 0.
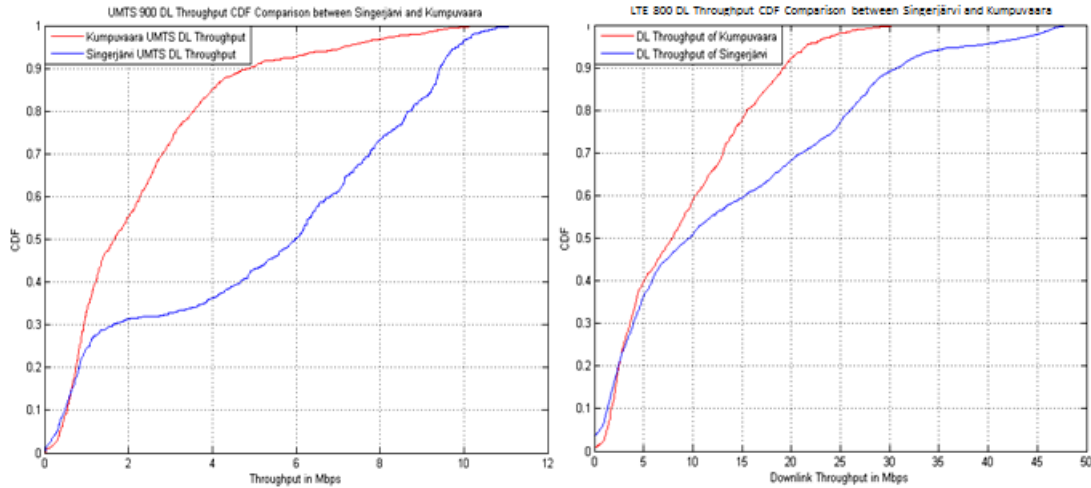
Figure 7.46: UMTS 900 network scenario at the area

Figure 7.46 shows the UMTS network scenario with multiple interfering sites along with Kumpuvaara and Singerjärvi. UMTS network in the area is a commercially launched network with multiple NodeBs in the area. The inherent feature of UMTS is that a UE can be associated with multiple NodeBs at a time. Thus the nearby NodeBs or

the neighboring cells that are on active list contribute together to the streaming of data on downlink path. Hence, the throughput did not drop to 0 even at the poor condition. But comparatively, LTE 800 test network has only two sites placed such that the coverage area of two sites are mostly adjacent and with very less intersection. Thus at few measurement points, the UE was deprived of coverage and hence the throughput was ceased to 0.

Figure 7.47: *DL throughput comparison between Singerjärvi and Kumpuvaara*

Figure 7.47 shows the CDF comparison between the DL throughput of Kumpuvaara and Singerjärvi sites. Range of throughput for Kumpuvaara site is 8.8 Kbps to 10.3 Mbps while that of Singerjärvi site is 8.8 Kbps to 11.2 Mbps. Mean downlink throughput with the Kumpuvaara cells as active site is 2.3 Mbps while that of Singerjärvi cells have mean downlink throughput of 5.1 Mbps. 50th percentile for Kumpuvaara site is 1.6 Mbps while that of Singerjärvi site is 5.9 Mbps. Higher percentiles when compared between Kumpuvaara and Singerjärvi show wider variations while the lower percentiles almost align to one another. Lower percentile indicates the cell edge conditions are similar for both of the sites. High deviation in higher percentiles indicates that Singerjärvi site has better throughput within its coverage area. The coverage however for Kumpuvaara site is higher and thus has more samples. 90% of the samples have throughput below 5 Mbps while 90% of samples in Singerjärvi have throughput below 9.4 Mbps. The right plot in Figure 7.47 shows the LTE 800 CDF for both sites. Initial observation indicates that the trend of throughput in LTE 800 is similar to that of UMTS 900. Plot of lower percentiles remain align for both sites till 40%. 90% of samples have throughput below 20 Mbps approx. for Kumpuvaara while that for Singerjärvi is below 31 Mbps approx. Yet again, the number of samples for Kumpuvaara site is higher than that of Singerjärvi site with Kumpuvaara site serving at greater distance. The cell edges or the site is served with poor CQI and resulting in lower application throughput.

8. CONCLUSION AND DISCUSSION

8.1. Measurement analysis

Analysis of the measurements has been appropriately and sequentially divided into:
- CQI and link adaptation
- RSRP analysis
- RSRQ analysis
- SNR analysis
- Throughput analysis

CQI and link adaptation analysis initially give the radio status of the channel and indicates how the UE has adapted to the channel variation. Interdependence of CQI and Link adaptation in a closed loop can be seen in the analysis. Variation of CQI with the varying distance and link adaptation is shown clearly.

RSRP analysis is directly related to the radio signal power in LTE. The reference signal power measured at UE degrades along with the CQI and modulation order. The loss of signal power comes from the free space model but not entirely. The other factors affecting the signal loss are diffraction, scattering, slow and fast fading and interference. RSRP measured has been compared with the theoretical value from link budget to find the difference in the estimated path loss. The measure of attenuation a signal bears being associated with the particular cell gives the cell dominance. RSRQ, which gives the signal quality, has also been studied for both of the bands.

SNR and throughput are important planning parameters for network planners. For a particular band, the analysis of SNR or SINR gives the measure of effect of noise and interference to the signal power. The downlink throughput measured has been compared with the Shannon's theoretical limits with peak throughputs ranging from 48 Mbps approx. and 36 Mbps at max. for two sites. Threshold throughput of 1 Mbps has been maintained in the border of both cells. Cell edge throughput thresholds defined by the service provider also limits the cell edge SINR. These throughput and SINR limits can also be considered as the performance border lines in the measurement data. The comparison clearly indicates that the coverage radius is almost half for LTE 1800 compared to LTE 800 in all of the perspectives taken for the analysis.

A comparison of LTE 800 with the UMTS network was also done although limited by the parameters matched for comparison. RSCP was compared with the RSRP and the downlink throughputs were also compared.

8.2. Reliability and validity test

Reliability of the measurements was tested and elaborated in Section 7.1.3.3 by performing a multiple run test on the same measurement route. The parameter tested was RSRP. Graphical and statistical analyses shown in the section indicate that for a particular measurement route, measurement data was found to be reliable and statistically consistent (refer to Figure 7.11 and Table 7.6). The setup of test network with single test UE ensured that the interference from other UEs was negligible and the data observed was consistent. Thus, the data can be considered reliable.

The analyses can also be called valid as it adheres to the theoretical and empirical models. The downlink throughput has stayed within the Shannon and Rayleigh capacity limitations. The maximum throughput observed was about 28 Mbps below the theoretical maximum. The theoretical capacity however does not include the control channel traffic and other radio environment related losses which could account for some of the lost 28 Mbps. The cell radius as calculated from the link budget was 29.3 km which is approximately equal to the maximum detected set range observed i.e. 30.2 km. Performance of different bands was also calculated with analysis of SNR against the throughput and both bands performed 90% of the sample duration. The minor deviations of the observed values from the theoretical limits and the performance show that the measured data and the conclusions drawn are valid.

8.3. Limitations of the analysis

Theoretical coverage calculations of the different bands of LTE and UMTS Network are made with the Link Budget. Theoretical throughputs limits are given by Shannon bound on different channels. However, theoretical calculations are always subject to larger deviations in a time varying radio channel. Slow and fast fading that act upon a radio signal in a wireless channel make the estimation difficult. The trend of radio signal or RSRP in case of LTE from transmitter to the receiver at different distance can be predicted. However, an exact or a close estimate again is hard to make. RSRQ, yet another radio signal parameter associated with RSRP is similarly difficult to precisely estimate. Theoretical coverage estimation models one such as Okumura-Hata model has its own limitations; affect or terrain type, elevation etc. Rather than relying on just the link budget, a proper industrial standard network planning tool or a simulation tool would be more precise.

8.4. Moving ahead

This project on LTE 800 coverage analysis was done with the test network set in the rural area. Being the test network, the measurement did not consist of other UEs or other interfering sites. With an unloaded and interference free network, the measurements and conclusions might not depict the exact scenario that occurs in a typical radio environment. Also, the measurement cases could be expanded to other environments such as

urban, sub-urban etc. or a topographically challenging environment. The inter-frequency handover related measurements for co-located cells were not conducted due to the limitations of the UE. Analysis of this feature will give the true interaction of different LTE bands; showing how the coverage of different bands are laid over one another for co-located cells.

Future path of wireless communication as seen by 3GPP is largely based on LTE; an evolution in RAT that would provide service beyond consumer's satisfaction levels and sustainable for a considerable span of time. OFDM, the inherent multiple access technology associated with it has provided consortiums such as 3GPP an opportunity to provide high throughputs to larger number of users. LTE-A, predecessor of LTE will surely give an exponential rise to the radio performance in the coming dates.

REFERENCES

[1]   GPRS downlink throughput, http://www.3gpp.org/article/gprs-edge/

[2]   HSPA, http://en.wikipedia.org/wiki/Evolved_HSPA

[3]   3GPP ETSI TR 125.913 V8.0.0 Release 8. 2009. Requirements for Evolved
        UTRA (E-UTRA) and Evolved UTRAN (E-UTRAN)

[4]   Motorola Inc. 2007. Spectrum Analysis for Future LTE Deployments. A white
        paper on overview of spectrum trends related to LTE , highlighting the issues and
        opportunities that potentially lie ahead

[5]   3GPP TS 136.306 V10.5.0 Release 10. March 2012. LTE Evolved Universal Ter-
        restrial Radio Access (E-UTRA): User Equipment (UE) radio access capabilities

[6]   ETSI TS 24 301 V10.4.0 Release 10. October 2010. Universal Mobile Telecom-
        munications System (UMTS) LTE: Non-Access-Stratum (NAS) protocol for
        Evolved Packet System (EPS); Stage 3

[7]   3GPP TS 21.905 v10.3.0 Release 10. March 2011. LTE-Vocabulary for 3GPP
        Specifications

[8]   3GPP TS 23.203 V8.1.1 Release 8. March 2008. Technical Specification Group
        Services and System Aspects: Policy and charging control architecture

[9]   IXIA. 2009. SC-FDMA Single Carrier FDMA in LTE. A white paper on SC-
        FDMA technology, its use in LTE and its extension from OFDM

[10]   ETSI TS 136 101 V10.5.0 Release 10. January 2012. LTE Evolved Universal
        Terrestrial Radio Access (E-UTRA): User Equipment (UE) radio transmission
        and reception

[11] 3GPP TS 124.301 V10.4.0 Release 10. October 2011. Technical Specification Group Core Network and Terminals: Non-Access-Stratum (NAS) protocol for Evolved Packet System (EPS); Stage 3

[12] 3GPP ETSI TS 136 304 V8.10.0 Release 8. June 2011. LTE Evolved Universal Terrestrial Radio Access (E-UTRA): User Equipment (UE) procedures in idle mode

[13] 3GPP ETSI TS 123 401 V8.14.0 Release 8. June 2011. LTE General Packet Radio Service (GPRS) enhancements for Evolved Universal Terrestrial Radio Access Network (E-UTRAN) access Section 5.3.3. Page Number 63

[14] Kurjenniemi, J., Henttonen, T. & Kaikkonen, J. 2008. Suitability of RSRQ Measurement for Quality Based Inter-Frequency Handover in LTE. IEEE International Symposium on Wireless Communication Systems

[15] 3GPP ETSI TS 123 401 V8.14.0 Release 8. June 2011. LTE General Packet Radio Service (GPRS) enhancements for Evolved Universal Terrestrial Radio Access Network (E-UTRAN) access. Section 5.5.1.2.2 Page Number 119

[16] 3GPP ETSI TS 136 331 V10.3.0 Release 10. November 2011. LTE Evolved Universal Terrestrial Radio Access (E-UTRA): Radio Resource Control (RRC) Protocol specification

[17] 3GPP ETSI TS 136 213 V10.5.0 Release 10. March 2012. LTE Evolved Universal Terrestrial Radio Access (E-UTRA): Physical layer procedures

[18] 3GPP ETSI TS 136 214 V10.1.0 Release 10. April 2011. LTE Evolved Universal Terrestrial Radio Access (E-UTRA) Physical layer Measurements

[19] Dahlman, E., Parkvall, S. & Sköld, J. and Beming, P. 2008. 3G Evolution HSPA and LTE for Mobile Broadband. Elsevier Limited

[20] 3GPP ETSI TS 125 215 V10.0.0 Release 10. April 2011. Universal Mobile Telecommunications System (UMTS): Physical layer Measurements (FDD) Section 5.1.1, 5.1.17 & 5.1.19

[21] Salo, J., Nur-Alam, M. & Chang, K. 2010. Practical Introduction to LTE Radio Planning. A white paper on basics of radio planning for 3GPP LTE in interference limited and coverage limited scenarios, European Communications Engineering (ECE) Ltd, Espoo, Finland

[22] Holma, H. & Toskala, A. 2009. LTE for UMTS OFDMA and SC-FDMA based Radio Access. John Wiley and Sons Ltd.

[23] Chiang, M., Hande, P., Lan, T. & Tan, C.W. 2008. Power Control in wireless cellular networks. From the journal Foundations and Trends® in Networking. Now Publishers Inc.

[24] Castellanos, C.U., Villa, D.L., Rosa, C., Pedersen, K.I., Calabrese, F.D., Michaelsen, P.H. and Michel, J. Spring 2008. Performance of Uplink Fractional Power Control in UTRAN LTE. IEEE Vehicular Technology Conference

[25] Li, J. Bose, A and Zhao, Y.Q. 2005. Rayleigh flat fading channels' capacity, Proceedings of the 3rd Annual IEEE Communication Networks and Services Research Conference

[26] Matlab DCMC Capacity. http://users.ecs.soton.ac.uk/rm/resources/matlabcapacity/

[27] Molisch, A.F. 2011. Wireless Communications, Second Edition John Wiley & Sons, Ltd

[28] Shuttle RADAR Topography Mission (SRTM) 90m Digital Elevation Database v4.1. ftp://e0srp01u.ecs.nasa.gov/srtm/version2/SRTM3/

[29] Fujitsu. Enhancing LTE Cell-Edge Performance via PDCCH ICIC. A white paper on challenges of optimizing cell-edge SINR and various strategies to enhance the cell-edge performance of PDCCH using the existing LTE standard.

[30] PCTEL. April 2011. Maximizing LTE Performance Through MIMO Optimization. A white paper on capabilities and challenges posed by MIMO in LTE networks

APPENDIX

Appendix A: LTE Downlink Link Budget

Parameters	Unit	LTE 800 DL	LTE 1800 DL
Boltzmann Constant		1.38E-23	1.38E-23
Room Temperature	Kelvin	2.90E+02	2.90E+02
Base Station Height	meters	81.00	77.00
Mobile Station Height	meters	1.50	1.50
Carrier Frequency	MHz	800	1800
Bandwidth	Hz	1.00E+07	1.00E+07
Number of Resource Blocks		50.00	50.00
Number of Sub-carriers per Resource Block		12	12
Bandwidth per Sub-carrier	Hz	1.50E+04	1.50E+04
Effective Bandwidth	Hz	9.00E+06	9.00E+06
Time Period per resource block	s	5.00E-04	5.00E-04
Total Number of Sub-carriers		600	600
Transmitter Power	dBm	46	46
Antenna Gain (From manufacturer's specifications)	dBi	17.1	17.8
Cable Losses	dB	0.25	0.34
Antenna Diversity Gain	dB	0	0
Body Loss	dB	0	0
EIRP	**dBm**	**62.85**	**63.46**
Thermal Noise Density	dBm/Hz	-2.04E+02	-2.04E+02
Total Thermal Noise of the system	**dBm**	**-104.43**	**-104.43**
Receiver Antenna Gain	dB	0	0
Receiver Noise Figure	dB	7	7
Receiver Losses	dB	0	0
Modulation Scheme		QPSK	QPSK
No of Bits per Symbol		2	2
Coding Rate		0.1	0.1
Useful Bits per Symbol		0.2	0.2
No. Of Bits per Resource Block		16.80	16.80
Spectral Efficiency	**bps/Hz**	**1.68E-01**	**1.68E-01**
Required SINR at the Cell Edge	dB	-9.08	-9.08
Receiver Sensitivity	**dBm**	**-106.52**	**-106.52**
Fading Margin	dB	0	0
Interference Margin	dB	4	4
Coverage Probability	%	95	95
Indoor Path Loss	dB	0	0
Control Channel Overhead (29%)	dB	-0.53	-0.53
Total Path Loss	**dB**	**165.9**	**166.5**
Cell Radius (Okumura Hata Model)	**Km**	**29.3**	**12.7**

Appendix B: *UMTS Link Budget*

General info	Unit	Value
Frequency	MHz	900.00
Chip rate	cps	3.84E+06
Temperature	K	290
Boltzman's constant	J/K	1.38E-23
Noise Bandwidth	Hz	3.84E+06
Base Station Height	meters	8.10E+01
Mobile Station Height	meters	1.50E+00
Service profile	**Unit**	**Downlink**
Load	%	50
Bit rate	kbps	1024
Receiving end		**Mobile**
Noise figure	dB	7
Thermal Noise power	dBm	-108.13
Cell Interference margin (noise rise)	dB	3.01
Total interference level	**dBm**	**-98.12**
Required E_b/N_o	dB	7
Processing Gain	dB	5.74
Antenna diversity gain	dB	0
SHO diversity gain	dB	2
Power control headroom	dB	0
Fading Margin (rural)	dB	0.8
Required C/I	**dB**	**0.06**
Receiver sensitivity	**dBm**	**-98.06**
RX antenna gain	dBi	0
LNA gain	dB	0
Cable loss	dB	0
Required signal power	**dBm**	**-98.06**
Transmitting end		**NodeB**
TX Power / connection	W	40
TX Power / connection	dBm	46.02
Antenna gain	dB	1
Cable loss	dB	0.2
Peak EIRP	**dBm**	**62.7**
Isotropic path loss	**dB**	**160.8**
Cell Radius (Okumura Hata Model)	**Km**	**18.1**